The functional role of Tspan2 in anti-infectious immune responses

Inaugural dissertation

for the attainment of the title of doctor
in the Faculty of Mathematics and Natural Sciences
at the Heinrich Heine University Düsseldorf

presented by

Marcel Marson

from Marl

Düsseldorf, January 2025

from the Institute for Medical Microbiology and Hospital Hygiene
at the Heinrich Heine University Düsseldorf

Published by permission of the
Faculty of Mathematics and Natural Sciences at
Heinrich Heine University Düsseldorf

Supervisor: Prof. Dr. Stefanie Scheu

Co-supervisor: Prof. Dr. Lutz Schmitt

Date of the oral examination: 21.07.2025

Summary

Members of the tetraspanin (Tspan) superfamily are attracting increasing interest as molecular organizers of the cell membrane. With their strong influence on the stability and functionality of protein complexes they are involved in a variety of processes, including cell migration, adhesion, proliferation, fertilization and multiple cancer-associated functions. While most Tspans have been characterized in different cell types of the immune system, knowledge about Tspan2 is limited to the central nervous system, so far. There, Tspan2 is expressed by oligodendrocytes with a crucial role during myelination and in stabilizing the mature myelin sheath.

In this doctoral thesis it is shown for the first time that Tspan2 is expressed by a variety of immune cells, including conventional and plasmacytoid dendritic cells, monocytes/macrophages and especially neutrophils. The application of state-of-the-art single-cell sequencing analyses of purified neutrophils from Tspan2$^{-/-}$ and wild type (WT) mice allowed the identification of accurate differences in the transcriptome of these neutrophils and their maturation stages. In particular, genes associated with motility-related ontologies, such as recruitment, migration, adhesion or chemotaxis, were found to be differentially expressed in Tspan2 deficiency. Furthermore, a number of genes were also directly related to individual effector functions and antimicrobial immune response.

Following the knowledge obtained by sequencing, Tspan2$^{-/-}$ mice were infected with the opportunistic pathogen *Candida albicans*. This resulted in a tendency towards a later onset of lethal symptoms as compared to WT mice, suggesting that the absence of Tspan2 may contribute to improved host survival. However, despite the large number of indicators, several studies conducted to elucidate the influence of Tspan2 on neutrophil motility showed no significant differences in recruitment behavior, (trans-) migration or chemotaxis. In contrast, neutrophils lacking Tspan2 were able to eliminate *Escherichia coli* bacteria considerably more efficient than WT neutrophils when directly exposed to them.

Although multiple studies were conducted to study different isolated aspects of motility, the loss of Tspan2 resulted in no alteration in neutrophil behavior. This indicates the complexity of the system, which can hardly be explained in studies with strictly defined conditions. In particular, the finding that the vast majority of neutrophils abundantly express Tspan2 indicates a certain role that it has to fulfil in these highly relevant immune cells. Therefore, this work demonstrates the high relevance of Tspan2 and provides a fundamental basis for further research on Tspan2-mediated influences.

Zusammenfassung

Mitglieder der Tetraspanin (Tspan) Superfamilie wecken als molekulare Organisatoren der Zellmembran ein zunehmend größer werdendes Interesse. Durch ihren starken Einfluss auf die Stabilität und Funktionalität von Proteinkomplexen sind sie an einer Vielzahl von Prozessen beteiligt, darunter die Zellmigration, Adhäsion, Proliferation, Fruchtbarkeit und mehrere mit Tumorerkrankungen verbundene Funktionen. Während die meisten Tspans in verschiedenen Zelltypen des Immunsystems charakterisiert wurden, beschränkt sich das Wissen über das Tspan2 auf das zentrale Nervensystem. Dort wird Tspan2 von Oligodendrozyten exprimiert, in denen es eine entscheidende Rolle bei der Myelinisierung und der Stabilität des maturierten Myelins spielt.

In dieser Doktorarbeit konnte erstmalig gezeigt werden, dass Tspan2 von einer Vielzahl an Immunzellen exprimiert wird, darunter konventionelle und plasmazytoide dendritische Zellen, Monozyten/Makrophagen und insbesondere Neutrophile. Die Anwendung moderner Einzelzell-Sequenzierungsanalysen von aufgereinigten Neutrophilen aus Tspan2$^{-/-}$ und Wild-Typ (WT) Mäusen, ermöglichte die Identifizierung von kleinsten Unterschieden im Transkriptom dieser Zellen und deren Reifungsstadien. Dabei zeigte sich, dass vermehrt Gene in Tspan2-Defizienz differenziell exprimiert waren, die mit Ontologien, wie der Rekrutierung, Migration, Adhäsion oder Chemotaxis assoziieren. Des Weiteren standen auch viele in direktem Zusammenhang mit einzelnen Effektorfunktionen und allgemein der antimikrobiellen Immunantwort.

Folgend der durch die Sequenzierung erzielten Indikationen, wurden Tspan2$^{-/-}$ Mäuse mit dem opportunistischen Pathogen *Candida albicans* infiziert. Letale Symptome traten in diesen Mäusen tendenziell später ein als in WT Kontrolltieren, weshalb die Abwesenheit von Tspan2 möglicherweise zu einer verbesserten Überlebensrate des Hosts beiträgt. Bei der Durchführung mehrerer Studien zur Aufklärung des Einflusses von Tspan2 auf die Motilität der Neutrophilen, zeigten sich trotz der Vielzahl an Indikatoren keine signifikanten Unterschiede im Rekrutierungsverhalten, der (Trans-) Migration oder der Chemotaxis. Dem entgegen sind Neutrophile ohne Tspan2 in der Lage, bei direkter Exponierung zu *Escherichia coli* Bakterien, diese deutlich effizienter zu eliminieren als WT Neutrophile.

Obwohl mehrere Studien durchgeführt wurden, um verschiedene Einzel-Aspekte der Motilität zu untersuchen, führte der Verlust von Tspan2 zu keiner Veränderung im Verhalten der Neutrophilen. Dies weist auf die Komplexität des Systems hin, die in isolierten Studien mit streng definierten Bedingungen nur schwer aufgeklärt werden kann. Insbesondere die Erkenntnis, dass die große Mehrheit der Neutrophilen Tspan2 stark exprimiert, deutet auf eine bestimmte Rolle hin, die es in diesen hochrelevanten Immunzellen erfüllen muss. Daher zeigt diese Arbeit die hohe Relevanz von Tspan2 und liefert eine fundamentale Grundlage für weitere Forschungen zu Tspan2-vermittelten Einflüssen.

Table of contents

1 Introduction

1.1 The innate immune system

The immune system is a highly complex network, which is traditionally divided into the innate and adaptive immune system, providing the host with protection against a wide range of foreign microorganisms. Although adaptive immunity is specifically customized to the invading pathogen, it takes several days to unleash the immune response upon first encounter. In contrast, the innate immune system requires minutes to hours to initiate a non-specific immune response with the aim of eliminating the pathogen, controlling the infection and facilitating the adaptive immune response (Medzhitov and Janeway, 2000, Kimbrell and Beutler, 2001). The innate immune system comprises several layers of protection, including anatomical and physical barriers as well as a range of soluble mediators and cellular components. In addition, for initiation of a robust immune response the innate immune system relies on a limited number of germ line-encoded pattern recognition receptors (PRRs) which sense with defined specificities conserved endogenous molecules and metabolites of microbial origin (Janeway and Medzhitov, 2002).

1.1.1 Cellular components in innate immunity

Major contributors of the innate immune system are neutrophils, macrophages, dendritic cells (DCs), natural killer (NK) cells, eosinophils and mast cells (Janeway and Medzhitov, 2002). Although these cells play indispensable roles, also non-professional cells such as epithelial and endothelial cells as well as fibroblasts are among the first to react once a microbial infection or tissue injury occurs. Using PRRs, cells can recognize evolutionary conserved structures on the surfaces of microbes, termed pathogen-associated molecular patterns (PAMPs), as well as endogenous molecules from damaged cells, called damage-associated molecular patterns (DAMPs). As a response to most PAMPs or DAMPs these cells can upregulate the expression of a range of proinflammatory mediators, including cytokines, type I interferons (IFNs), chemokines and antimicrobial proteins, depending on the type of activated PRR (Kumagai and Akira, 2010, Takeuchi and Akira, 2010).

1.1.2 Pattern recognition receptors

To date, four different classes of PRRs have been identified. These include Toll-like receptors (TLRs), C-type lectin receptors (CLRs), retinoic acid-inducible gene I (RIG-I)-like receptors, nucleotide-binding oligomerisation domain (NOD)-like receptors and intracellular DNA sensing receptors (Kumar et al., 2011). TLRs represent the best characterized PRRs, of which 12 different are present in the murine system. While intracellular TLRs mainly recognize nucleic

acids of viral origin, TLRs on the cell surface detect mostly bacterial components. This includes TLR4, which can recognize Lipopolysaccharide (LPS) found in the outer membrane of gram-negative bacteria (Kumar et al., 2011, Chow et al., 1999). Furthermore, in fungal infections, several TLRs, including TLR2 and TLR4, as well as CLRs, such as dectin-1 and dectin-2, are known to play an important roles as fungal sensors, emphasizing the importance and flexibility of PRRs (Inoue and Shinohara, 2014, Patin et al., 2019). Upon activation of TLRs by microbial substances, a signaling cascade is induced that can follow two main pathways, which are roughly divided into the MyD88- and TIR domain-containing adaptor inducing interferon-β (TRIF)-dependent signaling pathways. The dominant Myd88-dependent signaling pathway leads to the activation of the IκB kinase (IKK) complex and mitogen-activated protein kinase (MAPK) pathway. IKK activation allows phosphorylation and degradation of the NF-κB inhibitor IκBα, allowing NF-κB to translocate into the nucleus and induce the expression of proinflammatory genes, including type I IFNs (Kawasaki and Kawai, 2014).

1.2 Neutrophils – The front line of the immune system

Among innate immune cells, neutrophils represent 50-70 % of all circulating leukocytes under homeostatic conditions, however, their lifespan is very short. In humans, the average half-life is about 5 days, whereas in mice they last only 8-12 hours (Bartneck and Wang, 2019, Pillay et al., 2010). Neutrophils develop and accumulate in the bone marrow, where they develop from multipotent progenitors. The granulocyte colony-stimulating factor (G-CSF) acts as the essential factor for granulopoiesis, committing the multipotent progenitors to the myeloid lineage and stimulating the proliferation of granulocytic progenitors (Christopher and Link, 2007). In homeostasis, only a minor fraction of the neutrophil pool in the bone marrow is released into the circulation, while the majority is retained by the stromal cell-derived stromal-derived factor-1 (SDF-1, CXCL12) acting on the chemokine receptor C-X-C motif chemokine receptor 4 (CXCR4) expressed by neutrophils. Elevated levels of the multifunctional G-CSF counteract by decreasing the expression of CXCL12 and CXCR4 and additionally increasing the expression of CXCL2 by bone marrow endothelial cells. The CXCL2 acting on the CXCR2 of neutrophils antagonizes the CXCL12/CXCR4 axis and facilitates the directed egression of neutrophils into the blood circulation, thus enabling rapid mobilization of neutrophils in stress situations (De Filippo and Rankin, 2018, Eash et al., 2010). After a period in circulation, neutrophils switch to a senescent phenotype at the end of their life time and upregulate the expression of CXCR4, which mediates homing of the neutrophils (Rankin, 2010). Back in the BM they are cleared by local macrophages that in turn produce G-CSF to maintain neutrophil homeostasis (Furze and Rankin, 2008).

1.2.1 Neutrophil heterogeneity

Although neutrophils are the most abundant cells in the bone marrow, their functional diversity has long been questioned, partly due to their inability to divide after terminal differentiation. Nevertheless, neutrophils do not represent a homogeneous cell population neither in physiological nor pathological conditions (Scapini et al., 2016, Silvestre-Roig et al., 2016). Regarding neutrophil development, three neutrophil subsets have been defined in the bone marrow, including the proliferating neutrophil precursors and the non-proliferating immature and mature neutrophils (Evrard et al., 2018). However, naming cell subsets helps to simplify understanding, but can also mask the true biological context. In contrast, combining transcriptomic cell profiles, their functional properties and tissue distribution may provide a deeper insight into neutrophil plasticity in phenotype and function (Ng et al., 2019). An important factor for the functionality of neutrophils are the granules and their composition, which change with maturation, as do their functional capacities. They are divided into azurophilic (primary), specific (secondary), gelatinase (tertiary) granules and secretory vesicles (Borregaard et al., 2007, Xie et al., 2020). While secretory vesicles serve as storage for membrane proteins, such as integrins and selectins, neutrophil granules are loaded with specific anti-microbial and proteolytic proteins and whose physical size and content decreases progressively from primary to tertiary (Faurschou and Borregaard, 2003). Azurophilic granules mainly contain the characteristic myeloperoxidase (MPO) as well as defensins and the bactericidal permeability-increasing protein (BPI) (Dell'Angelica et al., 2000). In contrast, secondary granules typically contain lactoferrin (LTF) and tertiary granules gelatinase and matrix metalloproteinases (Borregaard and Cowland, 1997). In addition to neutrophil changes during maturation and differentiation, their exposure to environmental cues or even the mechanical stress from entering or leaving the blood circulation, can shape neutrophil behavior and heterogeneity (Wang and Doerschuk, 2002).

1.2.2 Neutrophils under inflammatory conditions

While neutrophils are patrolling in the bloodstream, tissue-resident cells, such as mast cells and a set of macrophages and DCs, serve as sentinels and are often the first to be exposed to PAMPs and DAMPs from invading pathogens or dying cells. They subsequently secrete pro-inflammatory mediators that activate the surrounding endothelium and direct leukocytes to the site of inflammation, among which neutrophils are typically the most rapidly recruited cells. (Medzhitov, 2008). Circulating neutrophils can then be captured by the selectins expressed on the activated endothelial cells and slow down until they finally arrest (Figure 1). This process is mainly mediated by the interaction of neutrophil receptors P-selectin glycoprotein ligand-1 (PSGL-1) and the glycoprotein CD44 with selectins as well as lymphocyte function-associated

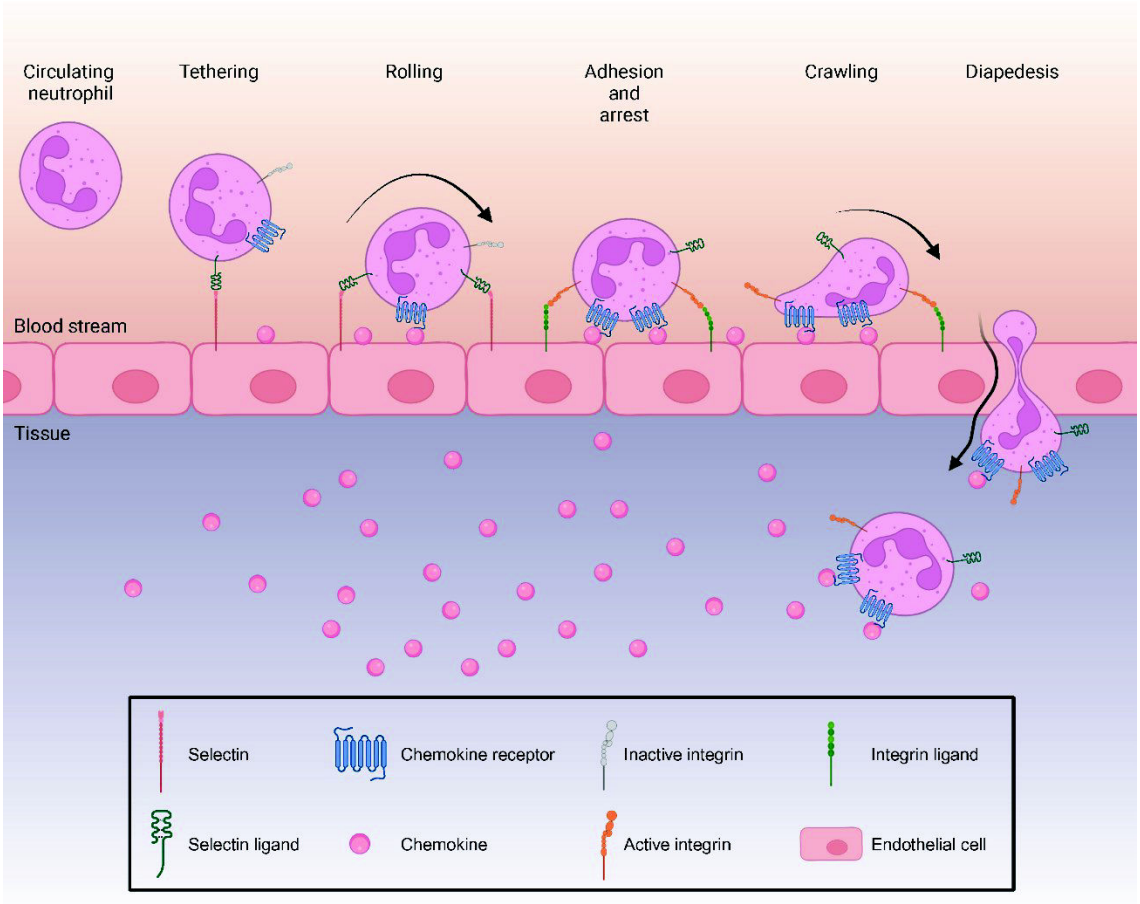

Figure 1: Sequential neutrophil recruitment from the vasculature into the inflamed tissue. The recruitment cascade is divided into the following step: Tethering of the circulating neutrophil in the blood stream; rolling on endothelial cells and activation; adhesion molecule-mediated arrest; crawling on endothelial cells; paracellular or transcellular diapedesis/transmigration from the vasculature into the tissue (paracellular shown here). Modified from (Nourshargh and Alon, 2014). Created with BioRender.com.

antigen 1 (LFA1) binding to intercellular adhesion molecule 1 (ICAM1) and ICAM2 (Nourshargh and Alon, 2014, Zarbock et al., 2011, Stadtmann et al., 2013).

The pro-inflammatory milieu generated by the resident cells or the direct contact with the activated endothelium stimulates the neutrophils, which in turn mobilize their cytoplasmic granules. While the contents of the tertiary granules are secreted, followed by those of the secondary and finally primary granules, the fusion of the secretory vesicles with the cellular membrane increases the arsenal of integrins and other transmembrane proteins that further enhance neutrophil functions (Faurschou and Borregaard, 2003, Summers et al., 2010). During extravasation, many of the adherent neutrophils extrude pseudopods to crawl along the endothelial cells and prepare for transmigration through the endothelial barrier, a process known as diapedesis. Neutrophils can conduct transmigration either paracellular through endothelial cell junctions or transcellular through the endothelial cell itself (Filippi, 2016, Rocheleau et al., 2016). Once entering the inflamed tissue, their navigation is dependent on the surrounding chemokine milieu, which is sensed via G-protein coupled receptors (GPCRs) on their cell surface. However, neutrophils are also capable of secreting chemoattractants

themselves, which act on the surrounding neutrophils and trigger a GPCR-mediated positive feedback mechanism. This enables the recruited neutrophils to communicate and allow a directed migration of the group, a process known as swarming (Mihlan et al., 2022). Finally, they reach the microbes or dying cells following target-derived attractants, such as formyl peptides which are sensed dominantly over regular cell-derived attractants (Witko-Sarsat et al., 2000).

As key players of innate immunity, neutrophils possess a remarkable arsenal of anti-microbial effector functions (Figure 2). During degranulation, neutrophils exocytose soluble granule

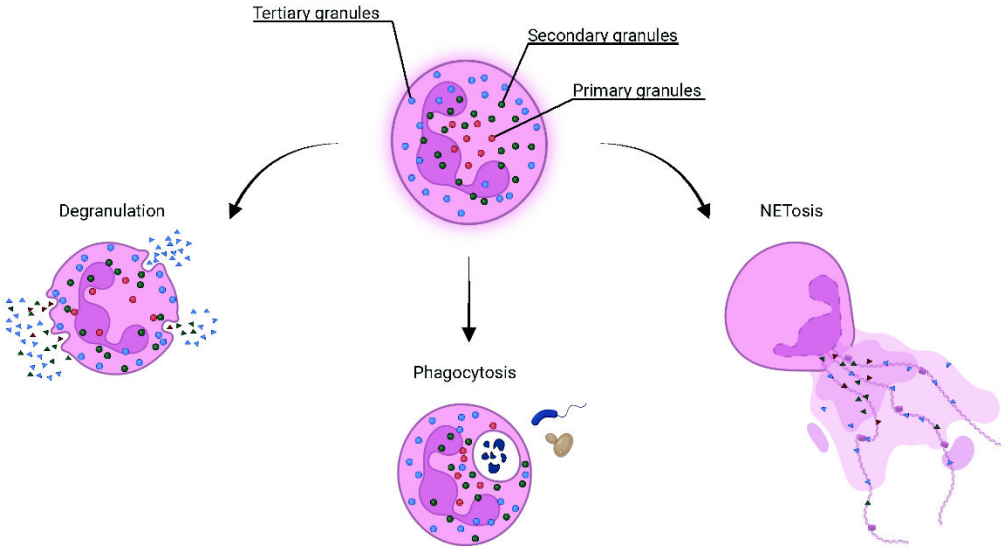

Figure 2: Neutrophil effector functions at sites of inflammation. Once activated, neutrophils start exocytosing anti-microbial substances stored in granules and released upon fusion with the cellular membrane. Tertiary granules are most rapidly mobilized, followed by secondary and primary granules. Receptor-mediated phagocytosis allows uptake of microbes or particles which are eliminated upon fusion of the phagosome with intracellular granules. The NETosis represents the last defense mechanism which can occur via lytic (shown here) or non-lytic mechanisms. In most cases neutrophils undergo suicidal NETosis with an explosive and membrane-rupturing release of NETs comprising the condensed chromatin and granule components. Modified from (Burn et al., 2021) and (Mollinedo, 2019). Created with BioRender.com.

protein, including extracellular matrix-degrading proteases, microbicidal peptides and reactive oxygen species (ROS) to generate a hostile environment that enhances the anti-microbial functions of proximal cells (Witko-Sarsat et al., 2000, El-Benna et al., 2016). Phagocytosis is a type of receptor-mediated endocytosis, including lectins and integrins, in which microbes are internalized. The internalization signal triggers the generation of ROS by activation of NADPH oxidase (NOX) and the mobilization of granules. Phagosome-granule fusion creates a lethal environment leading to the rapid elimination of most ingested microbes (DeLeo and Allen, 2020, Griffin et al., 1975). A special feature of neutrophils is their ability to form neutrophil extracellular traps (NETs), representing a final and lethal mechanism which is triggered by the enhanced ROS production. It induces an MPO-mediated escape of the neutrophil elastase (NE) from azurophilic granules and translocating into the nucleus. There, MPO and NE drive

chromatin decondensation synergistically and independent of their enzymatic activity (Papayannopoulos et al., 2010). Finally, NETs are explosively released by neutrophils comprising the condensed chromatin, anti-microbial mediators and enzymes in order to capture and eliminate microbes (Urban et al., 2009, Urban et al., 2006). In addition to the suicidal NETosis, in which the membrane ruptures during NET release, a non-lytic or vital NETosis also exists, which has been observed primarily in early recruited neutrophils. In this case, the condensed chromatin is expulsed in a controlled manner similar to degranulation leaving the cell membrane intact. The remaining envelope, the anuclear cytoplast, is still able to internalize microbes (Papayannopoulos, 2018, Yipp et al., 2012).

1.3 The tetraspanin superfamily

Tetraspanins (Tspans) are a family of integral membrane proteins that were discovered on human leukocytes but have progressively been found on almost all types of mammalian cells (Maecker et al., 1997, Oren et al., 1990a). With their four transmembrane domains, they form

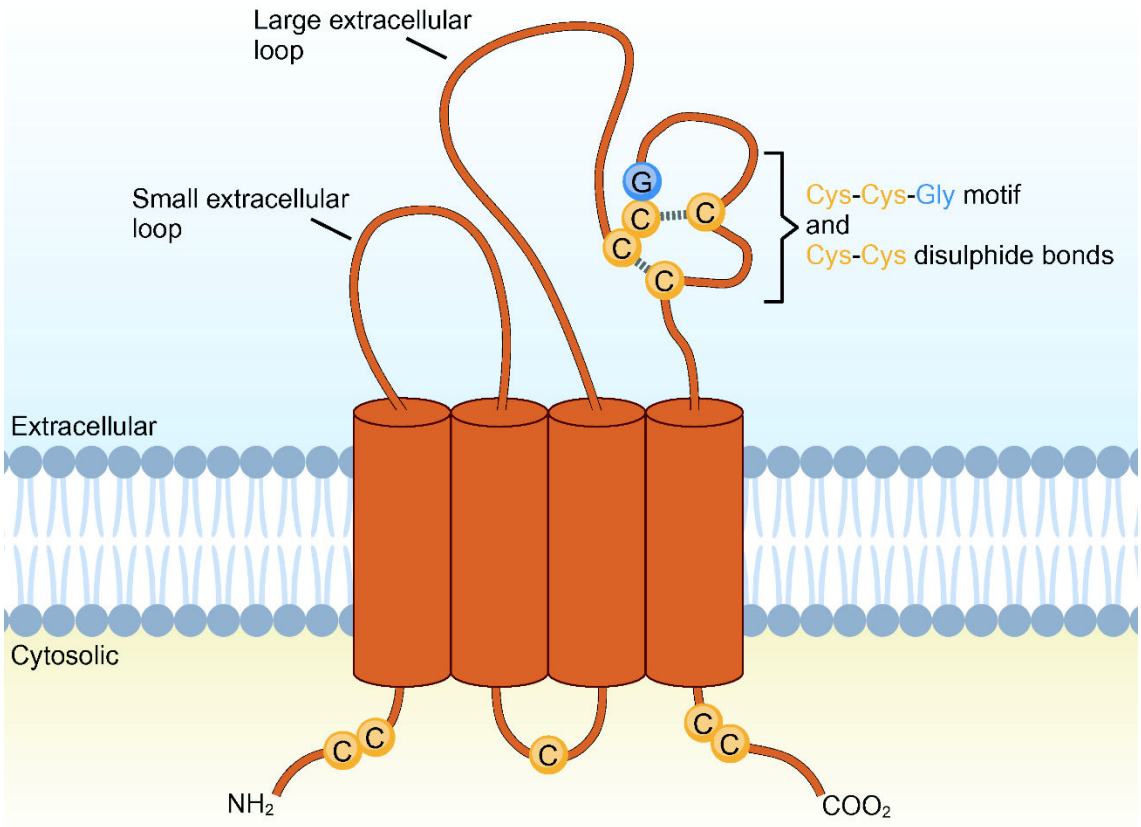

Figure 3: Illustration of the conserved Tspan structure. Tspans are found in cell membranes and contain four membrane-spanning domains. N- and C-termini are located intracellularly and have cysteine residues acting as potential palmitoylation sites. On the extracellular site they show a small and large loop, with the larger loop comprising an evolutionary conserved CCG-motif. Additional variable numbers of cysteines define the Tspan subfamily and shape their specificities. C (Cys, cysteine, yellow), G (Gly, glycine, blue), disulphide bonds (grey dashed line). Modified from (Levy and Shoham, 2005a). Created with BioRender.com.

a small and a large extracellular loop, as well as two short intracellular tails (Figure 3). Characteristic for the Tspan superfamily are a conserved CCG motif and two further cysteine residues within the large loop which form essential disulphide bonds (Stipp et al., 2003). Their structural composition allows them to interact in different ways which includes intramolecular interactions (Zimmerman et al., 2016), lateral associations with partner proteins and other Tspans or interaction with cytosolic proteins.

1.3.1 The tetraspanin web

While most immunomodulatory interactions of membrane proteins are limited to receptor-ligand associations, the Tspans serve as organizers of a variety of immune complexes in the membrane. Tspans interact in the membrane with their partner proteins while also associating with other Tspans and their respective partners, resulting in the formation of the so-called tetraspanin web (Rubinstein et al., 1996). As each cell typically expresses several different Tspans, the Tspan web is also cell type specific (Levy and Shoham, 2005b). While the Tspan web describes the network of Tspans and their interaction partners, the localization of this structure in the membrane, distinct from the well-known lipid rafts, is described as tetraspanin-enriched microdomains (Hemler, 2003).

1.3.2 Function in host immunity

Considering that each Tspan has its own expression profile and their interaction partners are highly cell type-dependent, they are involved in a variety of processes, including motility (Liu et al., 2007, Yeung et al., 2018), adhesion (Levy et al., 1998, Berditchevski, 2001), morphology (Furuya et al., 2005), proliferation (Franco et al., 2010), fertilization (Jankovičová et al., 2020) and cancer-associated functions (Wright et al., 2004b, Ono et al., 1999). Their functional roles are often described as being molecular facilitators that strongly influence the stability and functionality of immune complexes (Maecker et al., 1997). Before continuing with a breakdown of key involvements of various Tspans, the known Tspans are listed together with some of their functions in corresponding cell types and tissues (Table 1).

Table 1: Overview about functionalities of Tspan family members in mammals.

Tetraspanin	Cell type/ tissue	Function	Reference
Tspan1	Pancreatic cancer	Autophagy	(Zhou et al., 2021)

	Breast cancer	Proliferation, motility	(Wu et al., 2021)
Tspan2	Oligodendrocytes	Formation and stabilization of myelin sheath	(Birling et al., 1999)
	Lung cancer	Invasion, motility	(Otsubo et al., 2014)
	Pancreatic β-cells	Glucotoxicity-induced apoptosis	(Hwang et al., 2016)
Tspan3	Oligodendrocytes	Proliferation, migration	(Tiwari-Woodruff et al., 2004)
Tspan4	Glioblastoma	Proliferation, invasion	(Dong et al., 2024)
	Retinal pigmented epithelium	Migrasome formation, proliferation, migration	(Wu et al., 2022)
Tspan5	Endothelial cells	T lymphocyte transmigration	(Reyat et al., 2017)
	Hepatocellular carcinoma	Wound healing, migration, metastasis	(Xie et al., 2021)
Tspan6	Breast cancer	EV-mediated B cell recruitment	(Molostvov et al., 2023)
	Glioblastoma	Proliferation, metastasis	(Zhang et al., 2024)
Tspan7	Myeloma	Adhesion, transmigration	(Cheong et al., 2015)
Tspan8	Colorectal cancer	Proliferation, migration	(Zhang et al., 2020)
Tspan9	Gastric cancer	Proliferation, migration, invasion	(Li et al., 2016b)
Tspan10	Osteoclasts	Differentiation	(Zhou et al., 2014)

Tspan11	Osteoblasts	Adhesion	(Nakanishi et al., 2019)
Tspan12	Retinal vasculature	Development	(Junge et al., 2009)
Tspan13	Papillary thyroid cancer	Proliferation, Apoptosis	(Li et al., 2019)
Tspan14	Non-small cell lung carcinoma	-	(Jovanović et al., 2022)
Tspan15	Oesophageal squamous cell carcinoma	Metastasis	(Zhang et al., 2018)
Tspan16	-	-	-
Tspan17	Endothelial cells	T lymphocyte transmigration	(Reyat et al., 2017)
Tspan18	Prostate cancer	Metastasis	(Zhou et al., 2023)
Tspan19	-	-	-
Uroplakin-Ib (Tspan20)	Bladder epithelium	*E. coli* entry site	(Wu et al., 1996)
Uroplakin-Ia (Tspan21)	Bladder epithelium	*E. coli* entry site	(Wu et al., 1996)
Peripherin-2 (Tspan22)	Photoreceptor cells (rods and cones)	Photoreceptor complex formation	(Tebbe et al., 2020)
ROM-1 (Tspan23)	Photoreceptor cells (rods)	Disk morphogenesis, apoptosis	(Clarke et al., 2000)
CD151 (Tspan24)	Kidney, skin	Basement membrane integrity	(Karamatic Crew et al., 2004)
	T lymphocytes	Proliferation	(Wright et al., 2004a)

	Keratinocytes	Migration	(Wright et al., 2004a)
	NIH3T3	Adhesion	(Lammerding et al., 2003)
CD53 (Tspan25)	T and B lymphocytes	Trafficking/recirculation	(Demaria et al., 2020)
	B lymphocytes	Survival, development	(Greenberg et al., 2020)
CD37 (Tspan26)	T and B lymphocytes	T cell-B cell interaction	(Knobeloch et al., 2000)
	Neutrophils	Adhesion, (trans)migration	(Wee et al., 2015)
CD82 (Tspan27)	Macrophages	Infiltration, migration, activation, differentiation	(McGowan et al., 2022b)
	Hematopoietic stem and progenitor	Adhesion	(Termini et al., 2014)
	Non-small cell lung carcinoma	Migration	(Takahashi et al., 2007)
CD81 (Tspan28)	B lymphocytes	Activation, stabilization of immune signaling complexes	(Cherukuri et al., 2004)
	T and B lymphocytes	Proliferation	(Miyazaki et al., 1997)
	Hepatocytes, B lymphocytes	HCV entry site	(Pileri et al., 1998)
	Leukocytes	Migration	(Feigelson et al., 2003)
	Hepatocellular carcinoma	Invasion, migration	(Brimacombe et al., 2014, Mazzocca et al., 2008)

	Oocytes	Fertilization, gamete fusion	(Kaji et al., 2000, Le Naour et al., 2000)
CD9 (Tspan29)	Peripheral and central nervous system	Formation of paranodal junctions and compact myelin	(Ishibashi et al., 2004, Nakamura et al., 1996)
	Breast cancer, keratinocytes	Migration	(Jiang et al., 2013, Castro-Sanchez et al., 2010, Powner et al., 2011)
CD63 (Tspan30)	DCs	Migration	(Mantegazza et al., 2004)
Tspan31	Gastric cancer, Hepatocellular carcinoma	Proliferation, migration, apoptosis	(Ma et al., 2022, Wang et al., 2017)
Tspan32	T lymphocytes	Proliferation	(Lombardo et al., 2019)
Tspan33	B lymphocytes	Adhesion, migration	(Navarro-Hernandez et al., 2020)

1.3.2.1 Tspans in cell migration

Some members of the Tspan family, including CD9, CD37, CD63, CD81, CD82 and CD151 emerged to be key modulators of migration and adhesion processes in immune cells (Jiang et al., 2015, Yeung et al., 2018). Therefore, these Tspans need to associate with proteins that are indispensable for cell-cell and cell-extracellular matrix (ECM) adhesions as well as ECM and cytoskeletal remodeling (Friedl and Wolf, 2009). One of the best characterized family of interaction partners for Tspans are integrins which are crucial mediators of cell-cell and cell-ECM contacts (Berditchevski, 2001, Hynes, 2002). Regulation of cell migration by integrins can occur in different ways. CD151 has been shown to enhance migration capacities by modulating integrin internalization (Liu et al., 2007) but also to increase their ligand affinity (Nishiuchi et al., 2005). Beside integrin-mediated functions, CD9 can influence cell migration by regulating expression of MMP-9 (Jiang et al., 2013). Furthermore, CD81 and CD82 have been shown to act on the actin organization via regulation of the Rac/Rho signaling pathway, showing that Tspans comprise a multitude of mechanistics to regulate cell migration (Takahashi et al., 2007, Tejera et al., 2013). Less straight forward is the fact that Tspans can

both promote and inhibit a function on the same cell type, which can depend on a variety of factors. These include CD81 and CD9, both of which exert pro-migratory (Brimacombe et al., 2014, Castro-Sanchez et al., 2010) as well as anti-migratory (Mazzocca et al., 2008, Powner et al., 2011) influences on certain cancer cells under distinct environmental conditions.

1.3.2.2 Tspans in migration and recruitment

DCs are an essential component of the immune response, acting as a bridge between the innate and adaptive immune systems by shaping the specific T and B cell immune response through effective migration and antigen presentation (Yoneyama et al., 2005). Immature DCs express CD9, CD63, CD81, CD82 and CD151, all of which except CD151 affect interactions of DCs with their environment and reduce their chemokine-induced migration behavior (Mantegazza et al., 2004). In contrast, CD37-deficient neutrophils were unable to exert a directed movement towards a chemotactic gradient and showing an impaired adhesion to the β2 integrin ligand intercellular adhesion molecule-1 (ICAM-1), resulting in a reduced chemokine-induced adhesion and transmigration (Wee et al., 2015). A similar effect has been shown for CD151, whereas neutrophil migration capacity on fibronectin ECM *in vitro* abolished upon inhibition of CD151 (Yauch et al., 1998). In contrast, CD82 restrains the migration of neutrophils and macrophages and is for the latter important for normal morphology and activation. In addition, $CD82^{-/-}$ macrophages are unable to eliminate the parasite *Leishmania mexicana* as they are functionally impaired (McGowan et al., 2022a). Besides the influence of Tspans on leukocytes, they are also expressed on endothelial cells and can be decisive for efficient recruitment of leukocytes. For CD9 and CD151, it was shown that they associate laterally with ICAMs and vascular cell adhesion molecules (VCAMs) on the endothelial cell surface and that silencing of the two Tspans inhibits the adhesion and transmigration of recruited immune cells, as they fail to establish sufficient contact with the endothelium (Barreiro et al., 2005).

1.3.2.3 Tspans in infection

Interestingly, Tspans typically do not exhibit receptor-ligand-like functions, but can be misused as entry factors in the case of viral infections. This applies to CD151, and to a lesser extent to CD9 and CD63 in the case of human cytomegalovirus (HCMV) (Fast et al., 2017). A similar behavior emerges with human papillomavirus (HPV), where CD151 is the main mediator for HPV entry, while CD63 is responsible for viral trafficking and retrograde transport of viral DNA which subsequently leads to infection (Gräßel et al., 2016, Spoden et al., 2008, Fast et al., 2017). With increasing attention for Tspans, a crucial role for TEMs could also be attributed for

human immunodeficiency virus 1 (HIV-1) infection, featuring CD81 and CD63 during viral entry, assembly and intercellular spread (Suárez et al., 2018).

Tspans also play a decisive role in infection with a large number of bacteria. The intracellular *Listeria monocytogenes* infects epithelial cells via certain cellular receptors. CD81 is rapidly recruited to the *Listeria* entry site where it is thought to act as an organizer of the receptors and plays a crucial role in the internalization of the bacterium (Tham et al., 2010). Another intracellular bacterium, *Mycobacterium tuberculosis*, is able to survive and replicate in phagosomes of host cells. This involves the specific recruitment of CD63-positive lysosomes to the bacteria-containing phagosomes, which provides an escape mechanism for *M. tuberculosis* and simultaneously provides a source of nutrients (Seto et al., 2010). A similar behavior was observed during *Chlamydia* infection when trafficking of CD63-positive multivesicular bodies to bacteria-containing inclusion bodies provided essential lipids for maintenance of infection (Beatty, 2006). Another factor in the infection with gram-negative bacteria such as *Chlamydia* or *E. coli* is LPS, which is found in the bacterial cell wall and represents a potent inducer of inflammation. LPS binds to TLR4, which induces the expression of its co-receptor CD14 which is recruited to TLR4 to form a complex (Lu et al., 2008). However, CD9 prevents the formation of the LPS-receptor complex by associating with CD14. CD9-deficient mice that were subjected to intranasal challenge with LPS showed an overarching LPS-induced inflammation in the lung with strongly increased infiltration and production of proinflammatory mediators (Suzuki et al., 2009).

In addition to bacteria and viruses, fungi as well pose a serious threat, especially for immunocompromised patients. Following fungal infection, leukocytes express a number of anti-fungal receptors, including C-type lectins such as Dectin-1, whose loss is associated with a greatly increased susceptibility to fungal infections (Ferwerda et al., 2009). CD37, another member of the Tspan family, is essential for stabilization of Dectin-1 in the cell membrane of antigen-presenting cells and downstream interleukin-6 (IL-6) production upon Dectin-1-mediated phagocytosis (Meyer-Wentrup et al., 2007). In addition to the C-type lectins, cooperative recognition via TLRs, such as TLR4 and TLR2, are necessary to elicit a robust immune response against some fungi, such as *Candida albicans* and *Cryptococcus neoformans* (Dang et al., 2022, Netea et al., 2006).

Collectively, the strong involvement of Tspans in various viral, bacterial and fungal infections emphasizes their growing importance in various pathologically relevant processes during infection, including penetration, intracellular trafficking and modulation of a potent and balanced immune response.

1.4 Tetraspanin-2 structure and expression

After discovery of the Tspan family in 1990, further Tspans were discovered in different tissue types over the following years. This included the tetraspanin-2 (Tspan2) in 1998 by Todd et al. during a targeted screen for human Tspan consensus sequences in the expressed sequence tag (EST) database, which provided a source for molecular markers (Todd et al., 1998, Oren et al., 1990b). While the crystal structure of a full-length CD81 is known, only a predicted structure exists for Tspan2, as for most Tspans (Zimmerman et al., 2016). Nevertheless, Tspan2 and the two most well characterized Tspans CD9 and CD81 belong to the same paralogue group, which is why a functional similarity between these three Tspans is assumed (Garcia-España et al., 2008). Although right after the discovery of human Tspan2 its expression in rats was reported to be restricted to oligodendrocytes in the central nervous system (CNS) (Birling et al., 1999), Tspan2 expression was later shown in a variety of human cell lines, including hematopoietic, lymphoid, and carcinoma cell lines (Serru et al., 2000).

1.4.1 Tspan2 in the central nervous system

Oligodendrocytes are a crucial cellular component of the CNS generating myelin sheaths around axons to increase nerve conduction velocity (Stadelmann et al., 2019).

During the early development of the CNS Tspan2 gene expression peaks on myelin-forming oligodendrocytes and even upon myelination of axons Tspan2 gene expression remains in the myelin membrane. Tspan2 likely not only supports the myelination process around axons but additionally stabilizes the mature sheath (Birling et al., 1999). The Tspan CD9 is also expressed in rat oligodendrocytes, but with a less restricted expression pattern than its paralogue Tspan2, thus displaying a molecular link between CD9, Tspan2 and β1 integrin (Terada et al., 2002). While function of CD9 is suggested to be more supportive within this web, β1 integrins play indispensable roles during early development of oligodendrocytes (O'Meara et al., 2011).

The chemoattractant CXCL12 is primarily known to act in the immune system as a retention factor in the bone marrow, but it is also produced in the brain by glial cells and neurons and is considered an important factor in the neuro-immune interface (Guyon, 2014). During chronic neuroinflammation, microglia are continuously activated by proinflammatory stimuli and further worsen the situation by producing themselves additional inflammatory mediators finally resulting in neuronal death. The activation status is partially influenced by CXCL12, although Tspan2 modulates its transport and also binding efficacy to its receptor CXCR4, thereby also modulating microglial activation (Reynolds and Mahajan, 2020). In addition, the reduction in Tspan2 gene expression in microglial cells correlates with a reduction in expression of the highly anti-inflammatory cytokines IL-13 (Kolosowska et al., 2019) and IL-10 (Shemer et al.,

2020) and an increase of the pro-inflammatory tumor necrosis factor alpha (TNF-α) (Kleidonas et al., 2023, Reynolds and Mahajan, 2020).

1.4.2 Tspan2 in cancer

The mutation of p53, a tumor suppressor, is one of the main drivers of tumor development (D'Orazi, 2023). In human lung cancer, mutation of p53 is associated with increased gene expression of Tspan2, as well as increased invasiveness and motility of cancer cells (Otsubo et al., 2014). In addition, association of Tspan2 with CD44, an adhesion receptor (Idzerda et al., 1989), enhances its function as a ROS-scavenger supporting the tumor progressive phenotype. Knockdown, on the other hand, reduced metastasis to lung and liver (Otsubo et al., 2014).

1.4.3 Aim of the study

This doctoral thesis aims for the characterization of expression patterns and functions of Tspan2 in immune cells. For this purpose, transcriptional Tspan2 reporters and conventional gene knockout mice (Tspan2$^{-/-}$) were utilized. The use of the Tspan2 reporter mouse model allowed the identification of immune cells that express high levels of Tspan2. To determine Tspan2-dependent effector functions and underlying molecular mechanisms, state-of-the-art single cell RNA sequencing of neutrophils from the Tspan2$^{-/-}$ mouse model was employed followed by comprehensive omics data analysis. Finally, based on observations, specific anti-microbial functions and complex biological processes were further investigated using selected *in vitro* and *in vivo* studies.

2 Material

2.1 Disposable consumables

Table 2: List of single use consumables.

Consumables	Company
Acclaim PepMap100	Thermo Fisher Scientific, Waltham, USA
Acclaim PepMapRSLC	Thermo Fisher Scientific, Waltham, USA
Cell scraper	Greiner Bio-One International GmbH, Kremsmünster, AUT
Cell strainer (100 µm)	Corning, Brooklyn, USA
Corning HTS transwell-24 well permeable supports	Merck, Darmstadt, GER
Costor stripettes (1, 5, 10, 25, 50 ml)	Corning, Brooklyn, USA
Disposable hypodermic needle	Braun, Kronberg im Taunus, GER
Graduated (filter) tips	Starlab, Hamburg, GER
LS columns	Miltenyi, Bergisch Gladbach, GER
Medical examination gloves	Ansell, Richmond, AUS
Not-treated tissue culture dishes (100 x 20 mm)	Greiner Bio-One International GmbH, Kremsmünster, AUT
Not-treated tissue culture dishes (100 x 20 mm)	Sarstedt, Nümbrecht, GER
Sabouraud-Dextrose-GC-Agar Fertigplatten	Mast Group Ltd., Bootle, UK
Safe-lock tubes (0.5 ml, 2 ml, 5 ml)	Eppendorf, Hamburg, GER
Safe-lock tubes (1.5 ml)	Sarstedt, Nümbrecht, GER
Syringe	Braun, Kronberg im Taunus, GER
Tissue culture dishes (100 x 20 mm)	Corning, Brooklyn, USA
Tissue culture plates (6, 12, 24, 96 well)	Corning, Brooklyn, USA
Wiping cloth bucket	Schülke, Norderstedt, GER

2.2 Reagents, chemicals and buffers

Table 3: List of reagents, chemicals and buffers used.

Name	Company
1,2-dioleoyloxy-3-(trimethylammonium)propane (DOTAP)	Roche, Basel, CHE
10x EcoRI buffer	Thermo Fisher Scientific, Waltham, USA
10x Tango buffer	Thermo Fisher Scientific, Waltham, USA
5 carboxytetramethylrhodamine, succinimidyl ester (5-TAMRA SE)	Thermo Fisher Scientific, Waltham, USA
6x orange gel loading dye	Thermo Fisher Scientific, Waltham, USA
7-Aminoactinomycin (7AAD)	BD Biosciences, Franklin Lakes, USA
Ampicillin	Thermo Fisher Scientific, Waltham, USA
Bioparticles-texas red conjugate from staphylococcus aureus	Sigma Aldrich, St. Louis, USA
Biozym LE Agarose	Biozym Scientific, Hessisch Oldendorf, GER
CellTracker green	Thermo Fisher Scientific, Waltham, USA
ChromoTek GFP trap agarose beads	Proteintech, Illinois, USA
Collagenase	Roche, Basel, CHE
Complete protease inhibitor cocktail	Sigma Aldrich, St. Louis, USA
CountBright absolute counting beads	Thermo Fisher Scientific, Waltham, USA
Cytosine-phosphorothioate-guanosine (CpG) 2216	TIB Molbiol, Berlin, GER
Desoxyribonuclease (DNase) I	Roche, Basel, CHE
Dihydrorhodamine (DHR) 123	Thermo Fisher Scientific, Waltham, USA
Dimethyl sulphoxide (DMSO)	Sigma Aldrich, St. Louis, USA
eFluor 780	Thermo Fisher Scientific, Waltham, USA
Erylysis Buffer pH 7.2-7.4	Morphisto, Frankfurt, GER
Ethanol, absolute	VWR International, Radnor, USA
Fetal Calf Serum (FCS)	Pan, Aidenbach, GER
Glutamine	Biochrom, Cambridge, UK
HBSS	Thermo Fisher Scientific, Waltham, USA

HEPES	Thermo Fisher Scientific, Waltham, USA
JetPRIME buffer	Polyplus Transfection, Illkirch-Graffenstaden, FRA
Leukotriene B4 (LTB4)	Cayman Chemical, Michigan, USA
N-Formyl-Met-Leu-Phe (fMLP)	Merck, Darmstadt, GER
Penicillin/Streptomycin (P/S)	Biochrom, Cambridge, UK
Phenylmethylsulphonyl fluoride (PMSF)	Sigma Aldrich, St. Louis, USA
Phorbol myristate acetate (PMA)	Sigma Aldrich, St. Louis, USA
Pluronic F-127	Thermo Fisher Scientific, Waltham, USA
Polybrene	Merck, Darmstadt, GER
Quick load 1kb plus DNA ladder	NEB, Ipswich, USA
Recombinant murine PF-4 (CXCL4)	PeproTech, London, UK
Recombinant murine TNF-α	PeproTech, London, UK
Sodium azide (NaN_3)	Thermo Fisher Scientific, Waltham, USA
Sodium chloride (NaCl)	Thermo Fisher Scientific, Waltham, USA
Staphylococcus aureus Bioparticles opsonizing reagent	Thermo Fisher Scientific, Waltham, USA
SYTOX Green	Thermo Fisher Scientific, Waltham, USA
TRIS hydrochlorid (Tris-HCl)	Thermo Fisher Scientific, Waltham, USA
Triton X-100	Thermo Fisher Scientific, Waltham, USA
Trypan Blue Stain	Thermo Fisher Scientific, Waltham, USA
Type I bovine collagen	Nutacon, Leimuiden, NL
VLE DMEM medium	Sigma Aldrich, St. Louis, USA
VLE RPMI 1640 medium (w/o) Glu	Sigma Aldrich, St. Louis, USA
β-Mercaptoethanol	Thermo Fisher Scientific, Waltham, USA

2.3 Equipment/Instruments

Table 4: List of equipment used for experimental purposes or analysis.

Equipment	Company
BD FACSCanto II	BD Bioscience, Franklin Lakes, USA
Cell observer spinning disk	Zeiss, Oberkochen, GER
Heraeus Heracell 240 incubator	Heraeus, Hanau, GER
Laminar airflow workbench	BD Biosciences, Franklin Lakes, USA
LSM780 confocal laser scanning microscope	Zeiss, Oberkochen, GER
LSRFortessa	BD Biosciences, Franklin Lakes, USA
Milli-Q water	Merck, Darmstadt, GER
NanoDrop 1000 spectrophotometer	Peqlab Biotechnology, Erlangen, GER
NextSeq 2000 system	Illumina Inc., San Diego, USA
Orbitrap Fusion Lumos Tribrid mass spectrometer	Thermo Fisher Scientific, Waltham, USA
Rapid separation liquid chromatography system, ultimate 3000	Thermo Fisher Scientific, Waltham, USA
Rotanta 46 RC and 96 RC centrifuge	Hettich, Kirchlengern, GER
SilicaTip emitter	New Objective, Woburn, MA, USA
T25 digital ULTRA-TURRAX	IKA, Staufen, GER

2.4 Primer

Table 5: List of synthetic oligonucleotides used for molecular cloning.

Name	Sequence 5'-3'
Tspan2M1s-pWPXL_BamHI	AGGTTTAAACTACGGGATCC GCC ACC ATG GGG CGT TTT CGC GGG
Tspan2M1s-pWPXL-GFP_EcoRI	CTGAGCTCAACTTCGAATTC ATG GGG CGT TTT CGC GGG
Tspan2noStopas-pWPXL_MluI	GGTAGCGCTAGGACGCGT TGA GAT CAC ATC GCG TGA GT
Tspan2Stopas-pWPXL-GFP_NdeI	CCAGAGGTTGATTATCATATG TCA GAT CAC ATC GCG TGA GT

2.5 Plasmids

Table 6: List of plasmids purchased or generated by molecular cloning.

Name	Description	Company/Reference
pCMV-VSV-G	Encoding a VSVG glycoprotein for production of lentiviral particles; CMV promoter; Amp-resistance	Addgene, Watertown, USA
psPAX2	Encoding a Gag, Pol and Env for production of lentiviral particles; CMV promoter; Amp-resistance	Addgene, Watertown, USA
pWPXL-GFP-mut_kozak	Encoding an EGFP with mutated kozak sequence; EF-1alpha promoter; Amp-resistance	A kind gift from Elisabeth Kravets (lab of Klaus Pfeffer, Institute of Medical Microbiology and Hospital Hygiene, Heinrich Heine University Düsseldorf)
pWPXL-GFP-w/o-STOP	Encoding an EGFP without stop codon; EF-1alpha promoter; Amp resistance	A kind gift from Klaus Pfeffer (Kravets et al., 2012) (Institute of Medical Microbiology and Hospital Hygiene, Heinrich Heine University Düsseldorf)
pWPXL-EGFP-TSPAN2	Encoding an EGFP-Tspan2 fusion construct, N-terminal EGFP; EF-1alpha promoter; Amp resistance	Generated in this work, methods section 3.5.1
pWPXL-TSPAN2-EGFP	Encoding a Tspan2-EGFP fusion construct, C-terminal EGFP; EF-1alpha promoter; Amp resistance	Generated in this work, methods section 3.5.1

2.6 Enzymes

Table 7: List of enzymes used in context of molecular cloning and cDNA synthesis.

Name	Company
5x In-Fusion HD Enzyme Premix	Takara Biotechnology, Kyoto, Japan
BamHI	Roche, Basel, CHE
EcoRI	New England Biolabs, Massachusetts, USA

MluI	Roche, Basel, CHE
NdeI	Roche, Basel, CHE
Phusion High-Fidelity DNA Polymerase	Thermo Fisher Scientific, Waltham, USA

2.7 Cell lines

Table 8: List of cell lines that were received or generated.

Name	Origin
Human embryonic kidney (HEK) 293FT	Thermo Fisher Scientific, Waltham, USA
Mouse embryonic fibroblasts (MEF) 1117 mGBP2 WT	A kind gift from Julia Mock and Veronica Raba (lab of Klaus Pfeffer, Institute of Medical Microbiology and Hospital Hygiene, Heinrich Heine University Düsseldorf)
MEF-EGFP	A kind gift from Julia Mock and Veronica Raba (lab of Klaus Pfeffer, Institute of Medical Microbiology and Hospital Hygiene, Heinrich Heine University Düsseldorf)
MEF-EGFP-TSPAN2	Generated in this work, methods section 3.5.4

2.8 Pathogenic organisms

Table 9: List of pathogenic organisms used in *in vitro* and *in vivo* studies.

Strain	Origin
Candida albicans (Robin) Berkhout (ATCC MYA-2876), SC5314	A kind gift from the lab of Ursula Fleig (Institute for Functional Genomics of Microorganisms, Heinrich Heine University Düsseldorf)
Escherichia coli (DH5α), fhuA2 Δ(argF-lacZ)U169 phoA glnV44 ϕ80Δ(lacZ)M15 gyrA96 recA1 relA1 endA1 thi-1 hsdR17	American Type Culture Collection (ATCC), Manassas, Virginia, USA

2.9 Cell culture media

Table 10: List of cell culture media and their supplementation used for respective cell lines.

Name	Concentration/ Volume	Components
Bone marrow Flt3L-culture medium	500 ml	VLE RPMI 1640 medium (w/o) Glu
	10 %	Heat-inactivated FCS
	1 %	Glutamine
	1 %	Penicillin-streptomycin
	7.5-10 %	Flt3L supernatant
	50 µM	β-mercaptoethanol
Bone marrow GM-CSF-culture medium	500 ml	VLE DMEM medium
	10 %	Heat-inactivated FCS
	1 %	Penicillin-streptomycin
	4 %	GM-CSF supernatant
	50 µM	β-mercaptoethanol
Neutrophil medium	500 ml	VLE RPMI 1640 medium (w/o) Glu
	10 %	Heat-inactivated FCS
	1 %	Glutamine
	10 mM	HEPES
	50 µM	β-mercaptoethanol

2.10 Antibodies

Table 11: List of (conjugated) antibodies used for FACS staining.

Antibody	Reactivity	Isotype	Company
Alexa Fluor 700 rat anti-mouse/human CD11b, clone M1/70	Mouse, Human, Cynomolgus, Rhesus	Rat IgG2b, κ	BioLegend, San Diego, USA
APC rat anti-CD11b, clone M1/70	Mouse, Human	Rat IgG2b, κ	BD Biosciences, Franklin Lakes, USA

APC rat anti-mouse CD45R/B220, clone RA3-6B2	Mouse, Human	Rat IgG2a, κ	BD Biosciences, Franklin Lakes, USA
APC rat anti-mouse CD86, clone GL-1	Mouse	Rat IgG2a, κ	BioLegend, San Diego, USA
APC-Cy7 rat anti-CD11b, clone M1/70	Mouse, Human	Rat IgG2b, κ	BD Biosciences, Franklin Lakes, USA
BV421 rat anti-mouse Siglec-H, clone 440c	Mouse	Rat IgG2b, κ	BD Biosciences, Franklin Lakes, USA
BV421 anti-mouse Ly-6G, clone 1A8	Mouse	Rat IgG2a, κ	BioLegend, San Diego, USA
BV510 rat anti-mouse I-A/I-E (MHC II), clone M5/114.15.2	Mouse	Rat IgG2b, κ	BioLegend, San Diego, USA
BV605 anti-mouse Ly-6C, clone HK1.4	Mouse	Rat IgG2c, κ	BioLegend, San Diego, USA
BV650 anti-mouse CD317 (BST2, PDCA-1), clone 927	Mouse	Rat IgG2b, κ	BioLegend, San Diego, USA
BV711 hamster anti-mouse TCR β chain, clone H57-597	Mouse	Armenian Hamster IgG2, λ1	BD Biosciences, Franklin Lakes, USA
BV785 anti-mouse CD19, clone 6D5	Mouse	Rat IgG2a, κ	BioLegend, San Diego, USA
CD16/CD32 antibody, clone 96	Mouse	Rat / IgG2a, lambda	Thermo Fisher Scientific, Waltham, USA
PE anti-mouse/rat XCR1, clone ZET	Mouse, Rat	Mouse IgG2b, κ	BioLegend, San Diego, USA
PE CD317 (BST2, PDCA-1) Monoclonal Antibody, clone ebio129	Mouse	Rat IgG2b, κ	Thermo Fisher Scientific, Waltham, USA
PE rat anti-CD11b, clone M1/70	Mouse, Human	Rat DA, IgG2b, κ	BD Biosciences, Franklin Lakes, USA
PE-Cy7 hamster anti-mouse CD11c, clone N418	Mouse	Armenian Hamster IgG	BioLegend, San Diego, USA

PE-Cy7 hamster anti-mouse CD11c, clone HL3	Mouse	Armenian Hamster IgG1, λ2	BD Biosciences, Franklin Lakes, USA
FITC anti-mouse F4/80, clone BM8	Mouse	Rat / IgG2a, kappa	Thermo Fisher Scientific, Waltham, USA
BV421 anti-mouse NK-1.1, clone PK136	Mouse	Mouse IgG2a, κ	BioLegend, San Diego, USA
PerCP-Cy5.5 anti-mouse Ly-6G, clone 1A8	Mouse	Rat IgG2a, κ	BioLegend, San Diego, USA
PerCP-Cy5.5 hamster anti-mouse CD3ε, clone 145-2C11	Mouse	Armenian Hamster IgG1, κ	BD Biosciences, Franklin Lakes, USA
PerCP-Cy5.5 rat anti-mouse CD19, clone 1D3	Mouse	Rat IgG2a, κ	BD Biosciences, Franklin Lakes, USA
TotalSeq A0301 anti-mouse hashtag 1-6	Mouse	Rat IgG2a, κ/Rat IgG2b, κ	BioLegend, San Diego, USA

2.11 Commercial Kits

Table 12: List of Kits used.

Name	Company
Chromium Single Cell 3' NextGEM Reagent Kit v3.1	10xGenomics, California, USA
Neutrophil Isolation Kit, mouse	Miltenyi, Bergisch Gladbach, GER
Nucleospin Gel and PCR Clean-up kit	Macherey-Nagel, Düren, GER
Nucleospin Plasmid (no lid) Kit	Macherey-Nagel, Düren, GER
Plasmid DNA purification Maxi kit	Macherey-Nagel, Düren, GER

2.12 Buffers and solutions

Table 13: List of buffers and solutions with their respective composition.

Name	Concentration/ Volume	Components/Company
Digestion buffer	1.86 ml	PBS
	120 µl	DNase I
	20 µl	Collagenase
Dulbecco's Phosphate-Buffered Saline (PBS)		Thermo Fisher Scientific, Waltham, USA
FACS Buffer	500 ml	1x PBS
	2 %	FCS
	2 mM	EDTA
Lysis Buffer (in dH_20)	100 mM	Tris HCl, pH 7.4
	1.5 M	NaCl
	0.2 %	NaN_3
	1 %	Triton X-100
	40 µl/ml	Protease inhibitor cocktail
	10 µl/ml	PMSF
MACS Buffer	500 ml	1x PBS
	0.5 %	FCS
	2 mM	EDTA
RNA Sequencing Buffer	50 ml	PBS
	0.04 %	BSA
Solvent B (in dH_20)	0.1 %	Formic acid
	84 %	Acetonitrile
STOP buffer	500 ml	PBS
	10 mM	EDTA

2.13 Software

Table 14: List of software used for data analysis.

Software	Company
Adobe Acrobat Reader DC	Adobe Inc., San José, USA
Adobe Illustrator	Adobe Inc., San José, USA
FACS Diva	BD Biosciences, Franklin Lakes, USA
FlowJo v10	BD Biosciences, Franklin Lakes, USA
Geneious	Biomatters, Auckland, NZL
GraphPad Prism 9	GraphPad, San Diego, USA
Imaris Bitplane	Oxford Instruments, Abingdon, UK
Zen blue	Zeiss, Oberkochen, GER
10X Genomics CellRanger v7.0	10xGenomics, California, USA
R package ClusterProfiler v4.10.0	(Yu et al., 2012)
R package SingleR v2.4.1	(Aran et al., 2019)
R v4.3.2 and RStudio	(R Core Team, 2021), (RStudio Team, 2019)
Proteome Discoverer v2.4.1.15	Thermo Fisher Scientific, Waltham, USA
R package Seurat v5.0.1	(Hao et al., 2023)

3 Methods

3.1 Mice

Conventional Tspan2 gene knockout (Tspan2$^{-/-}$) mice (de Monasterio-Schrader et al., 2013) have been described previously (Yaseen et al., 2017) and were maintained in the animal facility of the University of Münster and the Heinrich Heine University of Düsseldorf. Newly generated bacterial artificial chromosome (BAC) transgenic mice were genetically engineered encoding an EGFP under an artificial Tspan2 promoter (unpublished). Mice were maintained in the animal facility of the University of Münster.

All mice in this work were maintained on a C57BL/6J background and housed under at least specific pathogen free (SPF) conditions. Procedures including animals were approved by the government of North-Rhine Westphalia (81-02.04.2022.A322). Experiments with the mentioned genotypes were performed with age and sex matched wild type (WT) littermates. Where indicated, Tspan2$^{-/-}$ mice were challenged intraperitoneally (i.p.) for 4 hours or intravenously (i.v.) for up to 30 days with *Candida albicans*.

3.2 Bone marrow isolation

Femur and tibia were isolated from a mouse using forceps and scissors sterilized in ethanol prior to use. After removing fur, feet, surrounding muscles and tissues the cleaned bones were placed in sterile phosphate buffered saline (PBS, Gibco). For sterilization, the bones were placed in sterile 70 % ethanol for 3 minutes and then returned into fresh PBS. Bones were further opened with a sterile scissor at the knee-side and placed with the open end down in a bottom-pierced 0.5 ml Eppendorf tube. Bone-containing tubes were placed in 1.5 ml tubes and centrifuged for 15 seconds at >10,000 x g. Bones were discarded and bone marrow (BM)-containing 1.5 ml tubes were kept to perform erythrocyte lysis for 3 minutes in erythrocyte lysis buffer (Morphisto). Erythrocyte lysis was stopped by adding 10 ml FCS-containing PBS. After centrifugation for 5 minutes at 300 x g BM cell suspension was filtered through a 100 µm cell strainer (Corning). After additional centrifugation and counting of the cells using a hemocytometer, BM cell suspension was used for further purposes.

3.3 Tspan2 gene expression in lymphoid tissues

3.3.1 Cell preparation from spleen and lymph nodes

Spleen, inguinal and mesenteric lymph nodes were isolated from Tspan2 reporter mice. Organs were further shred using forceps and digested in a DNase/collagenase-containing digestion buffer for 30 minutes at 37 °C. Subsequently, 5 ml STOP buffer (PBS supplemented

with 10 mM EDTA) was added to interrupt the digestion process followed by homogenization of cell suspensions. After filtering through a 70 µm cell strainer (Falcon) cells were centrifuged at 300 x g for 5 minutes and the supernatant was discarded. Only spleen-derived cell suspensions were additionally lysed in 3 ml erythrocyte lysis buffer (Morphisto) for 3 minutes. Erythrocyte lysis was stopped with PBS, the suspensions were centrifuged and resuspended in 5 ml RPMI-1640 medium to count cells. Cell suspensions from lymph nodes and spleens were used for downstream analysis.

3.3.2 Tspan2 gene expression pattern analysis

To determine the Tspan2 expression pattern among immune cell populations derived from different lymphoid tissues, cells were isolated from the BM, spleen, inguinal and mesenteric lymph nodes from Tspan2 reporter mice as described above in 3.2 and 3.3.1. For identification of Tspan2/EGFP-expressing cell populations ex vivo the following fluorophore-labeled antibodies were used upon treatment with anti-CD16/32 (1:50, eBioscience/Thermo, 93) to block Fc receptors: BV421-NK1.1 (1:150, BioLegend, PK136), Amcyan/BV510-anti-mouse I-A/I-E (1:100, BioLegend, M5/114.15.2), BV605-Ly6C (1:200, BioLegend), BV650-BST2/CD317 (1:100, BioLegend, 927), BV711-TCRβ (1:100, BD Biosciences, H750-597), BV785-CD19 (1:100, BioLegend, 6D5), FITC (Tspan2/EGFP), PE-XCR1 (1:100, BioLegend, ZET), PE-Cy7-CD11c (1:150, BioLegend, N418), PerCP-Cy5.5-Ly6G (1:150, BioLegend, 1A8), APC-B220/CD45R (1:100, BD Biosciences, RA3-6B2), AlexaFluor700-CD11b (1:200, BioLegend, M1/70). For staining of dead cells eFluor 780 (1:5000, eBioscience) was applied. All stainings for flow cytometry were prepared in PBS supplemented with 2 mM EDTA and 2 % FCS.

The following immune cells populations were identified upon single, live pregating: T cells ($CD19^-$, $TCR\beta^+$), B cells ($CD19^+$, $TCR\beta^-$), NK cells ($CD19^-$, $TCR\beta^-$, $CD45R/B220^-$, $NK1.1^+$), cDC1s ($CD19^-$, $TCR\beta^-$, $CD11c^{int\text{-}high}$, $MHCII^+$, $CD11b^-$, $XCR1^+$), cDC2s ($CD19^-$, $TCR\beta^-$, $CD11c^{int\text{-}high}$, $MHCII^+$, $CD11b^+$, $XCR1^-$), pDCs ($CD19^-$, $TCR\beta^-$, $CD11c^{int\text{-}high}$, $CD11b^-$, $XCR1^-$, $CD45R/B220^+$, $BST2/CD317^+$), Neutrophils ($CD19^-$, $TCR\beta^-$, $CD11c^{neg\text{-}int}$, $CD11b^+$, $Ly6G^+$), Monocyte/Macrophages ($CD19^-$, $TCR\beta^-$, $CD11c^{neg\text{-}int}$, $CD11b^+$, $Ly6G^-$). Flow cytometry acquisition was performed for all experiments on FACSFortessa (LSRFortessa, BD Biosciences).

3.4 Tspan2 gene expression *in vitro*

In order to determine the gene expression of Tspan2 in conventional and plasmacytoid dendritic cells (cDCs, pDCs) upon stimulation, BM cells isolated from Tspan2 reporter mice were isolated as described in 3.2 and cultured with Flt3L or GM-CSF.

3.4.1 Flt3L-culture

20 x 10^6 BM cells were cultured on 100 mm not-treated tissue culture dishes (Greiner) in 10 ml VLE RPMI 1640 medium (w/o) glutamine supplemented with 10 % FCS (Pan), 1 % glutamine (Biochrom), 1 % penicillin-streptomcyin (P/S, Biochrom), 50 µM β-mercaptoethanol (Thermo) and 7.5-10 % Flt3L supernatant to drive cDC and pDC differentiation (day 0). On day 5 half of the medium was replaced by fresh medium. Cells were placed at 4 °C for 30 minutes prior to harvesting using a cell scraper (Greiner) on day 7 and 0.5 x 10^6 were stimulated with 1 µM cytosine-phosphorothioate-guanosine (CpG) 2216 (TIB Molbiol) for 16 hours. To identify Tspan2/EGFP-expressing DCs the following fluorophore-labeled antibodies were used upon treatment with anti-CD16/32 (1:50, eBioscience/Thermo, 93) to block Fc receptors: APC-B220/CD45R (1:100, BD Biosciences, RA3-6B2), APC-Cy7-CD11b (1:100, BD Biosciences, M1/70), PE-BST2/CD317 (1:100, Thermo, ebio129), PE-Cy7-CD11c (1:100, BD Biosciences, HL3), BV421-Siglec-H (1:100, BD Biosciences, 440c), Amcyan/BV510-anti-mouse I-A/I-E (1:100, BioLegend, M5/114.15.2), PerCP-Cy5.5-CD3ε (1:100, BD Biosciences, 145-2C11), PerCP-Cy5.5-CD19 (1:100, BD Biosciences, 1D3). For staining of dead cells 7-Aminoactinomycin (7AAD, 10 µl/ml, BD Biosciences) was applied. All staining for flow cytometry were prepared in PBS supplemented with 2 mM EDTA and 2 % FCS.
The following immune cells populations were identified upon single, live-nonBT pregating: cDCs ($CD11c^+$, $B220^-$, $CD11b^+$), pDCs ($CD11c^+$, $B220^+$, $CD11b^{-\ to\ low}$). Flow cytometry acquisition was performed on FACSCanto II (BD Biosciences).

3.4.2 GM-CSF culture

2 x 10^6 BM cells were cultured on 100 mm not-treated tissue culture dishes (Sarstedt) in 10 ml VLE DMEM medium supplemented with 10 % FCS (Pan), 1 % P/S (Biochrom), 50 µM β-mercaptoethanol (Thermo) and 4 % GM-CSF supernatant to drive cDC differentiation (day 0). Further, 10 ml fresh medium was added on day 3 and half of the medium was replaced by fresh medium on day 6. On day 9 cells were placed at 4 °C for 30 minutes prior to harvesting using a cell scraper (Greiner). 0.5 x 10^6 cells were stimulated with 1 µM CpG 2216 (TIB Molbiol) for 16 hours. To identify Tspan2/EGFP-expressing DCs the following fluorophore-labeled antibodies were used upon treatment with anti-CD16/32 (1:50, eBioscience/Thermo, 93) to block Fc receptors: APC-CD86 (1:100, BioLegend, GL-1), APC-Cy7-CD11b (1:100, BD Biosciences, M1/70), PE-Cy7-CD11c (1:100, BD Biosciences, HL3), Amcyan/BV510-anti-mouse I-A/I-E (1:100, BioLegend, M5/114.15.2), PerCP-Cy5.5-CD3ε (1:100, BD Biosciences, 145-2C11), PerCP-Cy5.5-CD19 (1:100, BD Biosciences, 1D3). For staining of dead cells 7-Aminoactinomycin (7AAD, 10 µl/ml, BD Biosciences) was applied. All staining for flow cytometry were prepared in PBS supplemented with 2 mM EDTA and 2 % FCS.

The following immune cells populations were identified upon single, live-nonBT pregating: DCs ($CD11c^+$, $MHCII^+$). Flow cytometry acquisition was performed on FACSCanto II (BD Biosciences).

3.5 Generation of Tspan2 overexpressing cell lines

3.5.1 Molecular cloning

In order to generate a Tspan2 gene expression plasmid Tspan2-encoding sequence was inserted in the mammalian lentiviral expression plasmid pWPXL (Addgene). The Tspan2-encoding sequence was inserted in frame with the EGFP-encoding sequence at N- or C-terminal ends. The following expression plasmids were constructed:

1. pWPXL-EGFP-TSPAN2: This expression plasmid expresses an EGFP-Tspan2 fusion construct under control of an EF-1alpha promoter. The Tspan2-encoding sequence was cloned to the C-terminus of the EGFP-encoding sequences including a 32-base pair (bp) spacer sequence between *Egfp* and Tspan2 gene sequences.

2. pWPXL-TSPAN2-EGFP: This expression plasmid expresses a Tspan2-EGFP fusion construct under control of an EF-1alpha promoter. The Tspan2-encoding sequence was cloned to the N-terminus of the EGFP-encoding sequences including a 32 bp spacer sequence between *Egfp* and Tspan2 gene sequences.

3.5.1.1 Amplification of Tspan2 with site specific overhangs via PCR

To generate pWPXL-EGFP-TSPAN2 (N-terminal EGFP) and pWPXL-TSPAN2-EGFP (C-terminal EGFP) expression plasmids, the Tspan2-encoding sequence was amplified from murine lung cDNA by polymerase chain reaction (PCR). Tspan2M1s-pWPXL-GFP_EcoRI and Tspan2Stopas-pWPXL-GFP_NdeI were used as primers (section 2.4) to amplify the Tspan2 gene with overhangs specific for pWPXL-GFP-w/o-STOP plasmids (N-terminal *Egfp*) and Tspan2M1s-pWPXL_BamHI and Tspan2noStopas-pWPXL_MluI primers generating overhangs specific for pWPXL-GFP-mut_kozak plasmids. Both plasmids were kindly provided by the research group of Klaus Pfeffer (Institute of Medical Microbiology and Hospital Hygiene, Heinrich Heine University Düsseldorf).

Table 15: PCR program for the amplification of the Tspan2 gene fragment for pWPXL-GFP-w/o-STOP (666 bp + 41 bp) and pWPXL-GFP-mut_kozak (666 bp + 38 bp).

Cycle step	Temperature	Duration
Initial Denaturation	95 °C	3 min
Denaturation	95 °C	30 sec
Annealing	56 °C	30 sec
Extension	72 °C	30 sec
Final Extension	72 °C	10 min
Hold	4 °C	∞

3.5.1.2 Purification of PCR products

To allow efficient insertion of the gene of interest into target plasmids, PCR products containing the Tspan2-encoding sequence with site-specific overhangs for cloning into pWPXL-plasmids were applied on a 1 % agarose gel. The PCR products were excised under UV light and purified using a Nucleospin Gel and PCR Clean-up kit (Macherey-Nagel) following the manufacturers recommendations. The purified PCR products were directly used for homologous recombination or frozen at -20 °C.

3.5.1.3 Digestion of the pWPXL empty plasmids

To generate the desired Tspan2 gene expression plasmids, the empty pWPXL-GFP-w/o-STOP and pWPXL-GFP-mut_kozak plasmids were linearized to allow insertion of the Tspan2 gene amplification constructs by homologous recombination. For digestion of pWPXL-GFP-mut_kozak the restriction enzymes BamHI (Roche) and MluI (Roche) in combination with 10x Tango buffer were used to achieve maximum enzyme activity. For digestion of pWPXL-GFP-w/o-STOP the restriction enzymes EcoRI (BioLabs) and NdeI (Roche) were used with EcoRI buffer. The appropriate buffer system was applied using the recommendation of the DoubleDigest Calculator (Thermo Fisher Scientific).

Table 16: Double digestion of the pWPXL-GFP-mut_kozak empty plasmid.

Reagent	Digestion of pWPXL-GFP-mut_kozak [µl]
BamHI	3
MluI	3
10x Tango buffer	10
Plasmid DNA	4
ddH_2O	30
Total volume	**50**

Table 17: Double digestion of the pWPXL-GFP-w/o-STOP empty plasmid.

Reagent	Digestion of pWPXL-GFP-w/o-STOP [µl]
EcoRI	1.5
NdeI	3
EcoRI buffer	10
Plasmid DNA	4
ddH_2O	31.5
Total volume	**50**

Samples were incubated at 37 °C for 2 hours. The digestion reaction was stopped by incubation of the samples at 80 °C for 10 minutes to thermally inactivate the restriction enzymes. To confirm successful digestion and purify linearized plasmids, samples were loaded on a 1 % agarose gel as described in the following section 3.5.1.4.

3.5.1.4 Purification of linearized plasmids

Linearized plasmids pWPXL-GFP-mut_kozak and the pWPXL-GFP-w/o-STOP were applied on an 1 % agarose gel and as described in 3.5.1.2 excised under UV light and purified using a Nucleospin Gel and PCR Clean-up kit (Macherey-Nagel) following the manufacturers recommendations. Purified linearized plasmids were directly used for homologous recombination or frozen at -20 °C.

3.5.1.5 Homologous recombination

In order to generate the desired Tspan2 gene expression plasmids described in 3.5.1 homologous recombination was induced to hybridize the linearized plasmids with the insert containing site-specific overhangs. The reaction was enzymatically assisted using the 5x In-Fusion HD Enzyme Premix (Takara Biotechnology). Plasmid and insert were mixed in a molar ratio of 1:2, respectively. The reactions were incubated at 50 °C for 15 minutes at the following conditions.

Table 18: Approach to generate the desired Tspan2 gene expression plasmids via enzyme assisted homologous recombination.

Reagent	**1:2 (plasmid:insert) total ratio [µl]**	**1:2 (plasmid:insert) total ratio [µl]**
ddH_2O		
Plasmid	150 ng	150 ng
Insert	20 ng	40 ng
5x In-Fusion HD Enzyme Premix	2	2
Total volume	**10**	**10**

3.5.1.6 Plasmid transformation and amplification using *Escherichia coli*

With the aim to confirm successful generation of Tspan2 gene expression plasmids, 100 µl of chemically competent *E. coli* DH5α bacteria were treated with 2.5 µl purified plasmid DNA and incubated at 4 °C for 30 minutes. Afterwards the bacteria were heat-shocked at 42 °C for 1 minute and immediately placed back at 4 °C for 2 minutes. Then 400 µl Luria-Bertani (LB) broth was added to the bacteria followed by incubation at 37 °C for 45 minutes. For selective growth of bacteria successfully transformed with ampicillin resistance cassette containing Tspan2 gene expression plasmids, bacteria were plated on ampicillin containing LB agar plates. *E. coli* were grown over night at 37 °C.

In order to amplify transformed recombinant plasmids, several single colonies were picked and grown in glass tubes with 4 ml resistance containing LB broth (100 µg/ml ampicillin) shaking over night at 37 °C.

3.5.1.7 Analysis of Tspan2 gene expression plasmids

Bacteria cultures were further analysed for recombinant plasmids containing the previously described inserts. Therefore, the Nucleospin Plasmid (no lid) Kit (Macherey-Nagel) was used following the manufacturer's recommendations. Concentration of eluted plasmid DNA was measured via NanoDrop (Peqlab). Plasmids from individual bacterial colonies were digested with insert-matching restriction enzymes as described in 3.5.1.3. Every sample was supplemented with 6x orange gel loading dye (NEB) and loaded together with quick load 1kb plus DNA ladder (NEB) on a 1 % agarose gel. Insert-specific sizes of the bands were calculated using the geneious software in a virtually performed digestion. Two clones that were found positive for recombinant plasmids were amplified in a larger batch in *E. coli* bacteria. Plasmid DNA was then isolated and purified from the bacteria using the plasmid DNA purification Maxi kit (Macherey-Nagel). Plasmid DNA concentration was determined via Nanodrop.

3.5.2 Cultivation of HEK and MEF cell lines

Human embryonic kidney (HEK) cells and mouse embryonic fibroblasts (MEF) 1117 mGBP2 WT (kindly provided by Julia Mock and Veronica Raba from the Lab of Klaus Pfeffer, Institute of Medical Microbiology and Hospital Hygiene, Heinrich Heine University Düsseldorf) were cultured in Dulbecco's Modified Eagle Medium (DMEM, Gibco) supplemented with 10 % FCS (Pan), 2 mM L-glutamine (Biochrom) and 0.05 mM β-mercaptoethanol (Gibco) in a humidified cell culture specified incubator at 37 °C using 10 % CO_2.

3.5.3 Lentivirus production in HEK cells

For lentivirus production 3 x 10^6 HEK cells were seeded in 10 ml HEK cell medium (as described in 3.5.2) in 100 mm petri dishes (Corning) and grown overnight to achieve a confluence of 70-80 % at the time point of transfection. Transient transfection with 3.75 µg PAXII, 1.25 µg VSV-G and 5 µg pWPXL-EGFP-TSPAN2 or pWPXL-TSPAN2-EGFP was prepared in 500 µl jetPRIME buffer (Polyplus) for each plate. Transfection procedure was performed according to the manufacturer's recommendation. Afterwards HEK cells were incubated at 37 °C to allow lentivirus production. After two days the lentivirus-containing supernatant was harvested, aliquoted after removing big particles via passing through a 0.45 µm filter and frozen at -80 °C until use.

3.5.4 Lentiviral transduction of MEFs

For lentiviral transduction, 2.5 x 10^4 mouse embryonic fibroblasts (MEFs) were seeded in 24 well plates (Corning) and allowed to grow overnight. When cells reached confluence of

70-80 % on the next day, the supernatant was removed and replaced with lentivirus-containing supernatant and 5 µl/ml polybrene (Millipore). Cells were allowed to acclimatize for 30 min at 37 °C followed by centrifugation for 90 minutes at 300 x g at 30 °C. Afterwards, cells were placed back in an incubator at 37 °C. After 4-6 hours cell supernatant containing virus particles was replaced with fresh medium and plates were further incubated for 24-72 hours. Morphology and fluorescence of transduced cells were checked on a daily basis. After at least three passages, cells were subjected to fluorescence-activated cell sorting to purify EGFP-expressing cells. Sorted MEFs were expanded in cell culture and stored in liquid nitrogen until use.

3.6 Mass spectrometry screen

3.6.1 Co-immunoprecipitation

To enrich proteins that associate with EGFP-Tspan2 and EGFP, respectively, they were subjected to co-immunoprecipitation (co-IP). Therefore, approximately 1 x 10^7 MEFs stably expressing EGFP-Tspan2 and EGFP, respectively (as described in 3.5.4), were washed two times with PBS and lysed using lysis buffer containing 100 mM TRIS hydrochlorid (Tris-HCl, pH 7.4), 1.5 M sodium chloride (NaCl), 0.2 % sodium azide (NaN_3), 1 % triton X-100, 40 µl/ml protease inhibitor cocktail and 10 µl/ml Phenylmethylsulfonyl fluoride (PMSF). Lysis was performed for 30 minutes at 4 °C followed by centrifugation at 14,000 x g for 10 minutes at 4 °C and transfer of the clear supernatant to a fresh precooled tube. Cleared lysates were stored at -20 °C until use. Co-immunoprecipitation was performed using ChromoTek GFP Trap Agarose beads (Proteintech) following the manufacturer's recommendations.

3.6.2 LC-MS/MS analysis

The co-IP samples from five replicates of the EGFP-Tspan2 and EGFP (as described in 3.6.1) with a volume of about 45 µl, respectively, were processed using the single-pot, solid-phase-enhanced sample preparation (SP3) protocol modified according to Hughes et al. (Hughes et al., 2019) and essentially as described by Lenz and Stühler (Lenz and Stühler, 2022). Label-free peptide/protein identification and quantification was performed using nanoscale liquid chromatography coupled to tandem mass spectrometry (nanoLC-MSMS) in data-dependent acquisition (DDA) mode. Separation of peptides was performed on a Rapid Separation Liquid Chromatography System (Ultimate 3000, Thermo Fisher Scientific). Therefore, peptides were concentrated on a trap column (Acclaim PepMap100, Thermo Fisher Scientific) followed by peptide separation on an analytical column (Acclaim PepMapRSLC, Thermo Fisher Scientific). Separation was performed at 60 °C and a 2 hour gradient from 4 to 40 % solvent B (0.1 % formic acid, 84 % acetonitrile).

Eluted peptides were processed via a nano-source electron spray ionization (ESI) interface equipped with distally coated SilicaTip emitters (New Objective) into the online-coupled Orbitrap Fusion Lumos Tribrid mass spectrometer (Thermo Fisher Scientific) which was equipped with a field asymmetric ion mobility spectrometry (FAIMS) interface. Precursor mass spectra were recorded in the orbitrap analyzer within a scan range of 375–1500 m/z and a resolution of 120,000. MS2 spectra were recorded with rapid scan rate in the ion trap.

3.6.3 Protein identification and quantification

Mass spectrometry (MS) data analysis was performed using the Proteome Discoverer software (version 2.4.1.15, Thermo Fisher Scientific) and 55341 mus musculus protein entries from the UniProtKB (downloaded on 18 January 2022). Tryptic specificity was applied, allowing two missed cleavages, with fixed carbamidomethylation at cysteine residues and variable modifications for methionine oxidation and N-terminal acetylation. Peptides and proteins were identified with a 1 % false discovery rate (FDR) using a decoy database.
Statistical analysis was performed using the "R" programming language (v4.0.4), following the approach by Sinatra et al. (Sinatra et al., 2022), after removing potential contaminants and reverse hits. Protein intensities were normalized by median $\log_2$(fold change), and differential protein abundance between EGFP-Tspan2 and EGFP was assessed using the Significance Analysis of Microarrays (SAM) method (Tusher et al., 2001) within the Siggenes R package. For this approach, a minimum of four valid values had to be present per protein group in at least one group (EGFP-Tspan2 or EGFP), data were $\log_2$-transformed to reach a normal distribution like data structure, and missing values were filled in with random values from samplewise downshifted normal distributions (0.3 standard deviation (s.d.) width, 1.8 s.d. downshift).

3.7 Neutrophil isolation from murine bone marrow

For the isolation of neutrophils from a BM cell suspension (as described in 3.2), the magnetic activated cell sorting (MACS)-based neutrophil isolation kit (Miltenyi) was used. Up to 5 x 10^7 BM cells, isolated as previously described, were centrifuged for 10 minutes at 300 x g and 4 °C. For labeling and sorting, the manufacturer's recommendations were followed unless stated elsewhere. In addition, the labeled BM cells were loaded onto a LS column for magnetic separation via a sterile filter. Unlabeled cells that passed through were collected representing the enriched neutrophils and were used for all assays with purified neutrophils. Neutrophil purity was determined by flow cytometry. Cells were treated with anti-CD16/32 (1:50, eBioscience/Thermo, 93) for blocking and subsequently stained with APC-CD11b (1:150, BD Biosciences, M1/70) and BV421-Ly6G (1:150, BioLegend, 1A8). Dead cells were stained via

7AAD (10 µl/ml, BD Biosciencess) or eFluor 780 (1:5000, eBioscience). Flow cytometry acquisition was performed for all experiments on FACSFortessa (LSRFortessa, BD Biosciences).

3.8 Single cell RNA sequencing

3.8.1 Sample preparation for single cell RNA sequencing

BM neutrophils were purified from WT and Tspan2$^{-/-}$ mice and neutrophil purity and viability was confirmed as described in 3.7. Cells were washed two times in PBS supplemented with 2 mM EDTA and 2 % FCS. Upon an additional blocking step for 10 minutes at 4 °C, 2 x 10^6 purified neutrophils were subjected to labeling with TotalSeqTMA0301 anti-mouse Hashtag 1-6 antibodies (1:200, BioLegend) in PBS supplemented with 2 mM EDTA and 2 % FCS for 30 minutes at 4 °C. Unique hash tag oligos (HTOs) were used for WT (HTOs 1-3) and KO (HTOs 4-6) samples. Hashed samples were washed two times and resuspended in 500 µl PBS supplemented with 0.04 % BSA before pooling replicates of each genotype. WT and KO pools were centrifuged at 300 x g for 5 minutes and resuspended to 800 cells/µl with a total of 160,000 cells. Single cell RNA (scRNA) sequencing was performed in collaboration with Tobias Lautwein at the Biological and Medical Research Center (BMFZ, Heinrich Heine University Düsseldorf).

3.8.2 Single cell library generation

For generation of single cell libraries, a total of ~75,000 cells were used as input for the single-cell droplet libraries generation on the 10X Chromium Controller system utilizing the Chromium Single Cell 3’ NextGEM Reagent Kit v3.1 (10xGenomics, California, USA) according to manufacturer’s instructions. Sequencing was performed on a NextSeq 2000 system (Illumina Inc. San Diego, USA) with a mean sequencing depth of ~50,000 reads/cell.

3.8.3 Processing of 10X Genomics single cell data

Raw sequencing data was processed using the 10X Genomics CellRanger software (v7.0). Raw BCL-files were demultiplexed and processed to Fastq-files using the CellRanger mkfastq pipeline. Alignment of reads to the mm10 genome and UMI counting was performed via the CellRanger count pipeline to generate a gene-barcode matrix.

3.8.4 Filtering and demultiplexing

Analysis of the sequencing datasets were performed in R version 4.3.2 (R Core Team, 2021) and Seurat version 5.0.1 (Hao et al., 2023). Gene-barcode matrices and antibody capture information from WT and KO sequencing runs were loaded into R. Gene-barcode matrices were used to set up Seurat objects to which antibody capture information were added in an independent assay. For quality control gene-barcode data were filtered for mitochondrial gene counts greater than 5 % (Osorio and Cai, 2020) and cells that show amounts of unique features less than 500 or more than 5000 due to decreased features per cell correlation (*subset = nFeature_RNA > 500 & nFeature_RNA < 5000 & percent.mt < 5)*. Before analysing HTO representation, WT and KO objects were normalized using centered log-ratio (CLR) transformation. Cells of both datasets were independently demultiplexed using the *HTODemux()* method to assess HTO counts in the categories negatives, singlets and doublets followed by retaining exclusively singlets for downstream analysis.

3.8.5 Data integration

After quality control both data sets were normalized and scaled using the *SCTransform()* method. Furthermore, they were integrated into a single data set based on 1500 features selected by an algorithm of the *SelectIntegrationFeatures()* function followed by running *PrepSCTIntegration()*, *FindIntegrationAnchors()* and *IntegrateData()* resulting in one data set comprising WT and KO information.

3.8.6 Dimensional reduction and clustering

In order to reduce dimensionality a principal component analysis (PCA) was performed using *RunPCA()*. For subsequent uniform manifold approximation and projection (UMAP) using *RunUMAP()* dimensionality was reduced to 15 principal components. For final clustering *FindNeighbors()* was run followed by *FindClusters()* with a resolution of 0.4 resulting in a total of 16 clusters.

3.8.7 Identification of neutrophil maturation stages

To separate the purified neutrophils from possible contaminants an annotation approximation of the cluster was performed using SingleR v2.4.1 (Aran et al., 2019). As reference for annotation the built-in celldex MouseRNAseq database was used. Prior to downstream analysis all non-neutrophils were removed. In recent publications canonical markers were published to closely define and annotate neutrophil subpopulations in RNA sequencing data sets (Kim et al., 2022, Grieshaber-Bouyer et al., 2021, Xie et al., 2020). Considering this

knowledge gene expression of *Ifitm2, Ifitm3, Ifitm6, Gngt2, Gm2a, Fgl2, Csf3r, Il1b, Ccl6, Cxcl2, Mmp8, Retnlg, Camp, Ngp, Ltf, Chil3, Fcnb, Tuba1b, Mpo, Prtn3, Elane, Rpl12* was visualised for all clusters in a dot plot using the *Dotplot()* method.

3.8.8 Identification of DEGs

In order to identify differentially expressed genes (DEGs) among all neutrophils (Tspan2$^{-/-}$ compared to WT) and its maturation stages, the *FindMarkers()* function with bonferroni correction was used (test.use = “MAST”) which calculated adjusted p-values considering the total numbers of genes present. Differences in the transcriptome of Tspan2-deficient neutrophils were visualized in a ComplexHeatmap showing DEGs that represented highest and lowest fold changes (avg_log2FC). From these, top 30 most significant DEGs were determined and annotated. Investigating transcriptomic differences between KO and WT neutrophils at different maturation stages, DEGs were calculated for each neutrophil subcluster and visualized in volcano plots using the ggplot2 package. Top 30 DEGs with lowest p-values were annotated whereas DEGs with a p-value < 0.05 and an average fold change > 0.3 were annotated as upregulated genes, those with a p-value < 0.05 and an average fold change < -0.3 as downregulated genes. Considering that neutrophil transcriptome changes during maturation und normal conditions, highly significant DEGs that are either shared or unique for a specific neutrophil maturation state, a venn diagram was designed using the VennDiagram package. DEGs were individually weighted for their impact and a limited number was visualized within the diagram.

3.8.9 Gene ontology (GO) and gene set enrichment analysis (GSEA)

Functional analyses were performed using the R package clusterProfiler v4.10.0 (Yu et al., 2012). For gene ontology (GO) analysis correlation of significant DEGs (adjusted p-value < 0.05) with biological process associated gene sets were investigated. For visualization terms were sorted for their adjusted p-values followed by representation of the top 15 terms. Gene set enrichment analysis (GSEA) of Kyoto Encyclopedia of Genes and Genomes (KEGG) and GOs were performed using a pre-ranked list of significant DEGs for their adjusted p-values and gene sets comprising less than 20 terms were excluded from the analysis (minGSSize = 20). Most impactful terms of the results were visualized in gseaplots with respective normalized enrichment scores (NES) and false discovery rates (FDR).

3.8.10 Code availability statement

The R code used for the scRNA sequencing analysis in this dissertation is hosted on GitHub (https://github.com/MarcelMarson/scRNA-seq-of-Tspan2-deficient-neutrophils).

The repository is currently private but will be made publicly available upon publication of the associated data.

3.9 Neutrophil *in vitro* assays

3.9.1 Neutrophil kill assay

To investigate the capacity of neutrophils to eliminate *Escherichia coli* bacteria *in vitro*, purified Tspan2$^{-/-}$ and WT neutrophils were mixed with *E. coli* DH5α which were cultured until their late log phase (OD_{600} ≈ 0.9). Bacterial concentration was estimated using the chem.aligent optical density calculator (chem.aligent.com). To calculate the precise concentration for later analysis 1 µl of bacterial culture was 10^3-10^7 diluted in PBS, washed and plated on Luria-Bertani (LB) agar plates to count colonies after 16 hours at 37 °C. From estimated concentrations 10^5/10^6/5 x 10^6 bacteria/ml were prepared for co-cultivation with 10^6 purified neutrophils/ml. Neutrophils were acclimatized in a flat bottom not tissue culture treated 96 well plate for 30 minutes at 37 °C to allow attachment to the surface. Afterwards, bacteria were added to the neutrophils, the plates were centrifuged at 300 x g for 10 minutes and further incubated for 2 hours. As control bacteria were incubated without any neutrophils. After incubation, serial dilutions were prepared and plated on LB agar plates for 16 hours at 37 °C. On the next day colonies were counted and the percent of killing [%] was calculated using the colony forming units (CFUs) via the following formula:

$$Percent\ of\ killing\ [\%] = \left(\frac{CFU_{-Neutrophils} - CFU_{+Neutrophils}}{CFU_{-Neutrophils}}\right) * 100$$

3.9.2 Quantification of neutrophils intracellular ROS

In order to analyse the capacity of neutrophils from Tspan2$^{-/-}$ and WT mice to produce reactive oxygen species (ROS), 1 x 10^7 purified neutrophils/ml were allowed to acclimatize in a flat bottom not tissue culture treated 96 well plate (Corning) for 15 minutes at 37 °C. Subsequently cells were treated with 2 µM dihydrorhodamine 123 (DHR-123, Invitrogen) and stimulated with either DMSO (Sigma Aldrich) or 150 nM PMA (Sigma Aldrich). Over a period of 5 minutes, the neutrophils were allowed to oxidize the uncharged and non-fluorescent DHR 123 to the cationic and green fluorescent rhodamine 123. The reaction was stopped immediately after 5 minutes by transferring the plate to 4 °C. The amount of intracellular ROS was measured via the correlating intensity of fluorescent rhodamine 123 using flow cytometry (LSRFortessa, BD Biosciences).

3.9.3 Quantification of neutrophil NET formation

To investigate the capacity of Tspan2$^{-/-}$ and WT neutrophils to efficiently undergo neutrophil extracellular trap (NET) formation, 2 x 10^6 purified neutrophils/ml were allowed to acclimatize in a flat bottom not tissue culture treated 96 well plate for 15 minutes at 37 °C. Subsequently neutrophils were treated with 200 nM SYTOX Green (Invitrogen) and stimulated with either DMSO or 150 nM PMA. Cells were allowed to form NETs over a period of 2 hours at 37 °C, which were labeled with the nucleic acid dye SYTOX Green. Afterwards, the fraction of SYTOX Green positive signals were measured using flow cytometry (LSRFortessa, BD Biosciences).

3.9.4 Quantification of neutrophil phagocytosis

For the quantification of neutrophil phagocytosis, 2 x 10^6 purified neutrophils/ml from WT and Tspan2$^{-/-}$ mice were allowed to acclimatize in a flat bottom not tissue culture treated 96 well plate for 15 minutes at 37 °C. Furthermore, they were treated with 25 µg/ml of the pH-sensitive pHrodo E. coli (Invitrogen) and stimulated with either DMSO or 150 nM PMA. Subsequent to stimulation, cells were incubated for 1 hour at 37 °C. Phagocytosis was stopped by transferring the plate at 4 °C. To determine purity and quantify phagocytosing neutrophils they were stained as described in section 3.7 followed by flow cytometry analysis (LSRFortessa, BD Biosciences).

3.9.5 Under-agarose chemotaxis assay

Neutrophil migration capacity along a gradient of chemoattractants was investigated in an under-agarose chemotaxis assay (Heit and Kubes, 2003). Agarose gels were allowed to polymerize in 10 mm tissue culture dishes (Corning). Upon polymerization, wells with approximately 4 mm diameter were punched into the gel for the chemoattractant mixture. Four additional responder wells were punched surrounding the chemoattractant well with an approximate 3 mm distance using a template to ensure reliable technical replications.

For competitive analyses 2 x 10^7 cells/ml WT and Tspan2$^{-/-}$ purified neutrophils were labeled with either 0.5 µM CellTracker Green (CMFDA, Thermo Fisher Scientific) or 10 µM 5-carboxytetramethylrhodamine, succinimidyl ester (5-TAMRA SE, Thermo Fisher Scientific) for 25 minutes in PBS supplemented with 0.0002 % pluronic F-127 (Thermo Fisher Scientific) and pooled afterwards.

In addition, the dye combination was reversed to rule out unspecific effects. The central well was loaded with a 20 µl mixture of chemoattractants comprising 1 µM Leukotriene B 4 (LTB4, Cayman) and 1 µM murine CXCL2 (PeproTech). Surrounding responder wells in the agarose layer were loaded with 20 µl of a 1:1 ratio of the differentially labelled WT and Tspan2$^{-/-}$ neutrophils, in total 10^5 cells in 10 % FCS and 2 mM L-glutamine in phenolred-free RPMI

medium. Neutrophils were allowed to migrate for 4 hours underneath the agarose layer. End-point images were taken using a spinning-disk confocal microscope (Cell Observer SD system, Carl Zeiss, with a CSU-X1 confocal scanner unit, Yokogawa and an AxioObserver Z1 inverted microscope stand) equipped with a stage-top incubator (Tokai-Hit) or a LSM780 fluorescence confocal microscope (Zeiss). For image acquisition a Plan-Apochromat 10× 0.45 objective and multiple-tiles function in ZEN software were used. Tiles were stitched using ZEN blue software (Carl Zeiss Microscopy).

Neutrophil migration from the responder well towards the chemoattractant was measured using Imaris software (Bitplane). The displacement represents the distance from the responder well border to the end-point location of respective cells that migrated underneath the agarose layer. Displacement value were calculated for each migrated neutrophil. In addition, total numbers of cells found between the responder well border and the chemoattractant well were taken. In rare cases, neutrophils did not respond to the chemoattractant or were found in very few numbers, thus leading to the exclusion of the corresponding technical replicate.

This study was performed in close cooperation with Katharina Glaser (Max Planck Institute of Immunobiology and Epigenetics, Freiburg, Germany)

3.9.6 Swarming

In order to investigate neutrophil swarming behaviour in WT and Tspan2$^{-/-}$, manufactured microscale arrays of bioparticles clusters were used as described (Reátegui et al., 2017). For experimental pattern design, texas red bioparticle conjugates of *Staphylococcus aureus* (SA, Sigma Aldrich) were applied. In each experimental well single patterns had a diameter of 130 µm. Coating of wells was performed with 10 % SA-opsonization reagent (Thermo Fisher Scientific) and 10 µg/ml fibronectin in FCS for 1 hour followed by three washes with PBS.

2 x 10^7 cells/ml WT and Tspan2$^{-/-}$ purified neutrophils were labeled with either 0.5 µM CellTracker Green or 10 µM 5-TAMRA SE for 25 minutes in PBS supplemented with 0.0002 % pluronic F-127 and pooled afterwards. Neutrophil mixtures were pre-activated with 50 ng/ml TNF alpha (PeproTech) for 10 minutes followed by resuspension in 1 mg/ml type I bovine collagen (Nutacon) at a concentration of 2 x 10^6 cells/ml. For swarming, 180 µl of the neutrophil gel suspension was applied into each well and incubated for 2 to 3 hours at 37 °C before acquisition. Images were acquired at 10× magnification using the confocal spinning-disk microscope system as described above.

This study was performed in cooperation with Katharina Glaser (Max Planck Institute of Immunobiology and Epigenetics, Freiburg, Germany)

3.9.7 Transmigration capacity of neutrophils

3.9.7.1 Transmigration assays using Tspan2 reporter mice

In order to investigate whether Tspan2 has an impact on the transmigration mechanism of neutrophils, heterogeneous suspensions consisting of Tspan2-positive and Tspan2-negative purified neutrophils from Tspan2 reporter were used. For this purpose, neutrophil medium with either DMSO (Sigma Aldrich) or 1 µM N-Formylmethionyl-leucyl-phenylalanine (fMLP, Merck) was directly applied to the wells of a flat bottom not tissue culture treated 96 well plate followed by the placement of 6.5 mm transwell inserts with a 3.0 µm pore polycarbonate membrane (Merck) into the wells. 4×10^6 purified neutrophils/ml were loaded into each insert and transmigration was allowed for 4 hours at 37 °C. The reaction was then stopped at 4 °C for 10 minutes to loosen cells attached to the membrane. The inserts were removed and the cells that transmigrated into the wells were collected for flow cytometry analysis. Tspan2-positive and -negative fractions of transmigrated neutrophils were quantified by flow cytometry (LSRFortessa, BD Biosciences).
To determine purity and quantify Tspan2-positive and -negative fractions of transmigrated neutrophils they were stained as described in section 3.7 and quantified by flow cytometry (LSRFortessa, BD Biosciences).

3.9.7.2 Transmigration assays using Tspan2-deficient mice

Using purified neutrophils from Tspan2-deficient mice, 4×10^6 neutrophils/ml were processed as described above in section 3.9.7.1 and upon collection stained as described in section 3.7. For quantification of total neutrophil numbers which transmigrated, stained cells were resuspended in 250 µl and mixed with 50 µl of CountBright Absolute Counting Beads (Invitrogen). For data analysis, absolute numbers of defined neutrophils ($CD11b^+$ $Ly6G^+$) were correlated with absolute numbers of counting beads by flow cytometry (LSRFortessa, BD Biosciences). Exact numbers of transmigrated neutrophils were calculated as described in the manufacturer's protocol.

3.10 *In vivo* studies

3.10.1 Model of systemic candidiasis

C. albicans (SC5314) glycerol stocks were streaked on Sabouraud agar plates supplemented with gentamycin and chloramphenicol (Sabouraud^{+GC}, Mast) to form colonies at 30 °C for 24-48 hours. Single isolated colonies were cultured in 25 ml Sabouraud broth in a shaking incubator at 30 °C overnight. Fungi were washed extensively in PBS and resuspended at the desired concentration. 1×10^5, 5×10^5 or 1×10^6 *C. albicans* were administered i.v. in 100 µl

PBS in the dorsal tail vein of WT and Tspan2$^{-/-}$ mice (day 0). Animals were weighted and monitored on a daily basis. Animals that passed critical values in an animal welfare scoresheet or lost 20 % of their initial weight were sacrificed via cervical dislocation. Experiments continued for up to 30 days until surviving mice were sacrificed.

3.10.2 Model of intraperitoneal inflammation

C. albicans were grown as described in 3.10.1. 1 x 10^5 *C. albicans* were administered i.p. in 100 µl PBS into WT and Tspan2$^{-/-}$ mice which were sacrificed after 4 hours. The peritoneal cavity was washed twice with 5 ml PBS supplemented with 5 mM EDTA. Inflammatory infiltrates were collected from peritoneal lavage fluid. For identification of immune cell populations the following fluorophore-labeled antibodies were used upon treatment with anti-CD16/32 (1:50, eBioscience/Thermo, 93) to block Fc receptors: FITC-F4/80 (1:100, eBioscience/Thermo, BM8), BV421-NK1.1 (1:150, BioLegend, PK136), Amcyan/BV510-anti-mouse I-A/I-E (1:100, BioLegend, M5/114.15.2), BV605-Ly6C (1:200, BioLegend), BV650-BST2/CD317 (1:100, BioLegend, 927), BV711-TCRβ (1:100, BD Biosciences, H750-597), BV785-CD19 (1:100, BioLegend, 6D5), FITC (Tspan2/EGFP), PE-XCR1 (1:100, BioLegend, ZET), PE-Cy7-CD11c (1:150, BioLegend, N418), PerCP-Cy5.5-Ly6G (1:150, BioLegend, 1A8), APC-B220/CD45R (1:100, BD Biosciences, RA3-6B2), AlexaFluor700-CD11b (1:200, BioLegend, M1/70). For staining of dead cells eFluor 780 (1:5000, eBioscience) was applied. All stainings for flow cytometry were prepared in PBS supplemented with 2 mM EDTA and 2 % FCS.

The following immune cells populations were identified upon single, live pregating: T cells (CD19$^-$, TCRβ$^+$), B cells (CD19$^+$, TCRβ$^-$), NK cells (CD19$^-$, TCRβ$^-$, CD45R/B220$^-$, NK1.1$^+$), cDC1s (CD19$^-$, TCRβ$^-$, CD11c$^{int\text{-}high}$, CD11b$^-$, XCR1$^+$), cDC2s (CD19$^-$, TCRβ$^-$, CD11c$^{int\text{-}high}$, CD11b$^+$, XCR1$^-$), pDCs (CD19$^-$, TCRβ$^-$, CD11c$^{int\text{-}high}$, CD11b$^-$, XCR1$^-$, CD45R/B220$^+$, BST2/CD317$^+$), Neutrophils (CD19$^-$, TCRβ$^-$, CD11c$^{neg\text{-}int}$, CD11b$^+$, Ly6G$^+$), Ly6C^{high} Monocytes (CD19$^-$, TCRβ$^-$, CD11c$^{neg\text{-}int}$, CD11b$^+$, Ly6G$^-$, Ly6C^{high}, F4/80^{low}), resident Macrophages (CD19$^-$, TCRβ$^-$, CD11c$^{neg\text{-}int}$, CD11b$^+$, Ly6G$^-$, Ly6C^{low}, F4/80^{high}). Flow cytometry acquisition was performed for all experiments on LSRFortessa (BD Biosciences).

3.11 Statistics

Statistics were performed using GraphPad Prism 9 software. Either an unpaired two-tailed t-test, a one-way or two-way ANOVA was used, which is mentioned in the figure description of the respective experiments. Significances were determined and are shown based on the following p-values: ≥ 0.05 (ns), < 0.05 (*), < 0.01 (**), < 0.001 (***), < 0.0001 (****).

4 Results

Tetraspanins (Tspans) comprise a superfamily of transmembrane proteins that exhibit the ability to substantially modulate the functions of a variety of cells (Boucheix and Rubinstein, 2001, Hemler, 2005, Levy et al., 1998, Maecker et al., 1997, Tarrant et al., 2003). Although a range of Tspans are known to be expressed by different tissues and cell types, little is known about their specific expression patterns and their actual roles (Yaseen et al., 2017). One of the Tspans we have very limited knowledge about is the Tspan2, which has been identified and studied in oligodendrocytes of the central nervous system (Birling et al., 1999, de Monasterio-Schrader et al., 2013). CD9 has been shown to be located in Tspan-enriched microdomains of the cell membrane together with ß1 integrin, CD81 and Tspan2 in rat brain oligodendrocytes potentially creating an interactive signalling network with these proteins (Terada et al., 2002). Analysis of the Tspan2 genome revealed high sequence homology with CD9 and CD81, thus Tspan2, CD9 and CD81 are considered to be functionally related (Bassani and Cingolani, 2012, Garcia-España et al., 2008). CD9 and CD81 are two of the best characterized tetraspanins, while Tspan2 is poorly characterized, especially in the immune system (Bond et al., 2020, Furuya et al., 2005, Hong et al., 2014, Quast et al., 2011, Rubinstein et al., 1996, Ullah et al., 2019, Vences-Catalán et al., 2015).

Utilising transcriptional reporter and loss-of-function mouse models, we show Tspan2 gene expression in lymphoid organs, with neutrophils representing the predominant Tspan2 gene-expressing fraction. In addition, state-of-the-art single-cell transcriptome analyses enable the identification of potentially modulated processes, which are validated in downstream *in vitro* and *in vivo* studies.

4.1 Neutrophils show highest Tspan2 gene expression

The expression profile of Tspan2 has so far been limited primarily to oligodendrocytes, as well as some tumours and cell lines that have been investigated (Hwang et al., 2016, Otsubo et al., 2014, Birling et al., 1999). However, in particular the situation in the immune system remains unclear. To address this question among others in this doctoral thesis, transcriptional Tspan2 reporter animals were utilised and bone marrow (BM), spleen as well as inguinal and mesenteric lymph nodes were assessed for their Tspan2/EGFP expression by flow cytometry. Furthermore, a gating strategy with carefully chosen markers was established to allow identification of different immune cell populations (Figure 4). Using the all/single/live cell gate as the shared pre-gate, the following immune cells populations were identified: T cells ($CD19^-$, $TCR\beta^+$), B cells ($CD19^+$, $TCR\beta^-$), NK cells ($CD19^-$, $TCR\beta^-$, $NK1.1^+$), cDC1s ($CD19^-$, $TCR\beta^-$, $NK1.1^-$, $CD11c^{int\text{-}high}$, $MHCII^+$, $CD11b^-$, $XCR1^+$), cDC2s ($CD19^-$, $TCR\beta^-$, $NK1.1^-$, $CD11c^{int\text{-}high}$, $MHCII^+$, $CD11b^+$, $XCR1^-$), pDCs ($CD19^-$, $TCR\beta^-$, $NK1.1^-$, $CD45R/B220^+$, $BST2/CD317^+$),

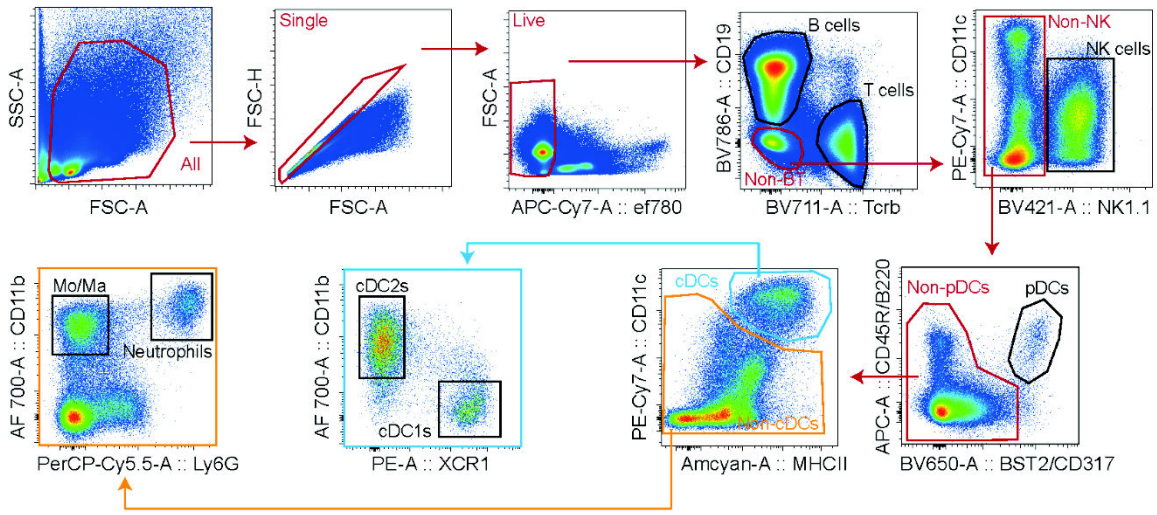

Figure 4: Gating strategy for identification of immune cell population among lymphoid organs. The gating strategy is shown for splenocytes from Tspan2 reporter mice and is representative for immune cell gating of all spleen and BM samples. Colored gates and arrows (red, blue, orange) indicate further downstream gating.

Neutrophils (CD19^{-}, TCRβ^{-}, NK1.1^{-}, CD11c$^{neg\text{-}int}$, CD11b^{+}, Ly6G^{+}) and Monocyte/Macrophages (CD19^{-}, TCRβ^{-}, NK1.1^{-}, CD11c$^{neg\text{-}int}$, CD11b^{+}, Ly6G^{-}).

The mesenteric and inguinal lymph nodes both show very low frequencies of Tspan2-positive cells (< 1 %), followed by up to 5 % in splenocytes compared to WT controls (Figure 5, Figure 6 A). In contrast, approximately 50 % of BM cells were found to express Tspan2, indicating a highly Tspan2-expressing population that is significantly more prevalent in the BM than in spleen or LNs. For cell type-specific expression pattern analysis, BM and spleen were

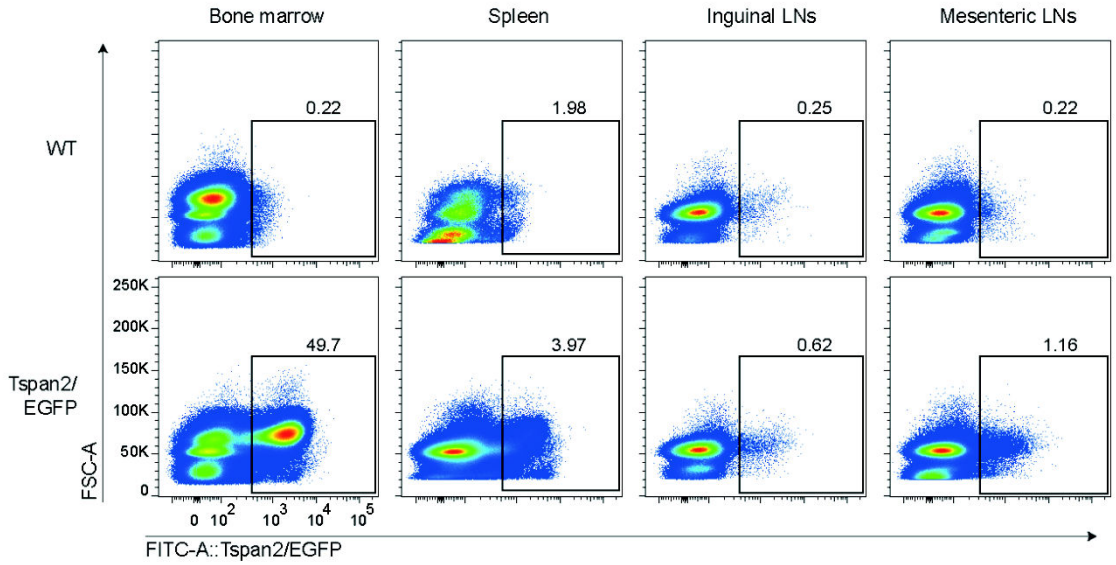

Figure 5: Tspan2 is highly expressed in cells from the BM. Tspan2/EGFP expression was quantified by flow cytometry from spleen, BM, inguinal and mesenteric LNs of Tspan2 reporter and WT mice. Cells pregated on all/single/live cells are shown in FACS blots presenting Tspan2/EGFP expression. WT gates represent negative controls for the respective organ.
BM: Bone marrow, LNs: lymph nodes. Shown is one of three independent experiments with n = 3.

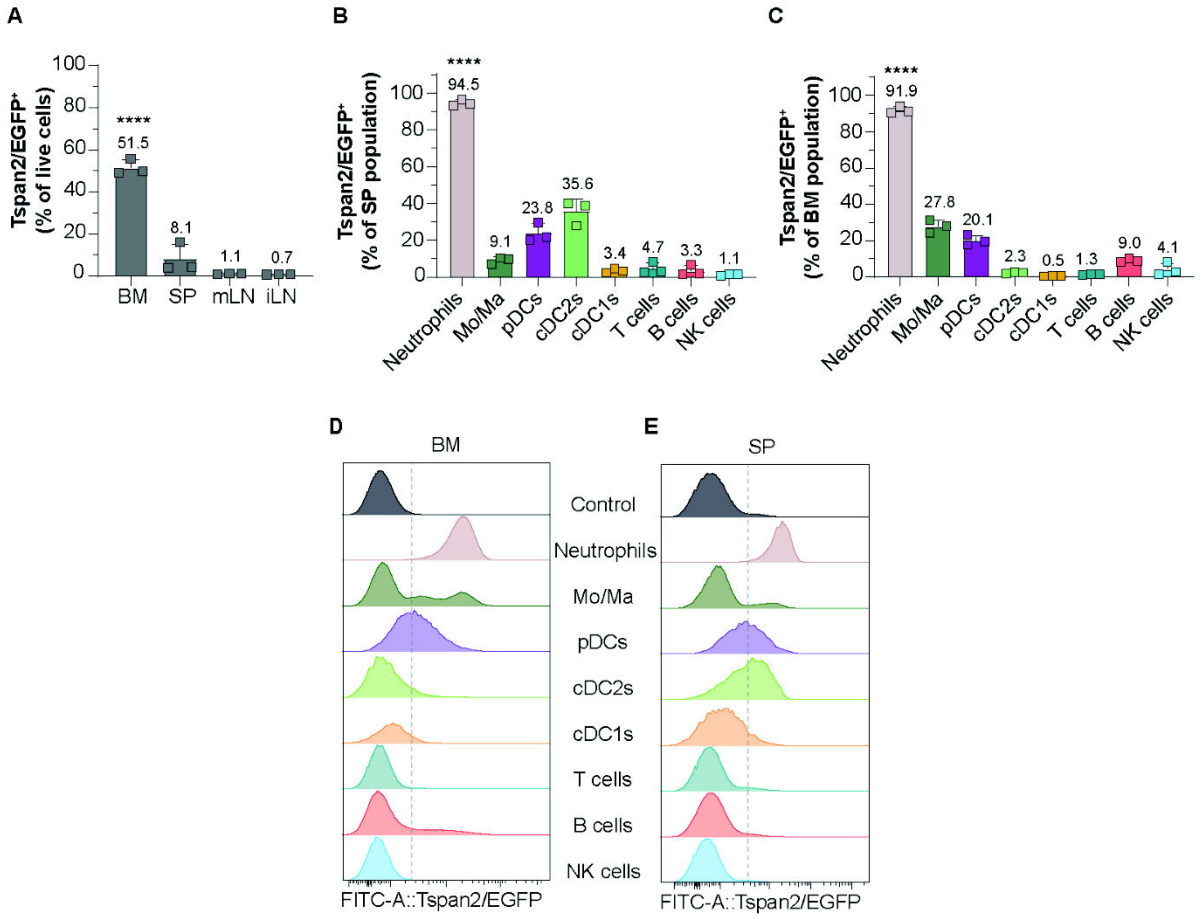

Figure 6: Neutrophils exhibit highest expression of Tspan2. (A) Frequency of Tspan2/EGFP expressing cells from SP, BM, iLNs and mLNs after pregating on single/live cells. (B) For Tspan2/EGFP⁺ fractions MFIs for cell type specific markers were calculated and displayed in heatmaps using the morpheus software from broad institute and the hierarchical clustering parameter (https://software.broadinstitute.org/morpheus/). (C and D) Tspan2/EGFP⁺ fractions of the defined immune cell populations and for (C) BM and (D) SP, additionally displaying their frequency values on top of each column. Further, MFIs of Tspan2/EGFP are shown for cell populations of (E) BM and (F) SP.
BM: Bone marrow, SP: Spleen, iLNs: inguinal lymph nodes, mLNs: mesenteric lymph nodes, MFI: Mean fluorescence intensity. Shown is one of three independent experiments with n = 3. Statistics were performed in Prism v9 using one-way ANOVA.

analysed in more detail. To this end, first a gating strategy with carefully chosen markers was established Both in the spleen and the BM only a minor fraction of Tspan2-positive cells is represented by B, T and NK cells as well as type I conventional dendritic cells (cDC1) (Figure 6 B and C). Interestingly, the proportion of Tspan2-positive cDC2s is approximately 33 % higher in the spleen compared to the BM, whereas the proportion of Tspan2-positive fractions within monocytes/macrophages (Mo/Ma) and pDC populations in spleen and BM ranges from 10 to 30 % (Figure 6 B and C). In comparison to all other immune cell populations, neutrophil granulocytes clearly dominate with > 90 % of their population being Tspan2-positive (Figure 6 B and C). Interestingly, when analysing mean fluorescence intensities (MFIs), cDC2s and pDCs in spleen and BM do not show clearly separated Tspan2-positive and Tspan2-negative populations but rather a shift, thus indicating that increasing Tspan2 gene expression might be

a progressing consequence of differentiation or activation (Figure 6 D and E). In contrast, Mo/Ma exhibit a more distinct population with regard to Tspan2 levels in spleen and even two peaks in the BM, which represent presumably monocytes and macrophages, respectively. As DCs showed a non-negligible proportion of Tspan2-positive cells, bulk DC populations were differentiated from murine BM of Tspan2 reporter animals in Flt3L cultures and

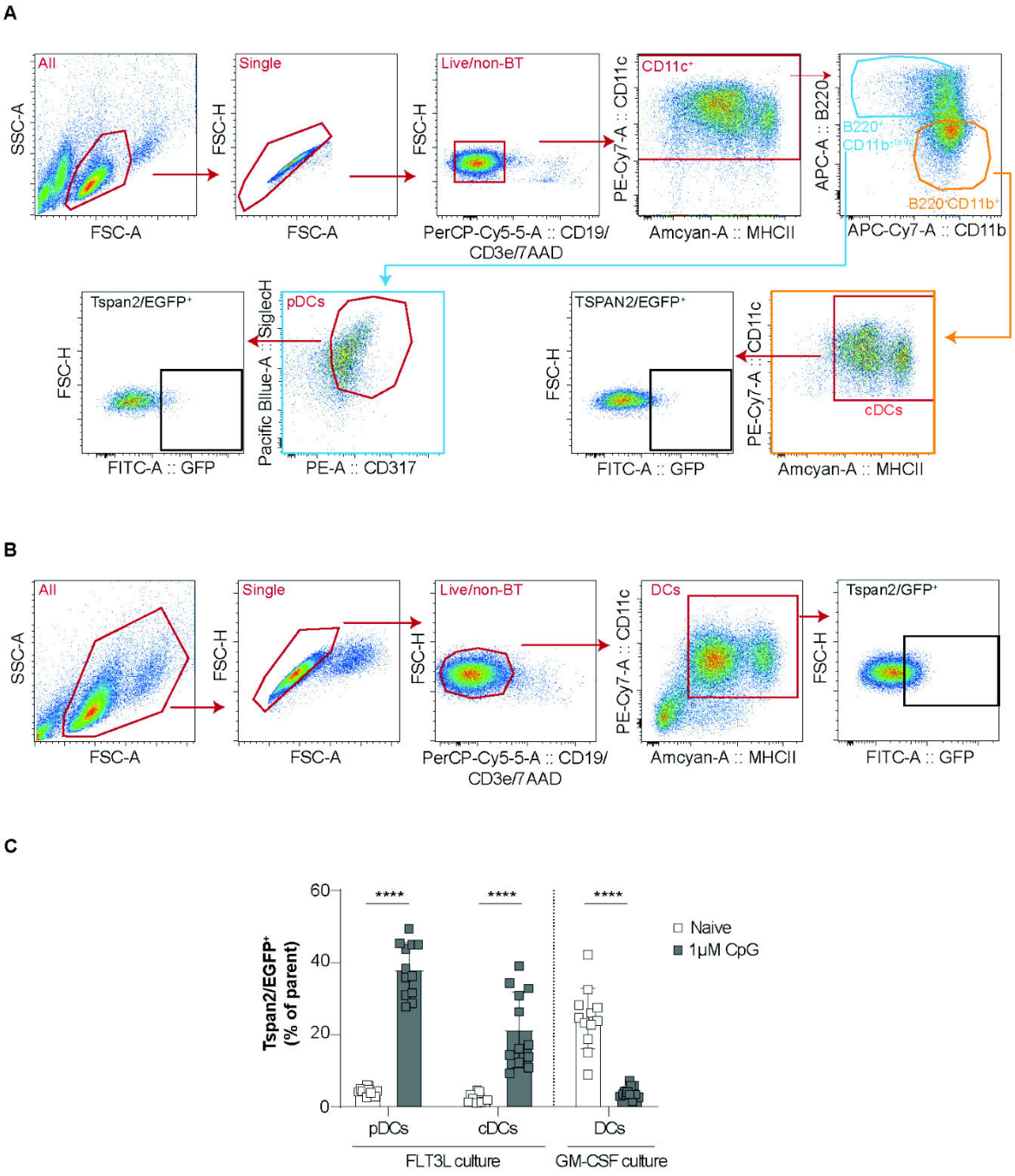

Figure 7: Tspan2 is differentially expressed in DCs upon CpG stimulation. BM cells from Tspan2 reporter mice were differentiated *in vitro* using Flt3L to drive differentiation into pDCs, cDCs and GM-CSF for generation of monocyte-derived DCs. Differentiated cell were further stimulated with 1 µM CpG for 16 hours. (A, B) Representative gating strategies of flow cytometry analysis for (A) Flt3L cultures and (B) GM-CSF cultures are shown for naive Tspan2 reporter-derived samples. (C) Quantification of Tspan2/EGFP expression is shown as pool of three independent experiments with n = 4, respectively. Statistics were performed in Prism v9 using one-way ANOVA.

monocyte-derived DCs in GM-CSF cultures to examine their Tspan2 levels after stimulation with the TLR9 ligand CpG. Surprisingly, Tspan2 levels of BM Flt3L culture-derived pDCs and cDCs were comparably low but significantly increased after stimulation (Figure 7). Inversely, BM GM-CSF cultures driving DC development primarily from monocytes, showed high basal levels of Tspan2 similar to CpG-stimulated Flt3L-derived DCs, but Tspan2 levels dropped significantly after stimulation, suggesting a complex regulation pattern of Tspan2 in DCs.
Nevertheless, neutrophils appear to be the only population that consistently expresses Tspan2 at high level among immune cells.
Taken together, these results show that Tspan2 is expressed in different immune cell populations, which include neutrophils, DC subtypes as well as monocytes and macrophages. Of these, neutrophils exhibit by far the highest expression levels of Tspan2 within a population, thus representing a highly interesting target to investigate the functional impact of Tspan2.

4.2 Identification of potential interaction partners of Tspan2 by mass spectrometry

Tspans undergo as scaffolding proteins a great number of interactions within Tspan-enriched microdomains. Although Tspans share a certain structural similarity, they are nevertheless unique, which inevitably means that one Tspan can interact better with some proteins than its other family members. Despite these different specificities, many of the Tspan interaction partners belong to the same group, such as integrins and growth factor receptors (Berditchevski, 2001, Tugues et al., 2013, Murayama et al., 2008). Investigation of interaction partners for Tspan2 will provide insight into potential Tspan2-mediated functions. Therefore, mouse embryonic fibroblasts, representing cells with a low level of differentiation, were lentivirally transduced to express either EGFP or an EGFP-Tspan2 fusion construct (Supplementary Figure 1). EGFP or EGFP-Tspan2-expressing cells were lysed and subjected to co-immunoprecipitation of Tspan2-interacting proteins using GFP-trap beads. Finally, enriched proteins were analyzed by mass spectrometry (MS) and samples were compared with each other to determine proteins that were specifically co-immunoprecipitated with Tspan2 (Figure 8). All proteins showing high $\log_2$ fold change in the EGFP-Tspan2 to EGFP comparison were considered potential interaction partners of Tspan2 or those that might be contained within the same Tspan2-enriched microdomains.
To reduce the number of potential interaction partners to the most likely interactors, only the proteins that matched the following parameters were highlighted by annotation: q-value ≤ 0.01 (red color), fold change ≥ 25 (x-axis), p-value ≤ 0.005 (y-axis), mean $\log_2$ intensity > 21.5 (dot size). In this context, the q-value additionally implements the false-discovery rate and the mean $\log_2$ intensity the protein abundance. To investigate potential direct and indirect interactions between these proteins and Tspan2 the powerful database STRING (v12.0, search tool for

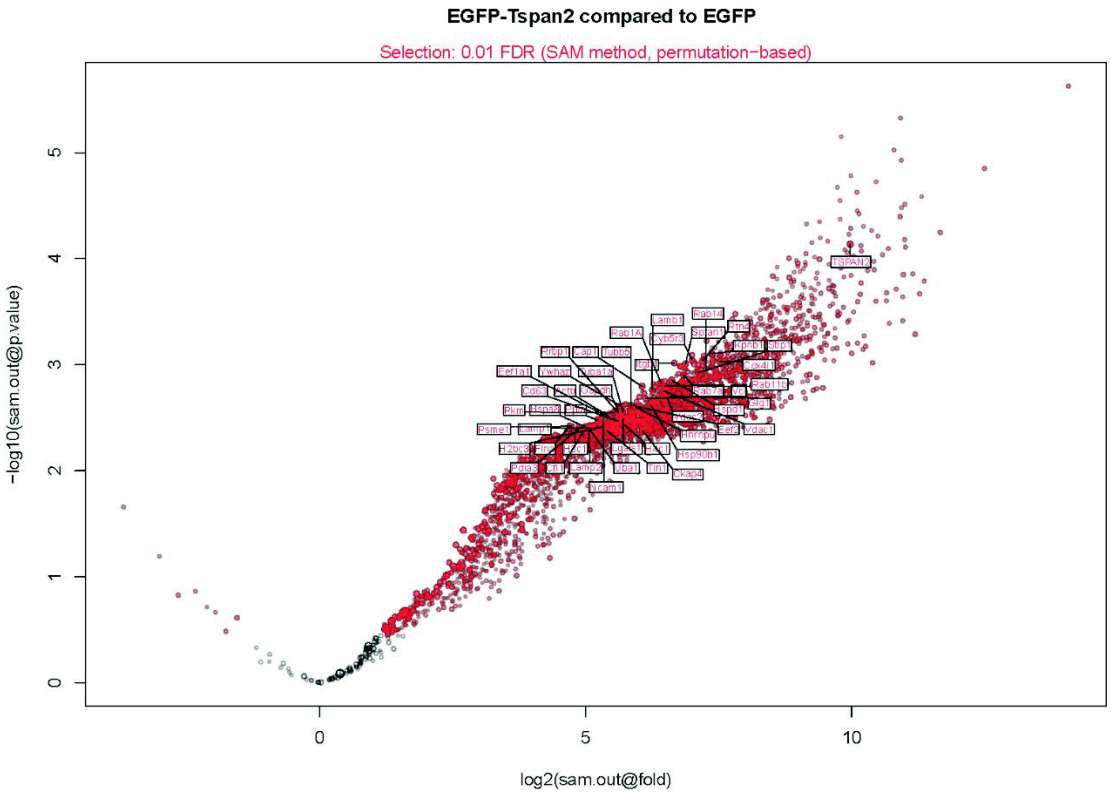

Figure 8: Mass spectrometry analysis of Tspan2 overexpressing MEFs. MEFs stably expressing either an EGFP-Tspan2 fusion construct or EGFP alone were lysed and co-immunoprecipitated via GFP-trapping beads. Finally, all proteins of five independent replicates, respectively, were analyzed in a MS screen. The volcano plot was generated using all identified proteins that were unique to one sample. Proteins that were considered to be most likely potential interaction partners of Tspan2 are annotated. The data was generated in close cooperation with Thomas Lenz (BMFZ, Heinrich Heine University Düsseldorf).
MEFs: Mouse embryonic fibroblasts, MS: Mass spectrometry.

recurring instances of neighboring genes) was used (Szklarczyk et al., 2022). Interestingly, Tspan2 is connected to the predicted network of protein-protein interactions, in total 47 proteins, via CD63 (Figure 9). This is suggested due to multiple factors, including protein homology, textmining, gene co-occurrence and experimental determination. With regard to the experimental determination, Tspan2 and CD63 were found to interact in *Homo sapiens* via an anti-tag co-immunoprecipitation assay (Huttlin et al., 2017), while in mouse there were no indications present. Furthermore, integrins are known to be common interaction partners of several Tspans (Berditchevski, 2001). In this analysis, the putative link between Tspan2 and ITGB1 arises from their respective direct associations with CD63. However, the interaction of CD63 and ITGB1 has not been confirmed either in mouse or in any other organism. Instead, the assumption that CD63 and ITGB1 may interact is based on the putative orthologues CD9 and CD81, as these Tspans were found associated with ITGB1 in humans (Serru et al., 1999, Radford et al., 1996). Interestingly, the STRING algorithm estimated edges for the proteins within the network which represent the predicted functional associations. In this respect, 63

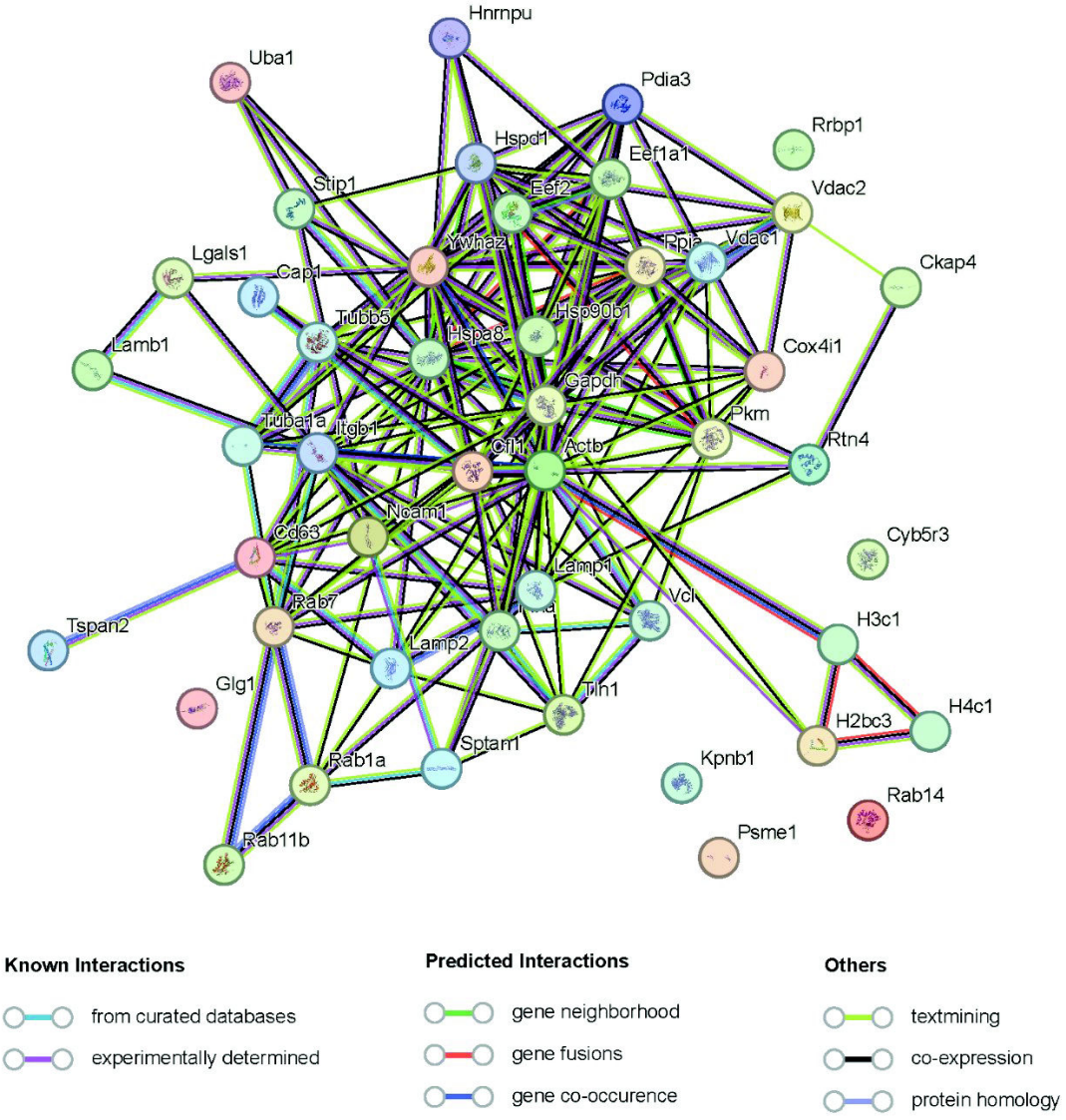

Figure 9: Tspan2 potentially interacts with CD63, ITGB1 and others. STRING analysis was performed by using the most likely interaction partners for Tspan2 determined by MS and analyzing the potential interactome via https://string-db.org. The protein network of a potential interactome was generated by the STRING (v12.0) algorithm based on known and predicted interactions and other indicators from literature.
STRING: Search tool for recurring instances of neighboring genes, MS: Mass spectrometry.

edges were predicted for the 47 proteins, whereas 194 edges were found in total. This indicates that this network potentially exhibits more interactions than expected and therefore this group of enriched proteins are likely to be biologically connected. Assignment of the 47 proteins to their ontologies of biological processes, the five most represented ones included ‘Formation of radial glial scaffolds’ and ‘Positive regulation of integrin-mediated signaling pathway’ (Szklarczyk et al., 2022). In this regard, it is well described that Tspan2 is expressed in rat myelinating oligodendrocytes (Terada et al., 2002). Furthermore, its association with

ITGB1 indicates a possible influence of Tspan2 on processes such as cell migration and adhesion.

4.3 Single cell RNA sequencing of Tspan2-deficient neutrophils

Utilising the Tspan2-deficient mouse model generally allows the investigation of differences in function-specific experimental models due to the absence of Tspan2. On the other hand, a non-specific assessment of potentially affected functions becomes possible by comparing

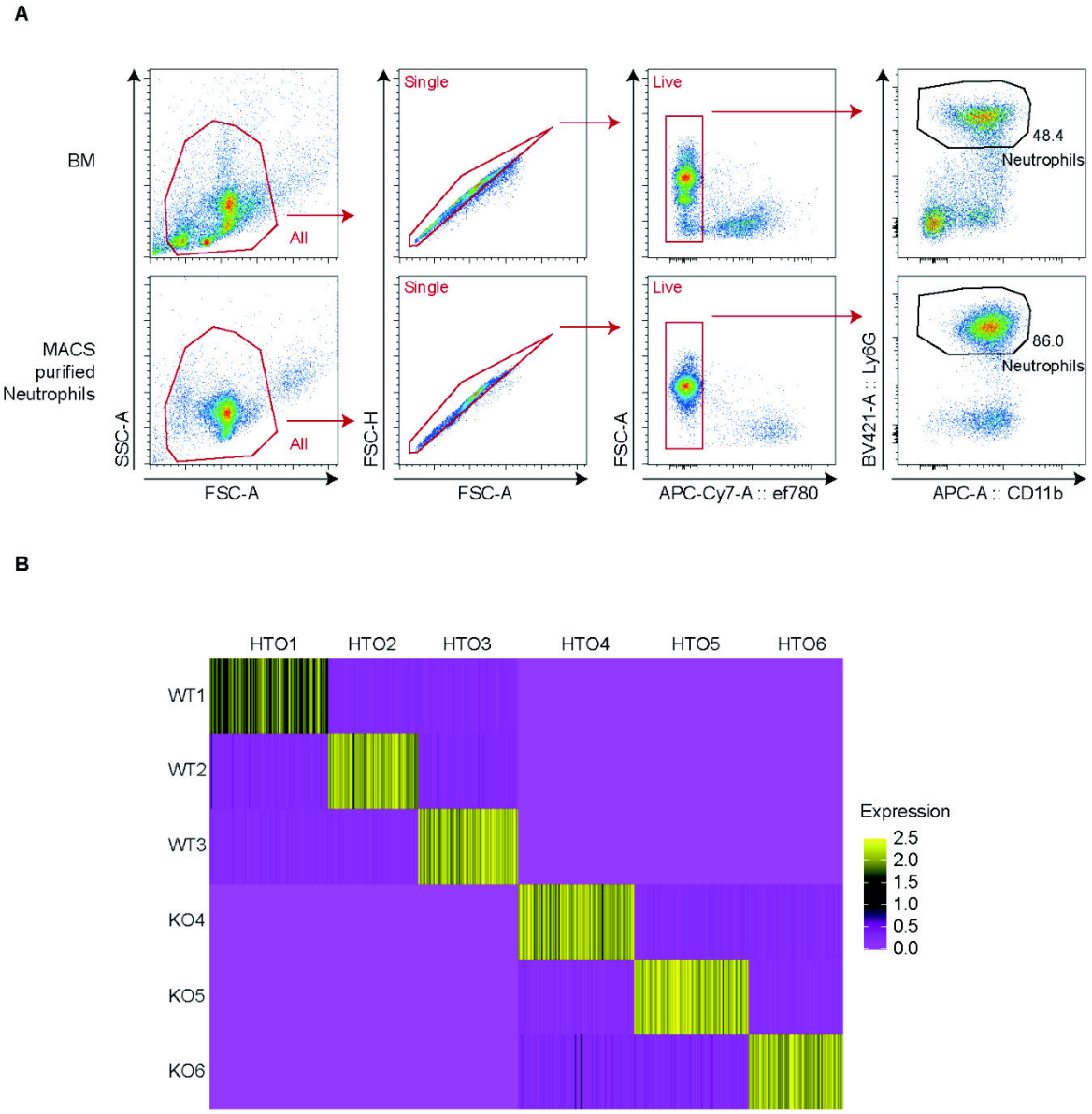

Figure 10: Neutrophil purity and separation of hashed biological replicates. For single-cell RNA sequencing neutrophils were isolated and MACS-purified from the BM of three Tspan2$^{-/-}$ and WT mice, respectively. (A) Neutrophil purity was confirmed by comparing Ly6G^{+}CD11b^{+} Neutrophil frequencies of live cells from BM and after MACS purification. Shown is a representative gating from the BM and MACS purified neutrophils of one WT mouse. Purified neutrophils were further hashed using TotalSeqTMA0301 anti-mouse Hashtag 1-6 antibodies. Biological replicates of WT and Tspan2$^{-/-}$ were pooled, respectively, and used as sequencing input. (B) The HTO Heatmap shows the remaining singlets representing the originally hashed samples.

in-depth the transcriptome of WT and Tspan2-deficient neutrophils. To achieve this, state-of-the-art single cell RNA (scRNA) sequencing analyses were performed using MACS purified BM neutrophils from three WT and Tspan2-deficient mice, respectively (Figure 10 A). Neutrophils were subjected to cell hashing, to allow separation of biological replicates during analysis and to ensure equality of samples derived from the same genotype. 20,000 purified BM neutrophils from WT and Tspan2$^{-/-}$ pools were sequenced at a depth of 50,000 to outline the potential functional alterations in Tspan2 deficiency. During quality control, samples were demultiplexed and analysed for their hashtag-based origin (Figure 10 B).

4.4 Annotation of neutrophils and their subclusters

To further remove contaminants representing non-neutrophil fractions and to appropriately annotate the neutrophil subsets, different resolutions were tested to closely define an appropriate number of clusters. Based on the experimental setup, a total of 16 clusters were chosen (Figure 11).

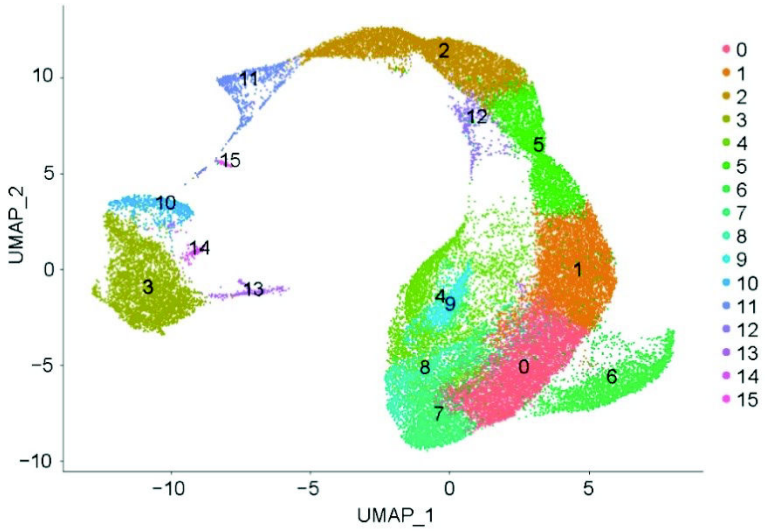

Figure 11: UMAP visualization of scRNA sequencing data. Cells are colored and numbered according to labels from clustering algorithm in Seurat. ScRNA sequencing of MACS purified BM neutrophils from three WT and Tspan2-deficient mice, respectively. For UMAP clustering a defined resolution of 0.4 was chosen resulting in 16 clusters.
BM: Bone marrow, UMAP: Uniform Manifold Approximation and Projection.

For the first line of cluster annotation, SingleR was used, which uses information from mass sequencing of sorted cell populations. The cluster classifications are presented in a SingleR heatmap, where the scores represent the expression of specific markers for the respective cell type (Figure 12 A). From 38,713 annotated cells 33,913 cells (87.70 %) were annotated as granulocytes (Figure 12 B, consisting of clusters 0, 1, 2, 4, 5, 6, 7, 8, 9, 11 and 12 shown in Figure 11), 4,688 as monocytes (12.11 %) and less than 0.3 % were referred to erythrocytes,

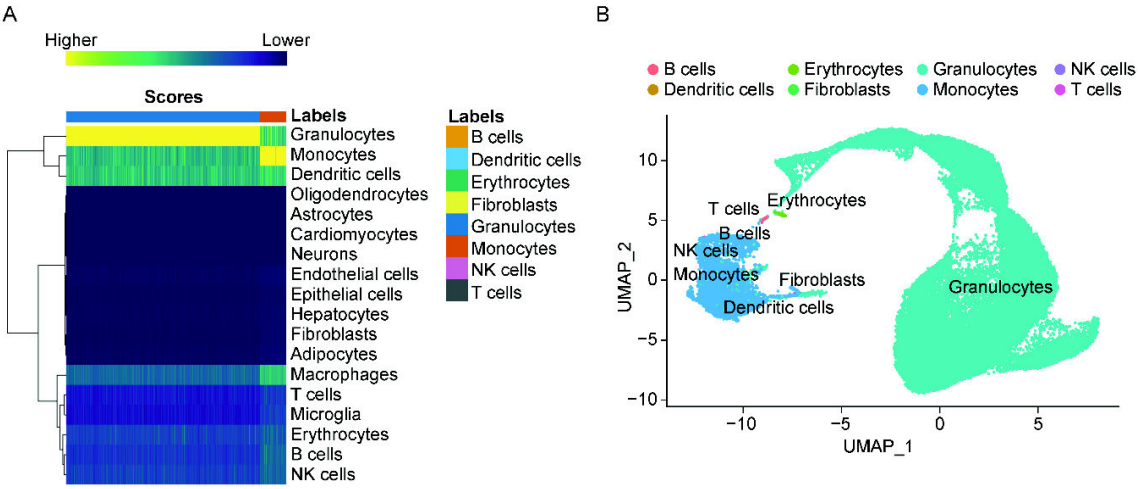

Figure 12: SingleR-based automated annotation identifies neutrophils and contaminants. Utilization of the SingleR package to predict with a MouseRNAseq database (Benayoun et al., 2019) and normal specificities a potential cell-type classification. (A) Scores (color scale from yellow to blue) for all cells across reference labels visualized in a heatmap. (B) Predicted cell types are additionally shown in a UMAP.
UMAP: Uniform Manifold Approximation and Projection.

dendritic cells, B cells, T cells, NK cells and fibroblasts. The frequency of here annotated granulocytes strongly correlates with the purity of neutrophils determined before running scRNA sequencing (≥ 85 %; Figure 10 A).

Subsequently, non-neutrophils were removed and published canonical neutrophil markers were used for annotation of neutrophil subclusters (Kim et al., 2022, Grieshaber-Bouyer et al., 2021, Xie et al., 2020). Mature neutrophils are cells that are incapable of dividing, which is why one of the first stages before the onset of their differentiation is the proliferative stage. This small subset was found to cluster among neutrophils and express genes associated with the proliferative trait, including ribosomal protein L12 (*Rpl12*) and tubulin alpha 1b (*Tuba1b*) (Figure 13). As neutrophil maturation progresses, different granules containing various anti-

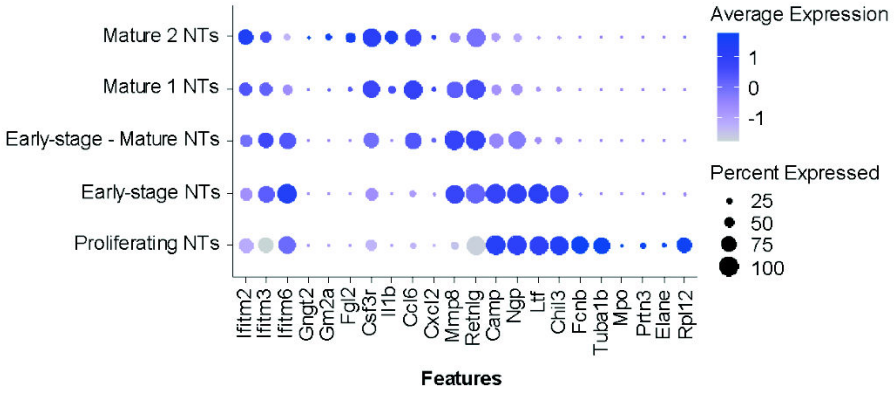

Figure 13: Annotation of neutrophil subclusters. The dot plot shows the average gene expression of published canonical gene markers (features) for neutrophil subclusters. Dot color indicates average expression values for each gene among all cells in the respective subcluster and dot size displays the proportion of cells expressing the gene.

microbial substances develop. In the early stages, secondary granule markers such as lactotransferrin (*Ltf*), antimicrobial cathelicidin peptide (*Camp*) and neutrophil granule protein (*Ngp*) reach their peak of expression, which continues to decrease as they mature. In contrast, other genes, such as C-C motif chemokine ligand 6 (*Ccl6*), interleukin-1β (*Il1b*) and colony-stimulating factor 3 receptor (*Csf3r*), correlate with the degree of neutrophil maturation with increasing expression as maturation progresses. In addition, interferon-induced transmembrane (*Ifitm*) genes show correlations with different stages of neutrophil maturation. In early, low-matured neutrophils, *Ifitm6* expression peaks and decreases progressively. In contrast, the expression of *Ifitm3* is maintained consistently while that of *Ifitm2* increases with maturation. Based on the distribution of the above mentioned and additional markers as well as their relation to the degree of maturation, the 11 subclusters of neutrophils were annotated accordingly (Figure 13) and visualised in a Uniform Manifold Approximation and Projection (UMAP; Figure 14 A). In the following, P_NTs (Proliferating Neutrophils), E_NTs (Early-stage

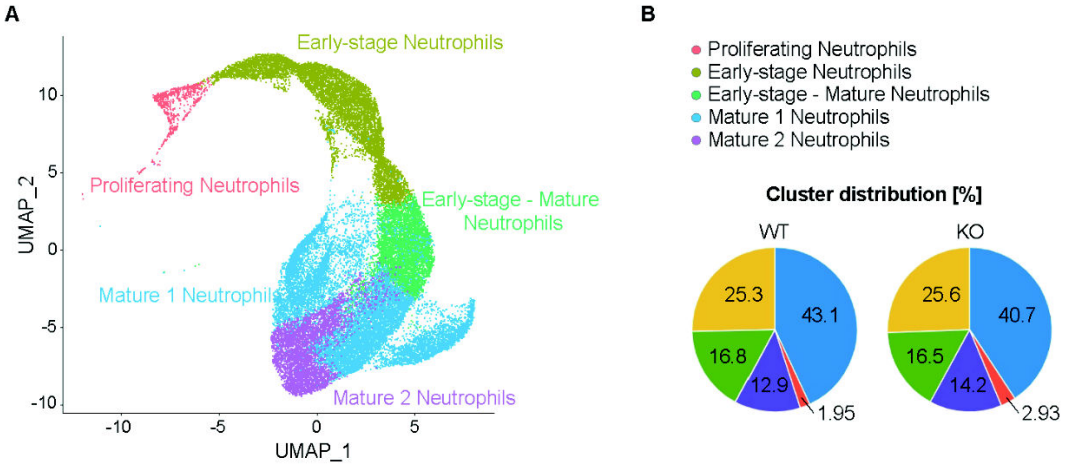

Figure 14: Abundance and distribution of BM neutrophil subsets. (A) UMAP visualized distribution of neutrophil subsets (Proliferating, Early-stage, Early-stage – Mature, Mature 1, and Mature 2 Neutrophils) among the WT and Tspan2$^{-/-}$ integrated data set. (B) Pie charts displaying neutrophil subset distribution between WT and Tspan2$^{-/-}$ pools.

Neutrophils), EM_NTs (Early-stage - Mature Neutrophils), M1_NTs (Mature 1 Neutrophils) and M2_NTs (Mature 2 Neutrophils) refer to the identified neutrophil subclusters. They represent the progression of neutrophil maturation in the bone marrow and their associated functional capacities.

4.5 Tspan2 does not impair neutrophil maturation in the BM

It is well known that some Tspans possess critical roles during cell development and maturation. These include CD53, which regulates the development of early B cells (Greenberg et al., 2020), or Tspan7, which is downregulated following stimulus-induced maturation of DCs and causes a change in their morphology (Perot et al., 2020).

To answer the question whether the loss of Tspan2 affects the maturation of neutrophils in the BM, the distribution of neutrophil subsets in the WT was compared against the KO. The M1_NTs turned out to be the most abundant population with 41-43 %, followed by the E_NTs (25-26 %), the EM_NTs (17 %), the M2_NTs (13-14 %) and the P_NTs (2-3 %), which constitute the smallest subset (Figure 14 B). However, there was no striking redistribution of the subsets between WT and KO neutrophils.

4.6 Several DEGs associate with inflammation in Tspan2-deficiency

The diverse functions neutrophils can and must perform, including their anti-microbial effector functions and recruitment capacity, can be significantly influenced by even minor changes in their transcriptome. To investigate relevant changes in the transcriptome, differentially expressed genes (DEGs) were identified in Tspan2-deficient neutrophils in comparison to the WT, resulting in a total of 3,695 DEGs. How DEGs were calculated choosing which parameters is described in detail in the material and methods section 3.8.8. To prove the representability of the determined DEGs, the most differentially regulated genes, based on their average log2 fold change, were determined and visualised for each replicate of the WT (green column) and KO (orange column) pools in a heatmap (Figure 15).

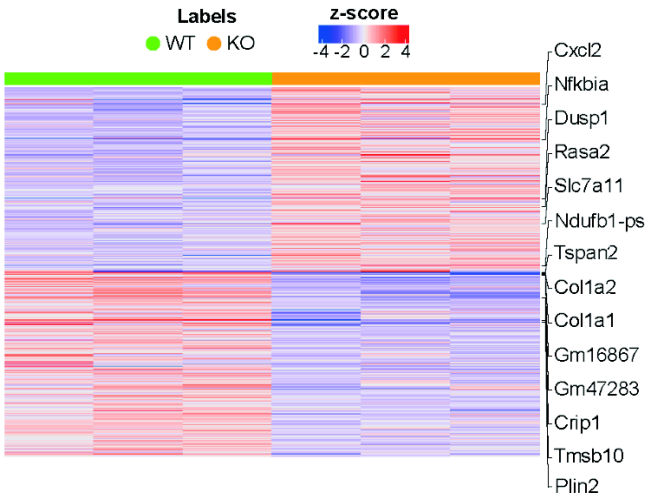

Figure 15: Many genes are differentially regulated in Tspan2-deficient neutrophils. Heatmap of the strongest 250 up- and downregulated DEGs in Tspan2-deficient neutrophils (orange) compared to WT (green). Shown is the average gene expression for each replicate. Top DEGs which additionally associate with effector, motility or anti-microbial functions are annotated.
DEGs: Differentially expressed genes.

Additionally, the most significant genes were annotated based on the adjusted p-value. Among them were several genes that possess a well-described role in neutrophils during an inflammatory response, such as C-X-C motif chemokine ligand 2 (*Cxcl2*), nuclear factor

kappa-B inhibitor alpha (*Nfkbia*) and dual specificity phosphatase 1 (*Dusp1*). Aside from these well-known genes, others were also found to be associated with various aspects of neutrophil capacities, such as Gm47283, a homologue of erythroid differentiation regulator 1 (*Erdr1*), thymosin beta-10 (*Tmsb10*), perilipin 2 (*Plin2*) and solute carrier family 7 member 11 (*Slc7a11*).

After determining the DEGs in Tspan2-deficient neutrophils, those of significance (adjusted p-value < 0.05) were isolated and used for downstream analyses. To provide an overview, all significant DEGs were first assigned to their associated ontologies and those that play an essential role in immune response-related functions were manually screened. Thereby, 55 genes were associated with migration, 19 with chemotaxis, 19 with anti-viral responses, 15 with reactive oxygen species, 14 with phagocytosis, 9 with anti-bacterial and 3 with anti-fungal immune responses. A number of these genes were placed in categories according to their ontologies and their respective average expression was visualised in a heatmap (Figure 16 A).

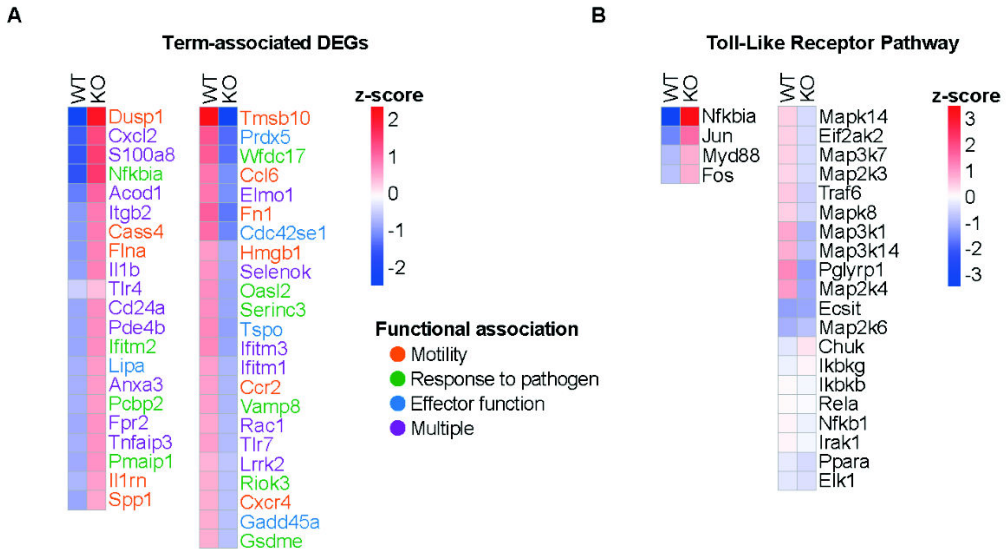

Figure 16: Multiple DEGs are involved in key processes during immune responses. Average expression of DEGs (A) of which gene ontology (GO) terms associate with motility (orange), response to various pathogens (green), neutrophil effector functions (blue), two or more of these terms (purple) or (B) with a toll-like receptor pathway (Biocarta, MM1518).

At first glance, many genes that belong to the same group appear to be regulated quite differently. However, this may conceal situation-dependent functional differences that can exert a decisive influence on key neutrophil capacities. The majority of genes upregulated in Tspan2-deficient neutrophils are involved in the regulation of migration and inflammatory processes. Among them are *Cxcl2* and *Il1b*, both essential mediators of a pro-inflammatory immune response, as well as integrin subunit beta 2 (*Itgb2*), which is part of one of the most frequent interaction partners of Tspans described and whose correct function is strongly dependent on them. However, anti-inflammatory mediators are also upregulated in the KO, such as *Nfkbia* and tumour necrosis factor-alpha-induced protein 3 (*Tnfaip3*), which are

involved in essential negative feedback mechanisms. However, just as many key contributors to important inflammatory processes are found among the downregulated genes. Neutrophil recruitment, a key process for the initiation of an effective immune response, requires sensitive regulation of chemokine receptors and adhesion molecules. C-X-C motif chemokine receptor 4 (*Cxcr4*) and C-C motif chemokine receptor 2 (*Ccr2*) are two of them and have been negatively associated with recruitment behaviour in immune cells. A similar regulation pattern can also be observed for toll-like receptor 7 (*Tlr7*) and *Ifitm3*, both of which are important participants in the antiviral immune response. Other rather less prominent genes, such as peroxiredoxin 5 (*Prdx5*) and selenoprotein K (*Selenok*) also play important roles in neutrophils, as they regulate susceptibility to oxidative stress.

In addition to the intracellular nucleic acid detector TLR7, TLR4 is also dysregulated, which recognises structures of bacterial origin, such as LPS (Chow et al., 1999), but also partially those of fungi, such as mannan (Tada et al., 2002) and viral RNA (Kurt-Jones et al., 2000). Both PRRs exhibit myd88-dependent downstream signalling, which leads to the activation of NF-κB followed by its translocation into the nucleus and thus to the induction of proinflammatory cytokines such as Il-1, Il-6 and TNF as well as anti-microbial and chemotactic mediators (Yu et al., 2020). Considering the possible involvement of these and other components downstream of TLR signalling, genes of the TLR signalling pathway (BIOCARTA_TOLL_PATHWAY, MM1518) were investigated for their expression levels in WT and KO (Figure 16 B). Among the components upregulated in Tspan2$^{-/-}$ were the innate immune signal transduction adaptor *Myd88* and downstream AP-1 transcription factor subunits *Jun* and *Fos* (Figure 16 B), as well as upregulated *Il1b* (Figure 16 A) (Kawai and Akira, 2006). Interestingly, *Nfkbia* was also present in steady state neutrophils, which encodes the potent NF-κB inhibitor IκBα. It inhibits the translocation of NF-κB into the nucleus until IκB kinases phosphorylate and degrade IκBα as a result of TLR activation, thereby releasing NF-κB (Baeuerle and Baltimore, 1988). This data may suggest that steady state neutrophils may elicit a stronger response to certain bacterial stimuli due to the high expression of many downstream PRR components.

4.7 Neutrophils lacking Tspan2 show potential impairment of key functions

To investigate the functional traits of the DEGs identified above, gene ontologies (GOs) associating with biological processes were quantitatively analysed. Therefore, the 15 most significant GO terms were highlighted in a bar chart, additionally displaying the total count of DEGs for each term. From the analysis, it was found that the majority of DEGs are strongly associated with various immunoregulatory and inflammatory functions (Figure 17). These include the particularly strongly represented processes of motility, cell migration and

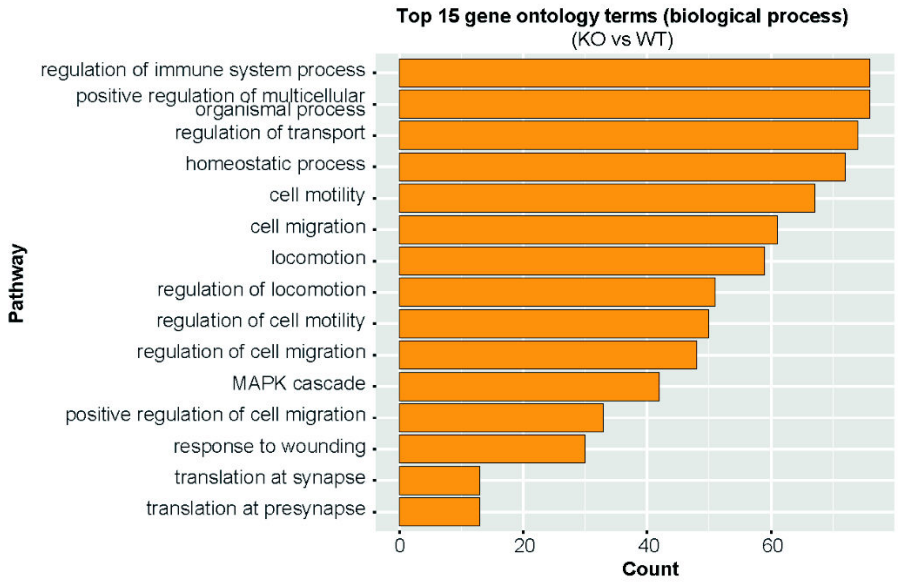

Figure 17: Tspan2 impacts multiple processes of neutrophils which are key during immune response. GO enrichment analysis of DEGs in Tspan2$^{-/-}$ compared to WT featuring biological processes. Terms shown in the bar plot represent the top 15 most significant GO terms with their respective gene counts.
GO: Gene ontology, DEGs: Differentially expressed genes.

locomotion. Furthermore, MAPKs play important roles in a variety of signalling pathways, including TLR-mediated ones. More than 40 of the significant DEGs appear to be directly related to the regulatory mechanisms within the MAPK cascade and several others to NF-κB signalling. Additional outstanding ontologies refer to pathways not yet addressed, such as those involved in response to wounding and DNA damage.

In order to further identify functions and pathways impaired by Tspan2, analyses were performed in which an ontology-specific gene set was mapped against the present DEGs. In a gene set enrichment analysis (GSEA) using the Kyoto Encyclopedia of Genes and Genomes (KEGG) over- and underrepresented pathways were determined and respective normalized enrichment scores (NES) displayed in a bar chart (Figure 18). Within this analysis an overrepresentation of the MAPK signalling pathway was found, similar to the previous GO term analysis. This, together with the aforementioned differentially expressed TLR components, indicate that there may be a strong impairment of neutrophil response mechanisms against specific pathogens. In addition to other significantly overrepresented categories, such as cell cycle and motor proteins, microRNAs in the context of cancer appear to play a central role. Thus, microRNAs are gaining growing attention and additionally have been found to function as regulators during the formation of neutrophil extracellular traps (NETs) (Águila et al., 2021). While microRNAs are receiving more attention, mechanisms of focal adhesions are one of the most studied fields of life science research. Focal adhesions are formed during a variety of processes, ranging from cell cycle progression to cell migration. This involves the interaction of the cytoskeleton of a cell with the surrounding extracellular matrix (ECM) via

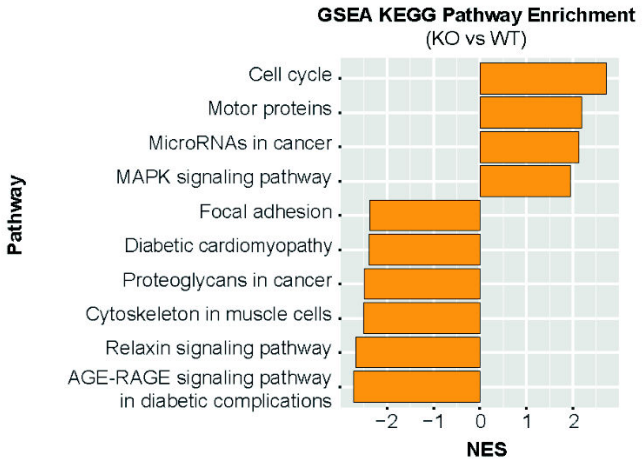

Figure 18: Neutrophils lacking Tspan2 show impaired formation of focal adhesions. Bar plot of a GSEA using KEGG pathways. The NES indicates over- or underrepresentation of the respective gene set.
GSEA: Gene set enrichment analysis, KEGG: Kyoto Encyclopedia of Genes and Genomes, NES: Normalized enrichment score.

integrin-dependent adhesion complexes (Mishra and Manavathi, 2021). Besides integrins, these complexes contain various receptors, GTPases and scaffolding proteins, such as Tspans. Here, Tspans play a key role in modulating protein cluster assembly within the cell membrane (Nakanishi et al., 2019). An underrepresentation of this gene set indicates that Tspan2 is potentially of high relevance for the maintenance of functional membrane protein networks. Interestingly, among the underrepresented terms were those associated with the immune situation in diabetes, although in previous analyses no significant DEGs were primarily associated with diabetes via GO terms.

However, the analysis of significant DEGs already provides valuable evidence for certain functions or immunoregulatory mechanisms that are potentially affected by the absence of Tspan2 in neutrophils. For further investigations, the exact expression differences will be taken into account in order to increase the value of significant genes with relatively high or low fold changes. For this purpose, a pre-ranked list of DEGs sorted by their fold changes was used to generate GSEA plots for terms of interest. Terms of interest refer to processes and mechanisms that have previously been emphasised. Many of the DEGs in Tspan2$^{-/-}$ showed a strong association with motility-related processes, which are essential for efficient neutrophil recruitment. When comparing the DEGs with a gene set associated with chemotaxis, most of the matching DEGs showed a positive fold change, with an overall NES of 2 (Figure 19 A). Meaning that chemotaxis-associated genes are highly overrepresented in Tspan2$^{-/-}$ neutrophils.

Another broad category consisted of DEGs that could be assigned to response mechanisms, such as the previously observed higher *Tlr4* and lower *Tlr7* expression in Tspan2-deficient neutrophils (Figure 16 A). In this regard, consistent results were found in which genes associating with the bacterial and xenobiotic responses were greatly overrepresented (Figure

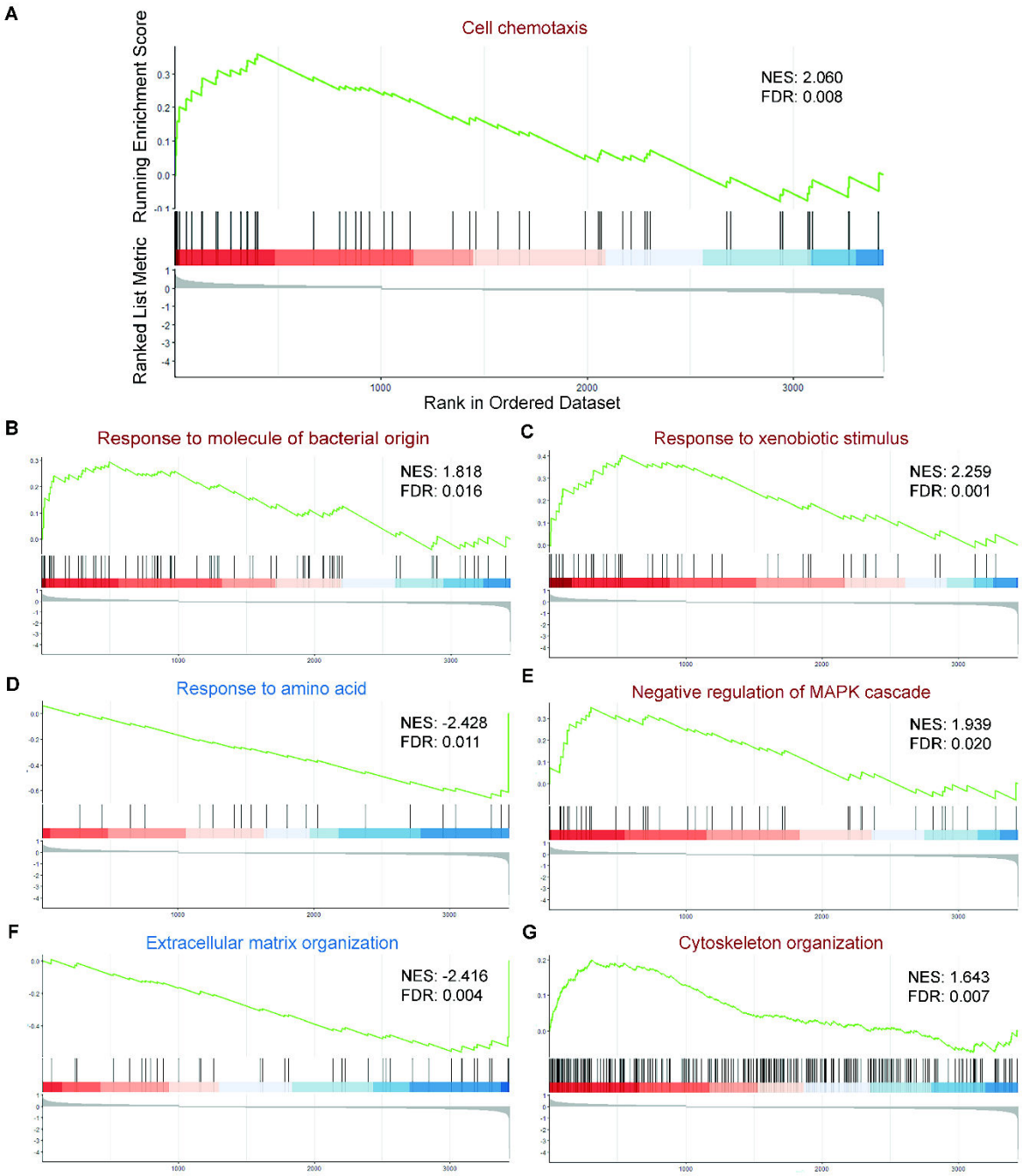

Figure 19: Several neutrophil motility and anti-pathogenic response mechanisms are differentially regulated in Tspan2-deficiency. (A-G) GO GSEA utilizing a pre-ranked list of DEGs (ranked list metric). Terms of interest were chosen and visualized in a GSEA plot. NES and FDR is shown for all overrepresented (red) and underrepresented (blue) GO term.
GO: Gene ontology, GSEA: Gene set enrichment analysis, DEGs: Differentially regulated genes, NES: Normalized enrichment score, FDR: False discovery rate.

19 B, C). Furthermore, the response to amino acids was underrepresented, which is presumably associated with the reduced expression of *Tlr7* (Figure 19 D). While MAPK signalling was a common term in the DEG analyses, a number of genes were found to be more abundantly expressed in the KO but negatively associating with the regulation of the MAPK cascade (Figure 19 E). In agreement with this GSEA, previous comparison of the average

expression of TLR components showed that MAPKs were expressed at a significantly lesser extent in the KO (Figure 16 B, Figure 19 E).

The third major aspect to consider is focal adhesion, which can be critical during immune cell recruitment in particular. In this type of interaction, the cytoskeleton of the cell forms a direct contact with the surrounding ECM. As the process of focal adhesion appears to be generally underrepresented, this may be either due to the impaired ability to remodel the cytoskeleton or to the interaction processes with the surrounding ECM (Figure 18). Interestingly, DEGs associated with each of these processes are differentially expressed in the KO. While genes for efficient organisation of the ECM are underrepresented, those for organisation of the cytoskeleton are overrepresented (Figure 19 F, G).

4.8 Multiple DEGs are unique to individual neutrophil subsets

In the previous sections, it was shown on the one hand that many function-specific genes are differentially expressed between the Tspan2-deficient and WT neutrophils and on the other hand that based on the defined neutrophil subsets, neutrophils are found in the BM at different stages of maturation. Therefore, it is reasonable to assume that some of the DEGs may be specific for a certain degree of neutrophil maturation. To obtain an individual overview,

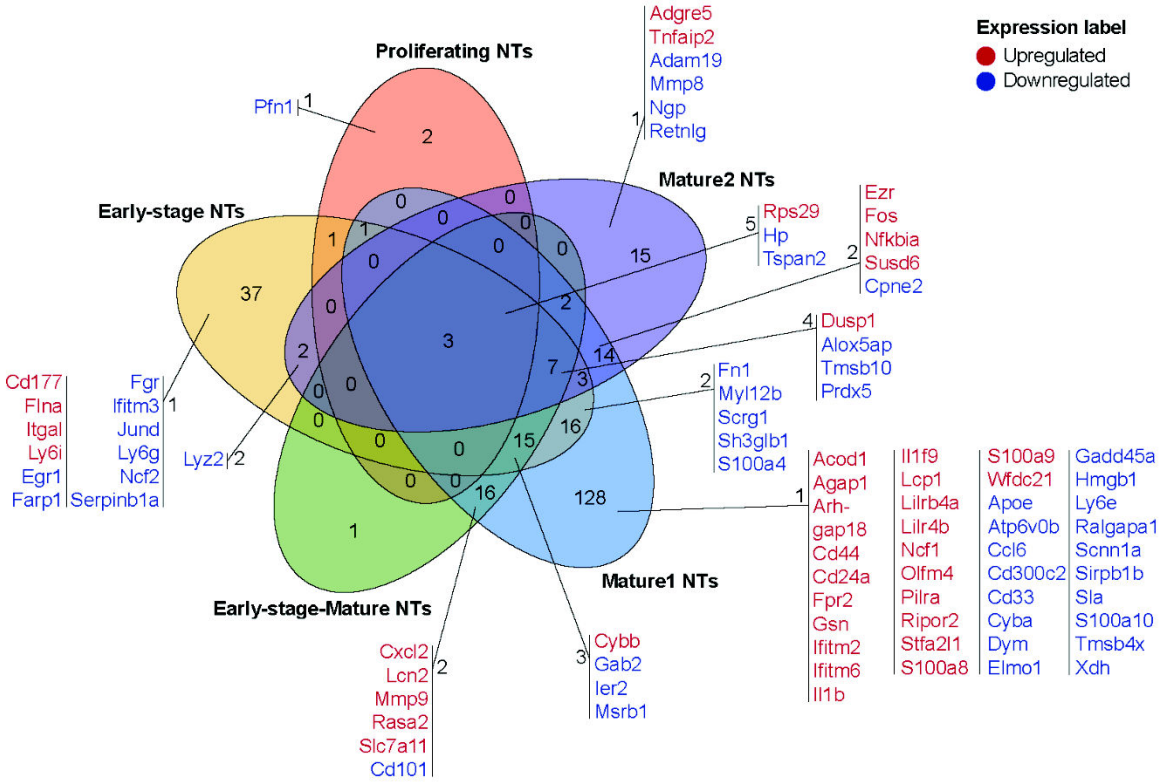

Figure 20: Several DEGs are dependent on neutrophil maturation levels. DEGs were determined for each subcluster. The Venn diagram shows the amount of DEGs that are shared or unique to one subcluster. Up- (red) or downregulated (blue) genes that are of potential interest were highlighted by name.
DEGs: Differentially expressed genes.

significant DEGs were determined for each subset independently and their average expression was mapped in a Venn diagram (Figure 20). Each area represents DEGs that only occur in those subsets that overlap at the respective position. Numbers indicate the count of DEGs in the respective delineated area and some prominent genes were annotated. Here, DEGs that exhibit patterns similar to the previously described *Ifitm* genes in the context of neutrophil maturation and show consistently decreasing or increasing expression patterns across different maturation stages may provide evidence for tightly controlled processes and mechanisms that are specifically influenced by Tspan2.

When comparing the subsets, it became evident that a small group of DEGs were consistently differentially expressed throughout the E-/EM-/M1-/M2-NTs. Two of these genes with the highest differential expression are *Dusp1* and *Tmsb10*, both of which associate with cellular motility. Among other genes showing consistent differential expression in the KO compared to WT among the E-/EM-/M1-NTs and the M1-/M2-NTs maturation stages the arachidonate-5-lipoxygenase-activating protein (*Alox5ap*) is specifically involved in leukotriene biosynthesis and thus plays a key role in neutrophil swarming, in which the synthesis and secretion of leukotrienes is essential for swarm coordination (Hopke et al., 2022). Furthermore, *Ier* and *Gab2* play important roles in motility and *Fos*, *Cybb* and *Ezr* fulfil functions during an anti-bacterial immune response.

4.9 Tspan2 induces maturation-dependent changes in the neutrophil transcriptome

The presence of shared DEGs across neutrophil maturation stages provides a good indication of which genes have a particularly strong association with Tspan2 and specific functions, pointing to constantly influenced pathways similar to the global analysis of the transcriptome from all neutrophils. However, the determination of genes that are unique to a subset can potentially identify maturation stage-specific processes that are dependent on Tspan2. In this regard, two subsets, the earliest P-NTs and the intermediate EM-NTs have very few significant subset-specific DEGs. In contrast, the clusters of E-, M1- and M2-NTs have larger groups of 37, 128 and 15 unique DEGs, respectively (Figure 20). With a subset abundance of approximately 40 % of the neutrophils in the BM, the M1-NTs also represent the largest subgroup with unique DEGs, thus potentially representing the subset most strongly influenced by Tspan2. In particular, this subset harbours DEGs that are associated with various essential processes of neutrophils, including immune response, inflammation and other cellular functions. Among the M1-NT-specific DEGs that participate in key mechanisms are the aconitate decarboxylase 1 (*Acod1*), *Il1b*, *Ifitm* and *S100* genes, which are of general relevance in inflammatory responses. Neutrophil processes such as chemotaxis, adhesion and migration are essential for the initiation of such an immune response. *CD44*, *CD24a*, formyl peptide

receptor 2 (*Fpr2*) and Rho GTPase activating protein 18 (*Arhgap18*) were directly associated with such gene ontologies. However, in addition to these genes, which are strongly upregulated in the KO, there are just as many that are downregulated despite similar functional associations, such as *CD33*, *Ccl6* and Engulfment and Cell Motility 1 (*Elmo1*), which can potentially influence neutrophil adhesion, recruitment and phagocytosis.

4.10 Tspan2-deficient mice can clear *C. albicans* infection

Following an infection, it is crucial for survival of the host that a successful immune response takes place, which depends on a large number of factors. The innate immune cells represent the first line of defense and utilize their broad repertoire of PRRs and anti-microbial mechanisms to control the infection and shape the establishment of a more specific immune response (Pradeu et al., 2024). Therefore, it is necessary to analyze the intactness of vital functions of innate immune cells in Tspan2 deficiency. The here shown sequencing analysis revealed a large number of DEGs associated with various aspects of neutrophil motility, including chemotaxis, migration and adhesion (Figure 17). Furthermore, a number of DEGs indicated an impairment of effector functions in Tspan2-deficient neutrophils. Among them, several genes were found to contribute to the response mechanisms in direct contact with viral, or especially bacterial or fungal components (Figure 16 and, Figure 19).

Following up on these findings, first *in vivo* studies on fungal infections with *Candida albicans* were conducted. Although *C. albicans* is a human pathogen, the systemic candidiasis induced by i.v. administration of the fungus closely models the infection observed in humans (Spellberg et al., 2005). After administration, *C. albicans* colonizes the organs of the host, with kidneys serving as the primary site of infection. If the infection fails to be controlled by the immune system, it results in death due to fungal sepsis (MacCallum and Odds, 2005). In the following section, the severity of the course of infection will be addressed, which refers to the development of non-specific symptoms such as weight loss and changes in behavior.

In a survival study, Tspan2-deficient and WT mice were administered 10^5 (low dose) and 10^6 (high dose) *C. albicans* intravenously (i.v.) to induce systemic candidiasis. While the low control dose only caused initial mild symptoms, which were rapidly resolved, many WT and KO animals receiving the higher dose were unable to control the Candida infection (Figure 21 A, F-G). Although the WT animals showed an earlier onset of loss of control of the infection, there was no significant difference compared to the Tspan2-deficient animals over the 30-day observation period. Interestingly, male mice appeared to be much more affected by the development of lethal symptoms as a result of systemic *C. albicans* infection than female counterparts (Figure 21 B-G). 8 of 10 males died from the infection independent of the genotype, compared to 1 of 10 females. Following this observation, a larger group of male WT and Tspan2$^{-/-}$ mice were challenged with an intermediate dose of 5 x 10^5 *C. albicans* i.v. and

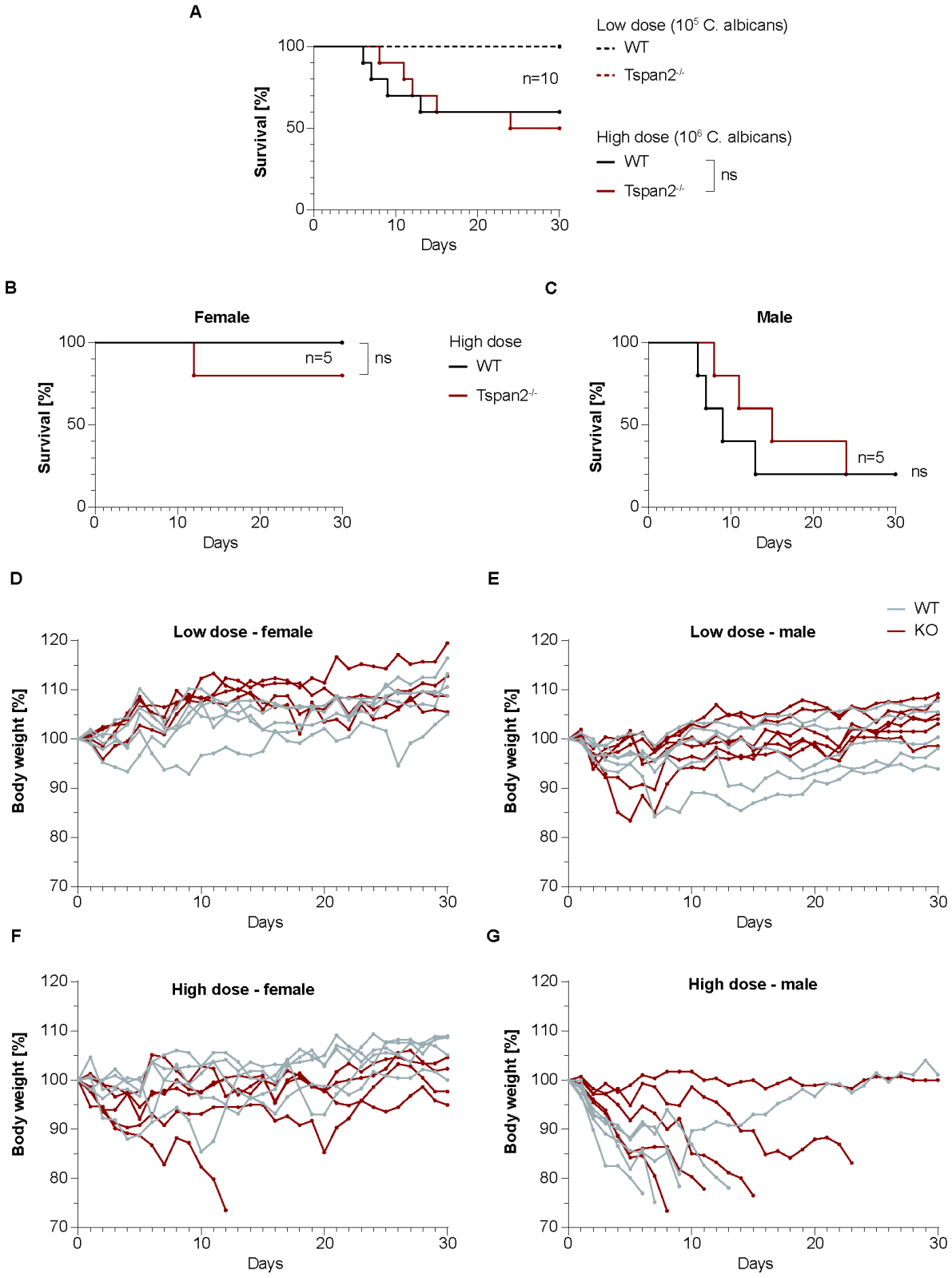

Figure 21: Male mice are more susceptible to systemic *C. albicans* infection. Administration of 10^5 (low dose) or 10^6 (high dose) *C. albicans* i.v. into WT and Tspan2$^{-/-}$ mice, respectively. (A-C) Mice were monitored on a daily basis over 30 days. Sex-dependent survival upon receiving high doses is shown for (B) females and (C) males. (D-G) Percentages of body weight over 30 days is shown for females and males receiving (D-E) low doses or (F-G) high doses, respectively. I.v.: Intravenously. Statistics were performed in Prism v9 using Log-rank (Mantel-Cox) test.

monitored over 30 days (Figure 22). Whereas Tspan2-deficient mice showed a later onset of

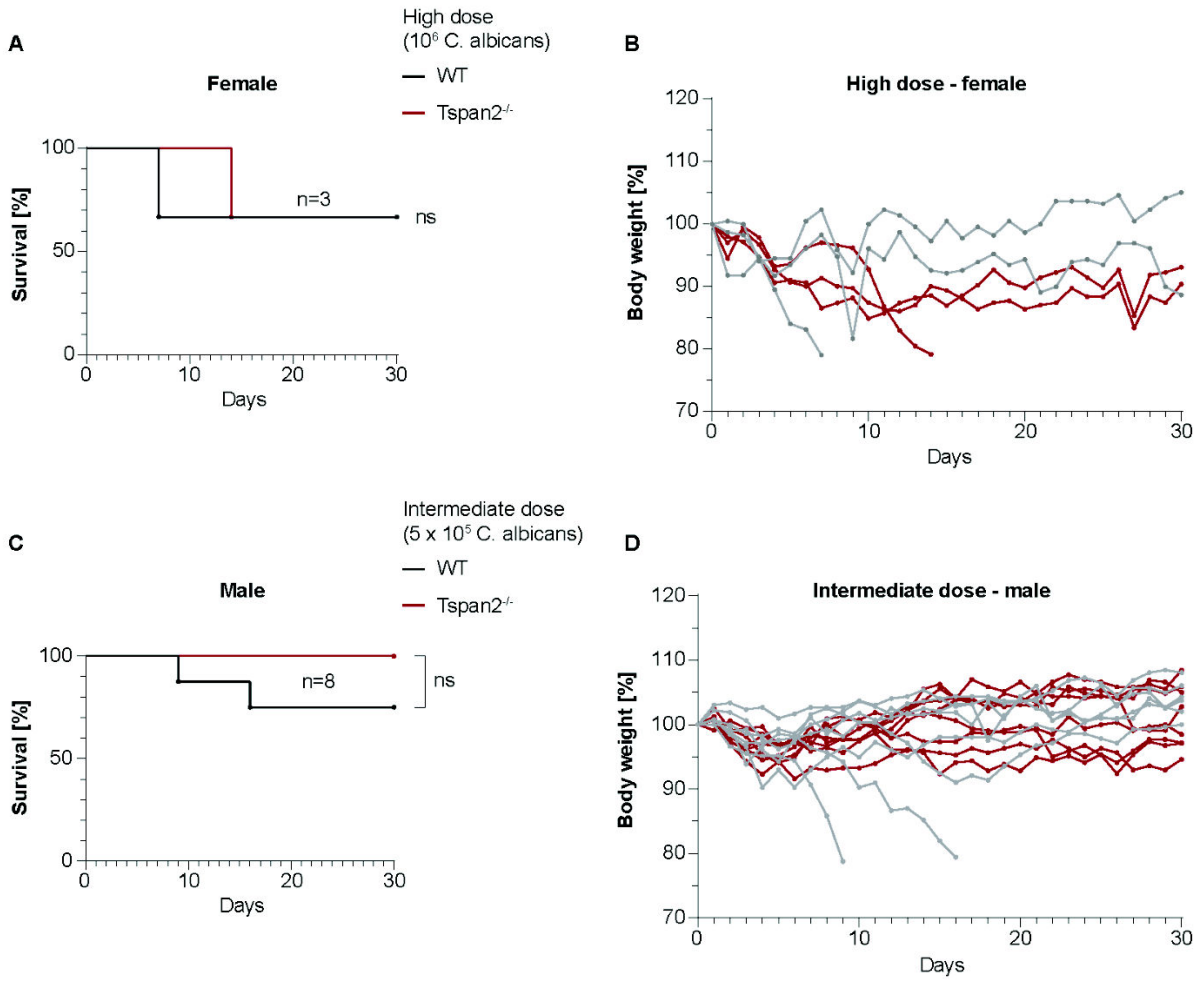

Figure 22: Tspan2-deficient mice show a tendency to better clearance of systemic *C. albicans*. Administration of (A-B) 10^6 (high dose) or (C-D) 5 x 10^5 (intermediate dose) *C. albicans* i.v. into WT (grey) and Tspan2$^{-/-}$ (red) mice, respectively. Groups of females received high while males received intermediate doses. (A, C) All mice were monitored on a daily basis over 30 days. (B, D) Percentages of body weight over 30 days is shown for groups of females and males
I.v.: Intravenously, Statistics were performed in Prism v9 using Log-rank (Mantel-Cox) test.

lethal symptoms upon administration of high doses (Figure 21 C, G), they survived after being challenged with intermediate doses of *C. albicans*, while 25 % of WT counterparts succumbed to the infection (Figure 22 C-D). Furthermore, a control group of female mice receiving a high dose of 1 x 10^6 *C. albicans* resulted in 33 % lethality (Figure 22 A-B). In line with previous observations Tspan2-deficient mice showed a later onset of lethal symptoms compared to WT, suggesting a slow but ongoing clearance behavior by the immune system.

4.11 Neutrophils lacking Tspan2 tend towards a loss of motility

Efficient recruitment of immune cells to the site of infection is crucial for a successful defense against invading microbes. The recruitment of neutrophils ranges from the release from the BM to the transmigration into the inflamed tissue. To study the effect of Tspan2 on motility associated mechanisms in more detail, different *in vivo* and *in vitro* assays were performed.

They focused on investigating the overall recruitment, the ability to sense attractants as well as the remodeling of the cytoskeleton and coordination of a swarm. To investigate the recruitment behavior, 10^6 *C. albicans* were administered intraperitoneally (i.p.) and the inflammatory infiltrates representing the recruited cells were collected after 4 hours via peritoneal lavage. Subsequently, neutrophils ($CD19^-$, $TCR\beta^-$, $NK1.1^-$, $CD11c^{neg\text{-}int}$, $CD11b^+$, $Ly6G^+$), proinflammatory monocytes/macrophages ($CD19^-$, $TCR\beta^-$, $NK1.1^-$, $CD11c^{neg\text{-}int}$, $CD11b^+$, $F4/80^+$, $Ly6C^{high}$) and cDCs ($CD19^-$, $TCR\beta^-$, $NK1.1^-$, $CD11c^+$, $MHCII^+$) were identified and the approximate total cell count was calculated based on their frequency (Figure 23 A).

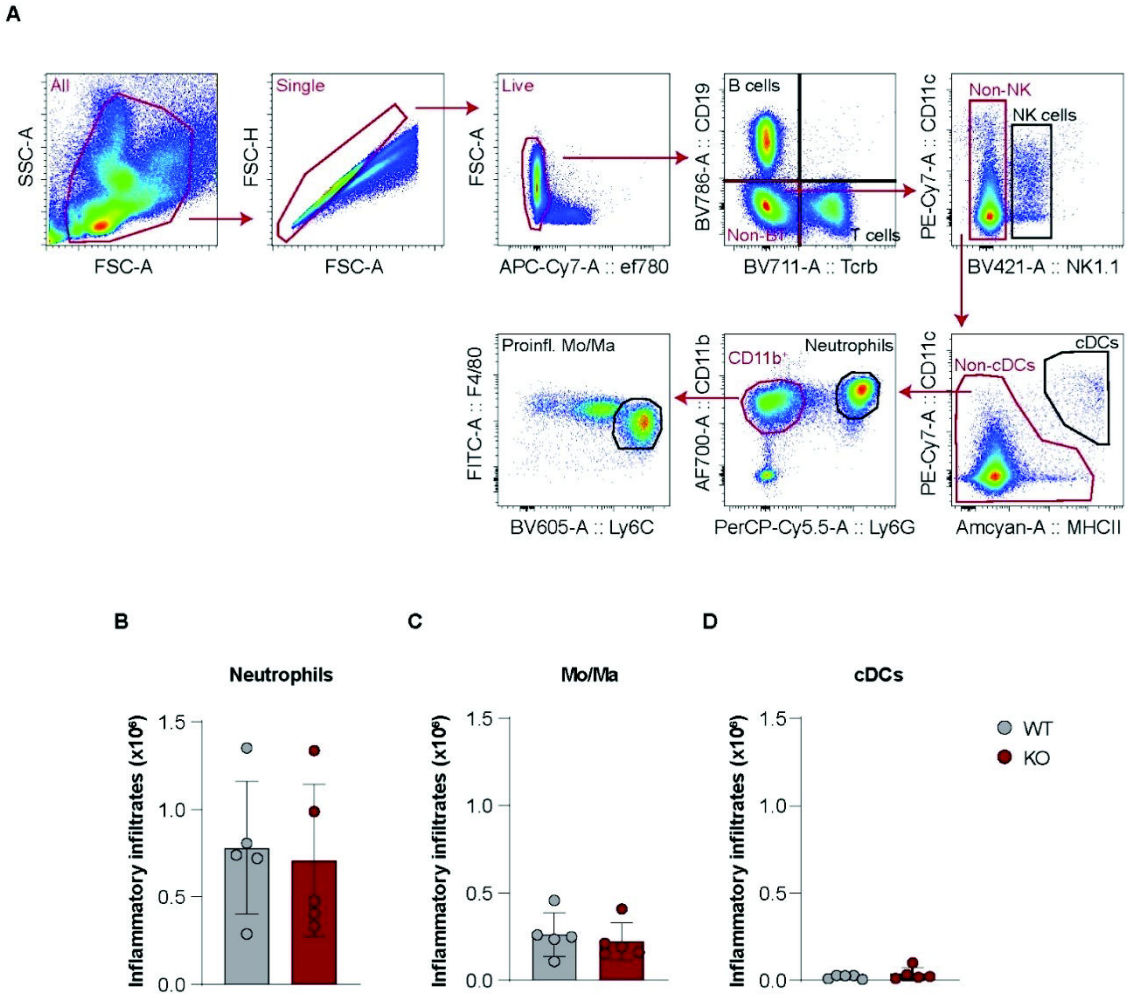

Figure 23: Recruitment into the peritoneal cavity upon inflammation is not altered in Tspan2-deficiency. Peritoneal inflammation was induced by i.p. administration of *C. albicans* for 4 hours. (A-D) Inflammatory infiltrates were collected by peritoneal lavage. (A) A gating strategy was established to identify (B) neutrophil, (C) Mo/Ma and (D) cDCs.
I.p.: Intraperitoneally. Shown are representatives of three independent experiments with n = 5. Statistics were performed in Prism v9 using student's t-test.

Even though neutrophil represent the immune cell population that is recruited to the highest extent into the peritoneal cavity upon onset of inflammation, only a slight decrease in cell numbers can be observed when mice lack Tspan2 (Figure 23 B). Furthermore, also total

numbers of Mo/Ma and cDCs recruited are not changed during Tspan2-deficiency (Figure 23 C-D).

When performing an under-agarose assay (UAA), WT and Tspan2-deficient neutrophils are expected to sense the attractant and migrate in its direction. To achieve this, neutrophils must be able to continuously rearrange their cytoskeleton as they navigate between a plate surface and a dense polymer. Both Tspan2$^{-/-}$ and WT neutrophils show the ability to migrate towards the attractant, which can be visually confirmed by the microscopic endpoint images (Figure 24 A). Further quantification of the distance migrated (displacement) and the absolute number of

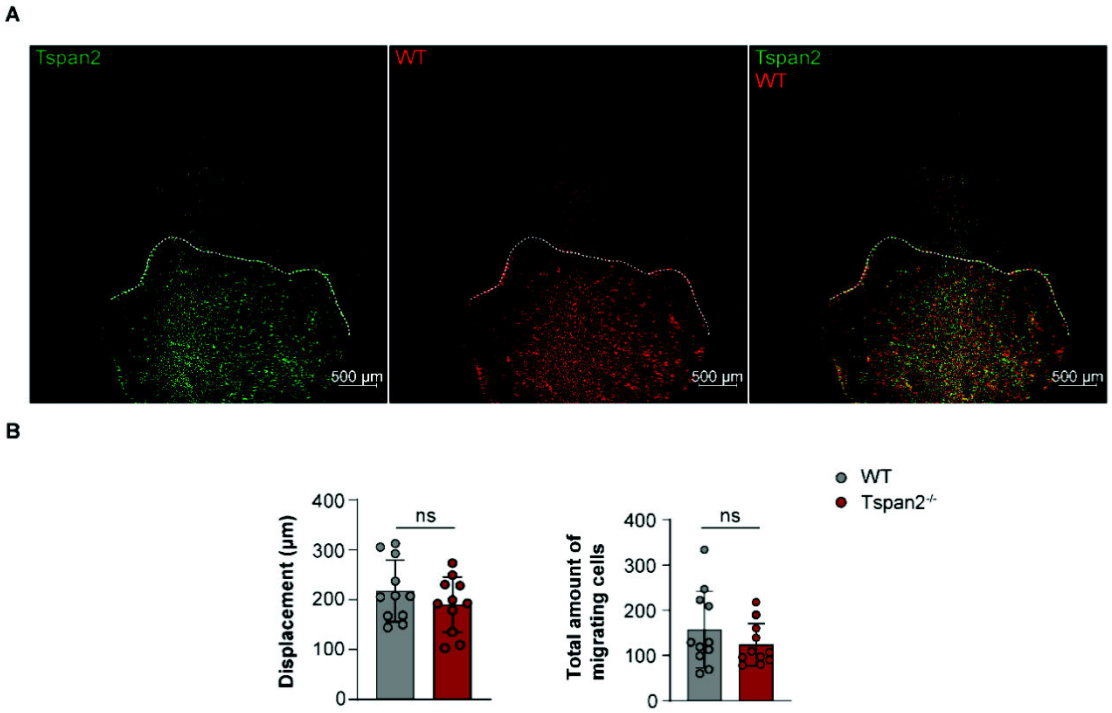

Figure 24: Tspan2-deficient neutrophils show slightly reduced migration capacities.
Competitive analysis of WT (red) and Tspan2$^{-/-}$ (green) neutrophils in an under-agarose assay. (A) Neutrophil pools were applied into punched holes of an agarose layer to migrate towards a CXCL2/LTB4 gradient. Endpoint images were taken after 4 hours. Thresholds of migration were illustrated manually as white ticked lines. (B) Total distances of migration (displacement) and absolute cell numbers of migrating neutrophils which passed thresholds were quantified.
Shown are representatives of three independent experiments with n = 8-11. Endpoint images in (A) show one sample well of migrating cells which represents one dot in (B). Statistics were performed in Prism v9 using one-way ANOVA. This figure was created in cooperation with Katharina Glaser, AG Lämmermann, Max Planck Institute, Freiburg.

migrated cells show no significant difference, although Tspan2-deficient neutrophils show a consistent tendency towards reduced motility (Figure 24 B). After successful guidance to site of infection, neutrophils must leave the bloodstream via transmigration and enter the inflamed tissue through an endothelial layer.

Once there, they follow the continuously secreted attractants by other cells and additionally utilize a mechanism in which they themselves release attractants into their environment. Surrounding neutrophils sense these attractants via G protein-coupled receptors (GPCRs),

which triggers further signaling cascades and enables nearby neutrophils to migrate as a swarm (Kienle et al., 2021). To investigate this unique mechanism, fluorescently labelled Tspan2$^{-/-}$ and WT neutrophils were exposed to surface-immobilized and heat-killed *Staphylococcus aureus* within a competitive study. Swarming was recorded in live cell imaging over 2 hours and 10 randomly selected cells were manually tracked over the first 30 frames (14.30 minutes) (Figure 25 A). In addition to the investigated capacities of neutrophils during

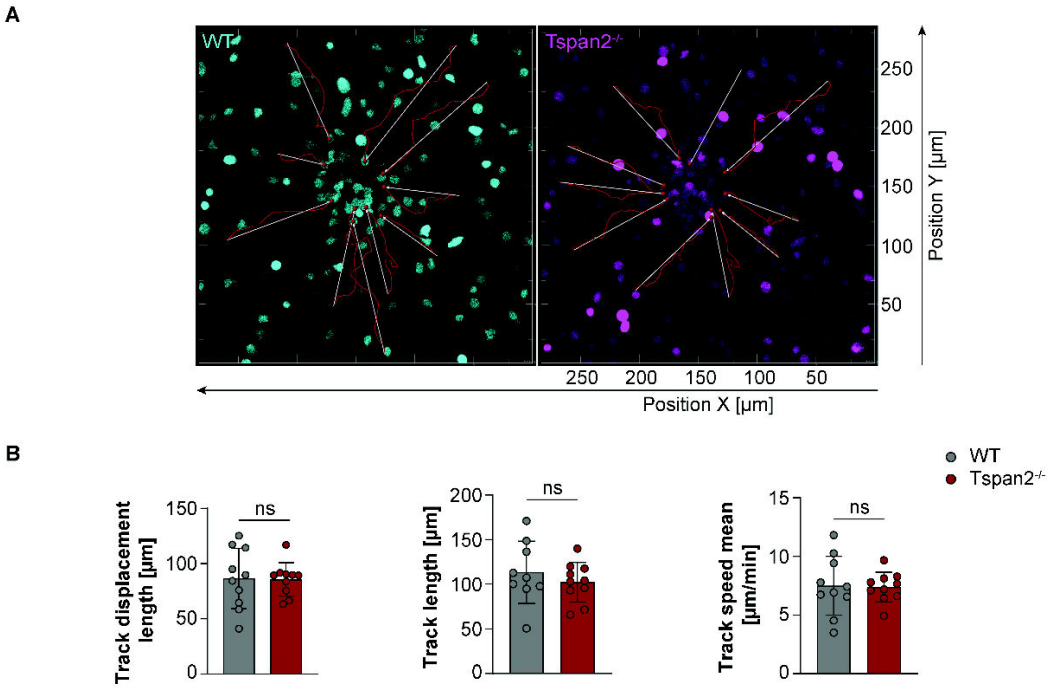

Figure 25: Neutrophils lacking Tspan2 show normal swarming behavior. WT (cyan) and Tspan2$^{-/-}$ (purple) neutrophils were comparatively analyzed for their swarming capacity. (A) Neutrophils swarming was captured over a time frame of 2 hours. 10 randomly chosen cells from each genotype were tracked over the first 30 frames (14 minutes 30 seconds). Red tails indicate frame-based track length and cell movement while arrows show total distances. (B) Cells tracked in (A) were analyzed for their track distance, exact length and average speed.
Shown are representatives of three independent experiments. Statistics were performed in Prism v9 using student's t-test. This figure was created in cooperation with Katharina Glaser, AG Lämmermann, Max Planck Institute, Freiburg.

the UAA, neutrophils must be able to both initiate and terminate the GPCR-mediated swarm. Observation of the swarming behavior in both WT and Tspan2$^{-/-}$ neutrophils revealed no visual difference (video not shown). Subsequent quantification of individual cells in terms of their directed displacement (grey arrows), the absolute distance covered (red tails) and their average speed also revealed no significant impairment by Tspan2 (Figure 25 B).

Transmigration of neutrophils was analyzed using a transwell system allowing them to migrate through pores along an fMLP gradient. Exact cell counts of the transmigrated fraction were determined by flow cytometry using counting beads. Both WT and Tspan2$^{-/-}$ neutrophils were able to show a strong transmigration behavior after exposure to fMLP (Figure 26 A, B). However, the absolute numbers of transmigrated cells were comparable in both genotypes.

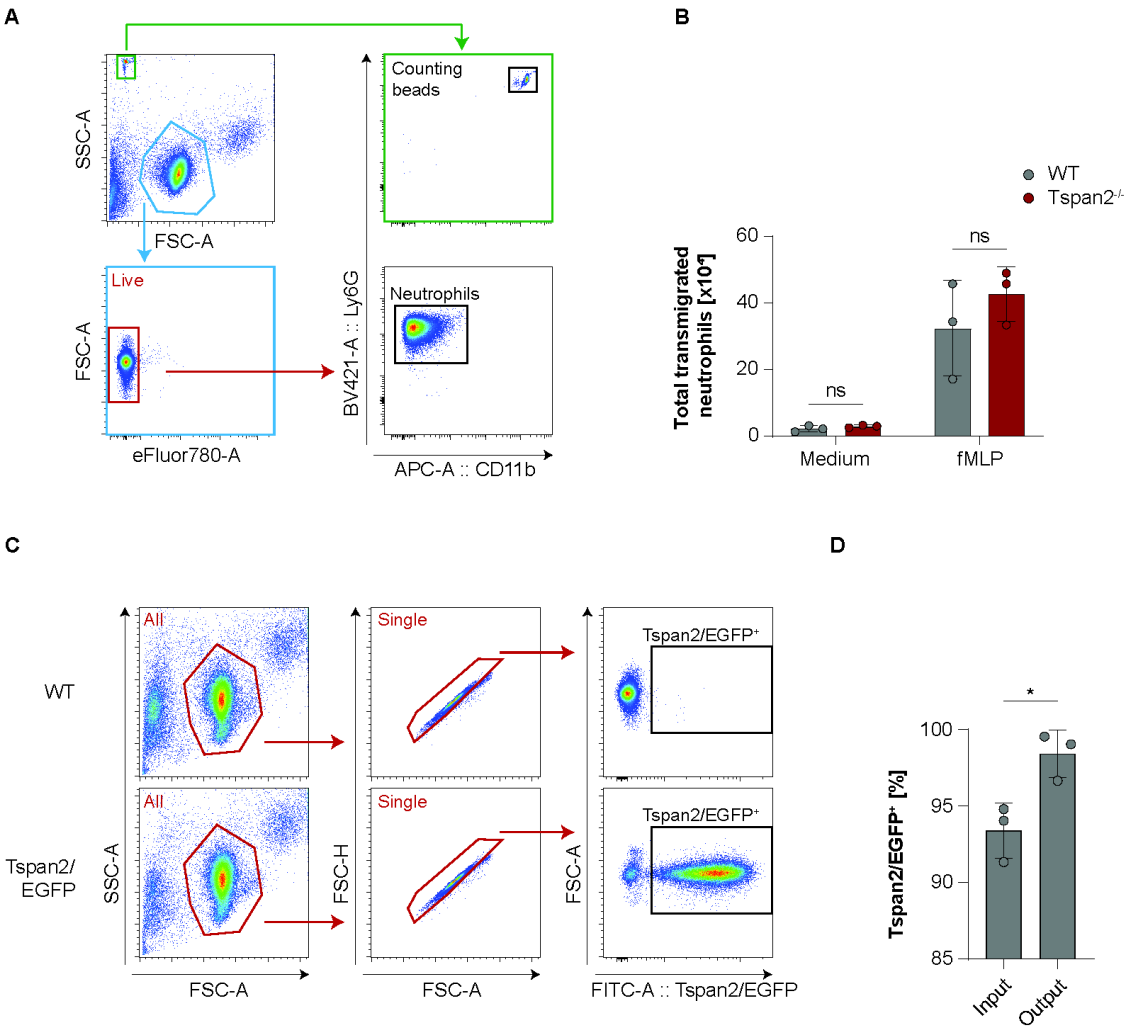

Figure 26: Tspan2 exhibits no overt influence on neutrophil transmigration behavior. (A-D) Transmigration of neutrophils was studied using an insertable transwell system. Transmigration was induced with 1 µM fMLP over 4 . (A-B) Tspan2-deficient and WT neutrophils that transmigrated through transwell pores were quantitatively analyzed using absolute counting beads. (C-D) Neutrophils from Tspan2 reporter mice were allowed to transmigrate as described above. Frequency of Tspan2/EGFP⁺ neutrophils were determined before starting the transmigration experiment and served as controls (Input). Input frequencies were compared to those of transmigrated cells.
Shown are representatives of three independent experiments, respectively, with n = 3. Statistics were performed in Prism v9 using student's t-test.

When performing a similar experiment with Tspan2 reporters, transmigration was analyzed in an alternative way. The frequencies of Tspan2/EGFP⁺ neutrophils were determined before the experiment and after successful transmigration. Neutrophils were already found to comprise an almost completely Tspan2-positive population between 90-95 %. However, the transmigrated fraction consisted of 96-99 % Tspan2-positive cells, which describes a significant increase (Figure 26 C, D). Contrary to the previous motility studies in the KO, this shows an inverse direction in which Tspan2 possibly favors the transmigration of neutrophils instead of negatively influencing it.

4.12 Tspan2 partially impairs neutrophil functions in vitro

During an infection event, neutrophils constitute a key component of the first line of defence. It is therefore crucial that they are efficiently recruited to the site of infection and can unrestrictedly utilise their wide range of effector functions to eliminate the threat. Expanding on the previous sequencing analyses, in vitro studies were performed to investigate the functional capacities of Tspan2-deficient neutrophils. Firstly, the primary overarching function of neutrophils was analysed, which describes the elimination of a pathogen. For this purpose, Tspan2$^{-/-}$ and WT neutrophils were co-cultured with gram-negative *E. coli* bacteria followed by quantification of the surviving bacteria via colony forming unit (CFU) counts. This revealed that neutrophils lacking Tspan2 have a significantly higher capacity to eliminate the bacteria than their WT counterparts (Figure 27). To model different bacterial burdens, neutrophils were

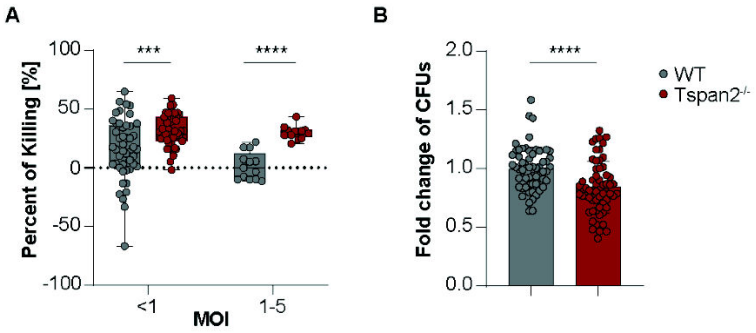

Figure 27: Tspan2$^{-/-}$ neutrophils show increased kill capacity against *E. coli* bacteria. Neutrophils co-cultured with *E. coli* DH5α at different MOIs. (A) Exact MOIs calculated from control CFUs were pooled into MOI ranges from <1 and 1-5. Percent of killing describes the percentage of bacteria killed by neutrophils in WT or Tspan2$^{-/-}$ co-cultures, respectively, compared to CFU controls cultured without neutrophils. (B) Fold change of CFUs compared to the average WT CFU count. MOI: Multiplicity of infection, CFU: Colony forming units. Shown are pools of three independent experiments with n = 6-7. Statistics were performed in Prism v9 using one-way ANOVA.

exposed to different multiplicities of infection (MOIs). At both low and higher MOIs, KO neutrophils were found to be superior to WT (Figure 27 A). This was also evident in the MOI-independent quantification of CFUs, which were significantly reduced in the KO (Figure 27 B). To eliminate microbes, neutrophils utilise their well-coordinated repertoire, comprising receptor-mediated microbial uptake, clearance through toxic substances after phagosome-granule fusion and the final formation of proinflammatory NETs. These individual mechanisms and further motility-related processes are very likely to underlie the phenotype observed in the bacterial kill, thus consequently subjecting them to investigation in further *in vitro* studies. During assessment of the phagocytotic activity, neutrophils were identified by their characteristic surface markers Ly6G and CD11b, with CD11b levels increasing after stimulation (Figure 28 A). This indicates that these neutrophils remained sufficiently unaffected after isolation from the BM until the experimental procedure and were not activated beforehand. The internalisation of fluorescently labelled pH-sensitive *E. coli* particles by neutrophils was quantified by flow cytometry. The fluorescence intensity of the particles

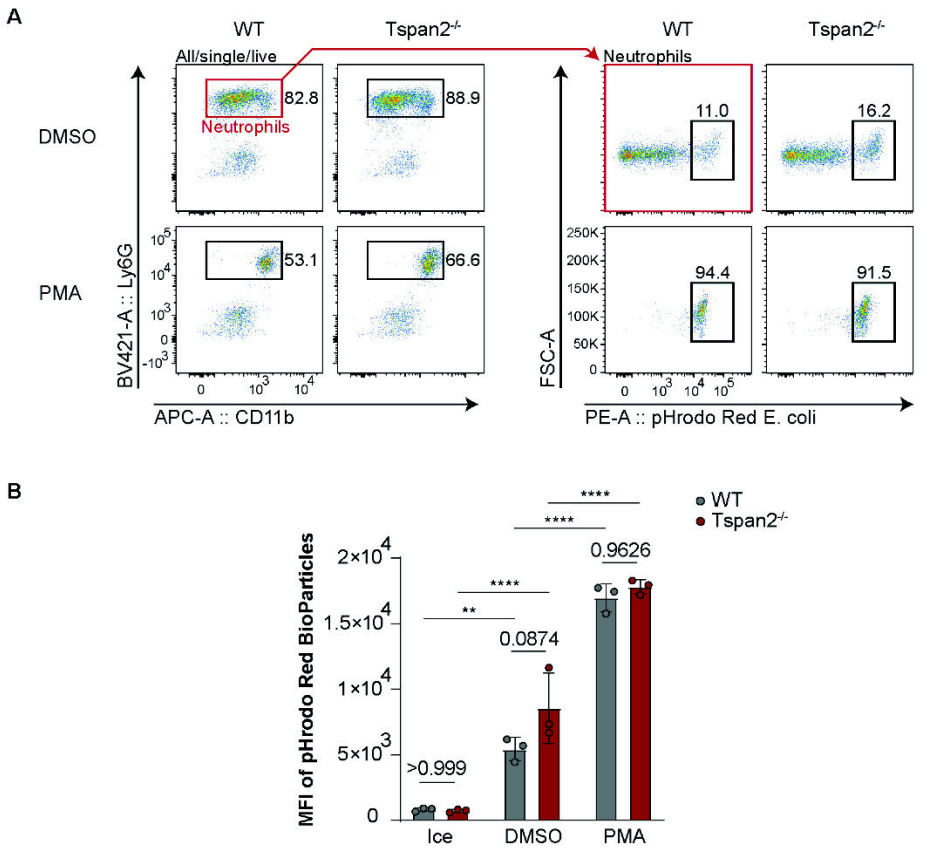

Figure 28: Tspan2 does not impact neutrophil phagocytosis. (A) Purified BM neutrophils from WT and Tspan2$^{-/-}$ mice were stimulated with 150 nM PMA and treated with 25 µg/ml pH-sensitive fluorescent *E. coli* particles. For flow cytometry analysis neutrophils were determined (Ly6G^{+} CD11b^{+}) and their phagocytosis capacity was analyzed by their frequency of *E. coli* particle uptake and quantification of neutrophil pHrodo Red *E. coli* MFI.
MFI: Mean fluorescence intensity. Shown are representatives of three independent experiments with n = 3-4. Statistics were performed in Prism v9 using one-way ANOVA.

gradually increased with growing acid environment, allowing to distinguish between surface-bound and phagocytosed particles. The phagocytosis capacity during Tspan2-deficiency showed a tendency towards an increase in DMSO and PMA-stimulated neutrophils, but was not significantly affected (Figure 28 B). Following activation of neutrophils, they start to produce reactive oxygen species (ROS), representing one of the absolute key functions, being crucial for subsequent processes, such as the intracellular kill of microbes and the formation of NETs. To analyse the presence of ROS in an unsaturated system, neutrophils were treated with sufficient amounts of dihydrorhodamine 123 (DHR) and stimulated with sensitively titrated levels of PMA. The intracellular ROS oxidises the DHR to the cationic and fluorescent rhodamine which is detectable by flow cytometry (Figure 29 A). The MFIs of the oxidised rhodamine showed comparably high values in both Tspan2$^{-/-}$ and WT controls (Figure 29 B). A unique feature of neutrophils is their ability to undergo NETosis, in which they condense their chromatin together with granule-stored anti-microbial substances before expulsing them as NETs into the extracellular space, thereby causing irreversible membrane rupture. This is a process that should exclusively occur during an infection, thus inactivated

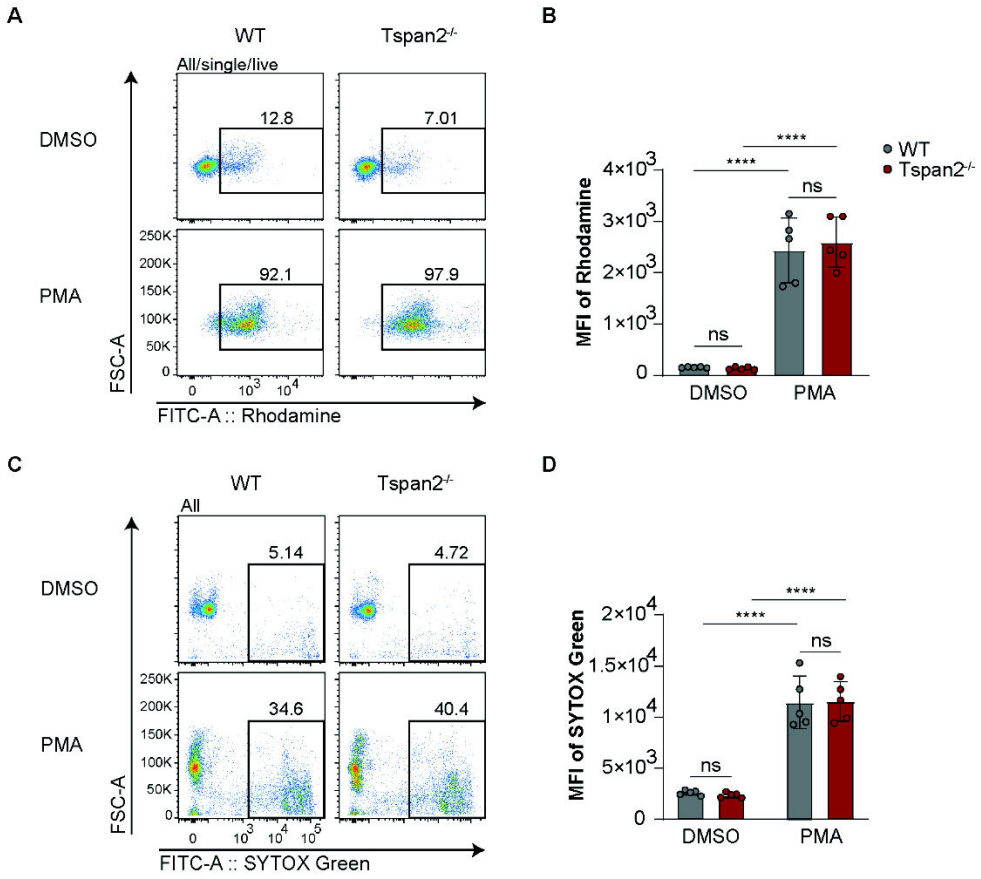

Figure 29: Neutrophils deficient in Tspan2 show normal ROS production and NETosis. Purified BM neutrophils were stimulated with 150 nM PMA and treated with 2 µM DHR-123 and 200 nM SYTOX Green, respectively, for analysis of intracellular ROS production and quantification of NETosis before analysis by flow cytometry. (A, C) Dot plots of ROS producing cells (Rhodamine$^+$) and those undergoing suicidal NETosis (SYTOX Green$^+$). (B, D) Bar plots showing respective quantifications of MFI.
ROS: Reactive oxygen species, NETs: Neutrophil extracellular traps, MFI: Mean fluorescence intensity. Shown are representatives of three independent experiments with n = 5. Statistics were performed in Prism v9 using one-way ANOVA.

aged neutrophils are cleared in healthy individuals. However, the release of NETs enables the capture of gram-negative and -positive bacteria and fungi, allowing clearance by other immune cells (Brinkmann and Zychlinsky, 2007). To investigate potential changes in NETosis during Tspan2-deficiency, neutrophils were stimulated with the potent NET-inducer PMA and further treated with a DNA-intercalating dye. However, flow cytometric quantification showed no significant difference in the amount of neutrophils forming NETs (Figure 29 C-D).

In summary, the functional *in vitro* analyses showed that the direct confrontation of neutrophils with *E. coli* bacteria is negatively affected by Tspan2. Interestingly, when analysing single mechanisms, including ROS production, phagocytosis and NETosis, no significant differences were observed.

5 Author contribution

Single cell RNA sequencing was performed in close collaboration with Tobias Lautwein (Lab of Prof. Karl Köhrer, Genomics & Transcriptomics Laboratory, Biological and Medical Research Center (BMFZ), Heinrich Heine University Düsseldorf). For scRNA sequencing cells were purified by myself and transported to BMFZ where single cell libraries were generated and 10X Genomics single cell data processing was performed by Tobias Lautwein (Lab of Prof. Karl Köhrer, Genomics & Transcriptomics Laboratory, Biological and Medical Research Center (BMFZ), Heinrich Heine University Düsseldorf). Downstream data analysis, including filtering, demultiplexing, data integration, cluster annotation, identification of DEGs and further analyses was done by myself.

Mass spectrometry screen was performed in close collaboration with Thomas Lenz (Lab of Prof. Kai Stühler, Molecular Proteomics Laboratory, BMFZ, Heinrich-Heine University, Düsseldorf). For mass spectrometry analysis co-IP samples were prepared by myself and transported to BMFZ. Sample processing, LC-MS/MS analysis, protein identification and quantification and generation of a volcano plot was performed by Thomas Lenz (Lab of Prof. Kai Stühler, Molecular Proteomics Laboratory, BMFZ, Heinrich-Heine University, Düsseldorf). Downstream data analysis, including STRING was done by myself.

All experiments that used Tspan2 reporter and knockout animals, except the *in vivo* studies, were performed in close collaboration with Prof. Judith Alferink (Department of Psychiatry, University of Münster). For these experiments, Rafael Leite-Dantas (Lab of Prof. Judith Alferink, Department of Psychiatry, University of Münster) kindly helped in preparing mouse organs. Mouse samples (e.g. femurs, tibiae, spleen, lymph nodes etc.) were prepared in Münster. Organ transport, cell preparation and assays were performed by myself.

Under-agarose chemotaxis and swarming assays were performed in cooperation with Katharina Glaser (Lab of Prof. Tim Lämmermann, Max Planck Institute of Immunobiology and Epigenetics, Freiburg, Germany).

Furthermore, the *Candida albicans* strain was kindly provided by the Ursula Fleig lab (Institute for Functional Genomics of Microorganisms, Heinrich Heine University Düsseldorf) which was used to perform *in vivo* studies.

Finally, Sonja Schavier (Lab of Prof. Stefanie Scheu, Institute of Medical Microbiology and Hospital Hygiene, Heinrich Heine University Düsseldorf) guided and helped in all *in vivo* studies. Culture and preparation of infection doses of *C. albicans* was performed by myself. I.v. and i.p. injections were performed by Sonja Schavier. Further monitoring and downstream analyses were done by myself.

6 Discussion

This doctoral thesis aimed to characterise the expression and function of Tspan2 in the innate immune system. For this purpose, Tspan2-reporter mice were initially used to determine Tspan2-expressing immune cell populations. Further a Tspan2-deficient mouse model was utilised in combination with modern scRNA sequencing analysis to determine functional aspects that are potentially impacted by Tspan2. Subsequently, those functions were investigated in *in vivo* and *in vitro* studies.

6.1 Tspan2 gene expression in neutrophils

Several immune cell populations were analysed to characterise the expression profile of Tspan2 across the investigated immune cells and to further target those highly expressing Tspan2 at steady state. In this doctoral thesis, the Tspan2 gene expression pattern was shown for the first time in selected primary and secondary lymphoid organs. The high expression levels in the murine bone marrow markedly differ from those found in the spleen and the inguinal and mesenteric lymph nodes, which, in contrast, exhibit only low overall gene expression of Tspan2. While in the spleen and bone marrow monocytes, macrophages and DC subtypes show low to moderate expression, neutrophils virtually hold exclusive rights to Tspan2 gene expression, as > 90 % of the neutrophils analysed were positive for Tspan2. Consequently, about half of the bone marrow cells were positive for Tspan2, given that neutrophils are most abundant in the bone marrow compared to the spleen and lymph nodes. Considering that ~ 10^7 neutrophils are produced daily in the bone marrow of mice and the vast majority expresses Tspan2, it exhibits great potential to modulate neutrophil functionality or their development and plasticity (Qu et al., 2023, Ng et al., 2019). So far multiple Tspans, including CD82, CD63, CD53, CD37 and CD9 (Wee et al., 2015, Källquist et al., 2008, Beinert et al., 2000, McGowan et al., 2022b, Bisson-Boutelliez et al., 2001) were shown to be expressed by and exert different functions in neutrophils. Nevertheless, monocyte/macrophage and DC populations were also found to express Tspan2 at certain levels depending on the tissue analysed. However, in addition to Tspan2, the expression of a variety of other Tspans is well described, including CD82, CD81, CD63, CD53, CD37 and CD9 in monocytes and macrophages. (Meyer-Wentrup et al., 2007, Suzuki et al., 2009, Hassuna et al., 2017, Tippett et al., 2013, McGowan et al., 2022b). While about as many Tspans were functionally analysed in dendritic cells, a study on the expression of Tspans in human and murine DC subtypes revealed the Tspan expression pattern as well as how this expression pattern differs between the two organisms. In the mouse, pDCs and cDC2s were shown to express Tspan2 mRNA, whereas cDC1s expressed Tspan2 mRNA only to a very small extent (Zuidscherwoude et al., 2017), which was also demonstrated within this doctoral thesis for BM-

and spleen-derived DCs. In human counterparts, however, only cDC2s expressed Tspan2 mRNA. A similar mouse versus human pattern was observed for CD9 mRNA, while CD151 and CD63 showed no difference in mRNA expression between mouse and human DCs (Zuidscherwoude et al., 2017).

Moreover, in this doctoral thesis it was shown with BM culture-derived DCs that the Tspan2 gene expression pattern can change drastically after stimulation. For instance, Flt3L-derived pDCs and cDCs possessed only a low percentage of Tspan2-expressing cells, which increased approximately fourfold after TLR9 stimulation with CpG. In contrast, the expression pattern was inverse when comparing unstimulated and stimulated GM-CSF-derived DCs. This again emphasizes that the functional network of Tspans is extremely complex and expression patterns only represent a snapshot of well-defined conditions. Nevertheless, they can provide valuable evidence of potentially modulated processes in comparable situations in a biological context.

6.2 Tspan2 potentially interacts with ITGB1 and CD63

Tspans are known as molecular organizers in the cellular membrane and can modulate a variety of processes by interacting with their partner proteins. By identifying Tspan2-specific interaction partners, further insights into the potential interactome of Tspan2 in Tspan-enriched microdomains can be obtained as well as predictions of potentially modulated functions based on the interaction partners. For this purpose, relatively undifferentiated cells, namely mouse embryonic fibroblasts, were used and lentivirally transduced with expression plasmids to generate cell lines that stably express EGFP-Tspan2 or EGFP. MS analysis of EGFP-enriched lysates resulted in approximately 4000 proteins that appear to associate with Tspan2. The most likely interaction partners were emphasized by increasing the stringency of selected parameters. It should be noted that not most proteins identified in this screen necessarily associate directly with Tspan2, but could also be located in the same microdomain. Interestingly, the STRING analysis links Tspan2 to the interaction network via CD63. On the one hand, a large number of these proteins could therefore interact with CD63 and thus merely indirectly with Tspan2. On the other hand, very little is known about the interactome of Tspan2, which is why no connection to other proteins can be established by the STRING algorithm without available information. Surprisingly, it is described that Tspan2 is expressed in rat oligodendrocytes in which a molecular link between CD9, CD81, ITGB1 and Tspan2 is described (Terada et al., 2002). Although the STRING database contains a repertoire of 5,090 organisms, no connection between Tspan2 and ITGB1 could be established by the algorithm (Szklarczyk et al., 2022). Furthermore, it also indicates no direct interaction between CD63 and ITGB1, only between ITGB1 and putative homologues of CD63, namely CD9 and CD81.

However, several studies have demonstrated an interaction of CD63 with ITGB1 (Jung et al., 2006, Radford et al., 1996).

Nevertheless, the MS screen provides a great overview of proteins that associate with Tspan2 in the membrane of MEFs and thus potentially interact with Tspan2 directly, independent of the cell type. Furthermore, the protein-associated ontologies suggest that Tspan2 may influence motility-related processes.

6.3 ScRNA sequencing revealed DEGs with high functional impact

6.3.1 Neutrophil recruitment behavior

Bone marrow neutrophils represent a confirmed heterogeneous population, ranging from the early proliferating neutrophils to the different stages of maturation, which were characterized by a variety of published conventional and maturation-specific markers (Grieshaber-Bouyer et al., 2021, Xie et al., 2020). Tspans typically do not possess natural ligands, with the exception of very few, for example the E2 envelope glycoprotein of HCV, which utilizes CD81 as an entry receptor (Wack et al., 2001), or the pregnancy-specific glycoprotein (PSG) 17, which directly binds CD9 for successful sperm-egg fusion (Ellerman et al., 2003). However, Tspans commonly associate laterally with other membrane proteins and influence both their localization and their functions. This ranges from proliferation and differentiation to the motility behavior of cells and their intercellular crosstalk. In the scRNA sequencing analysis, the vast majority of differentially expressed genes were found to be positively associated with motility and migration behavior. This is further supported by the significant overrepresentation of genes linked to functions such as chemotaxis and cytoskeletal organization.

In this context, the upregulated *Cxcl2* and the downregulated *Cxcr4*, *Ccr2* and *Ccl6* in the KO supported the hypothesis that Tspan2 influences the recruitment behavior and directional migration of neutrophils. CXCR4 and the antagonist CXCR2 are two GPCRs responsible for the retention of hematopoietic cells in the BM. Under normal circumstances, attenuation of CXCR4 signaling leads to the release of these cells into the circulation (Eash et al., 2010). Interestingly, we also found downregulation of *Ccl6*, a chemoattractant for monocytes and macrophages, and *Ccr2*, which can influence neutrophil recruitment behavior, although it is not known to be a primary neutrophil receptor (Reichel et al., 2005, LaFleur et al., 2004). CXCL2, on the other hand, plays a complex role in neutrophils by influencing their migration behavior at different levels (Lentini et al., 2020, Li et al., 2016a). A considerable source of the CXCL2 produced are the neutrophils themselves, which not only attracts other immune cells in a paracrine manner, but also exhibits an autocrine effect thereby triggering a gradual negative feedback mechanism, which, among others, causes the internalization of CXCR2 (Li et al., 2015). Furthermore, neutrophils require CXCL2 especially during recruitment, as they utilize CXCL2 to guide their way through the endothelial cell junctions during transmigration.

Dysregulation therefore results in either promotion of their transmigration capacity or in chronic neutrophil accumulation (Girbl et al., 2018). Along with CXCL1, CXCL2 is capable of binding glycosaminoglycans in the ECM, which enables the maintenance of a far-reaching chemoattractant gradient in tissues (Lentini et al., 2020).

Besides chemotactic signaling, other mechanisms such as integrin-mediated adhesion are also indispensable. Integrins are one of the best known and most important interaction partners of Tspans and collectively act as core players in adhesion- and ECM-associated processes. Interestingly, in the scRNA sequencing analysis, *Itgb2* was found to be strongly upregulated in Tspan2-deficient neutrophils. In this context, there was also a strong underrepresentation of genes related to the gene ontology of focal adhesions. These describe the direct interaction of the cytoskeleton of the cell with the ECM and significantly influence the ability of cell-cell communication and migration through large integrin-dominated clusters (Ivaska, 2012, Geiger and Yamada, 2011).

Two other Tspans have a very high evolutionary and molecular similarity to Tspan2, namely CD9 and CD81, which are also known as Tspan29 and Tspan28 (Dehler et al., 2023, Garcia-España et al., 2008). Given that these three Tspans belong to the same paralogue group, it has been hypothesized that they share a certain degree of functional similarity (Yaseen et al., 2017, Garcia-España et al., 2008). For CD9, it is known to organize lymphocyte function-associated antigen-1 (LFA-1) molecules on the cell surface in a large number of clusters, whereas in the absence of CD9, LFA-1 was found distributed over the entire surface, which consequently reduced adhesion capacities (Reyes et al., 2018). Given that LFA-1 is a heterodimeric integrin consisting of α_L (ITGAL) and β_2 (ITGB2) subunits, it is quite possible that Tspan2 exerts a comparable function to CD9 (Mezu-Ndubuisi and Maheshwari, 2021). A similar effect was observed in *Cd81*-deficient DCs, which were characterized by a defect in Rac signaling and associated with defective adhesion and migration (Quast et al., 2011). Small GTPases of the Rho family such as *Rac1* and *Cdc42* were found to be downregulated in Tspan2-deficient neutrophils in the scRNA sequencing, supporting the hypothesis that Tspan2 might exhibit mechanistic impairments comparable to CD9 and CD81.

Collectively, a number of genes were found to broadly facilitate processes such as chemotaxis and cytoskeletal organization in the absence of Tspan2, while others associating with GO terms of ECM organization and the formation of functional integrin-enriched focal adhesions were underrepresented. This suggests an imbalance between mechanisms of directed neutrophil recruitment and additional necessary interactions with other cells and the ECM. Thus, this may result in an impaired ability to migrate despite increased chemotaxis capacity.

6.3.2 Neutrophil subsets in the BM

As already mentioned, neutrophils mature in the bone marrow before they are released into the bloodstream. Accordingly, neutrophils were found in the bone marrow at different stages of their development, which could be precisely categorized using published markers (Grieshaber-Bouyer et al., 2021, Xie et al., 2020). Upon categorization of the neutrophil population approximately 55 % of the neutrophils were estimated to be fully mature. Beside the determination and analysis of DEGs within the complete neutrophil population, DEGs were additionally determined for each neutrophil subset. While the proliferating and early-stage to mature neutrophils showed very few genes that are differentially expressed, the mature 1 neutrophils represent the most impacted subset. In addition to a large number of genes which are shared among the subsets, they comprise 128 DEGs being unique. From this one might suggest that Tspan2 is impacting fully developed and mature neutrophils more than those of lower maturation grades. On the other hand, most DEGs were found in this subset which additionally represented the largest neutrophil population. Classification of a large population with a small set of markers might hide further heterogeneity within this subset which could lead to the determination of DEGs belonging to a slightly separate group of matured neutrophils.
However, as shown at the beginning Tspan2 gene expression was found in more than 90 % of neutrophils from the BM and spleen, decreasing the chance that Tspan2 gene expression and function is highly specific for one single neutrophil subset of a certain maturation grade.
The analysis of the individual maturation stages performed here is based on the expression profiles of the individual cells, representing the power of scRNA sequencing. By dividing the neutrophils into the maturation stages, not only the number of cells to be analyzed was substantially reduced, but also the resulting number of DEGs. Although DEGs could be reliably identified, they could not be functionally categorized by GO-term or GSE analysis as in the global analysis. A probable reason for this are the high p-adjusted values when determining the DEGs, which may be a result of the multiple testing correction that controls the FDR. These corrections are essential to reduce the number of false positives but may also have a greater impact on smaller datasets. Although the maturation stages were determined based on solid and published parameters, unknown factors within a subset can lead to heterogeneity, increasing statistical noise and variability and making it difficult to detect subtle expression changes.

6.3.3 Response to pathogens

With increasing maturation of neutrophils their functional capacities increase, including their ability to clear pathogens efficiently. When investigating potential influences of the absence of Tspan2 on neutrophil function, many key components required for successful clearance of pathogens were found differentially regulated. Among these, *Tlr4*, *Il1b* and other pro-

inflammatory mediators were significantly upregulated. Interestingly, it has been shown that *Cd9*-KO in macrophages leads to CD14-TLR4-mediated hyperactivation upon LPS stimulation. The absence of CD9 led on the one hand to higher basal levels of CD14 and on the other hand removed potential direct interaction of CD9 with CD14 in specific microdomains. This resulted in a loss of spatial separation of CD14 from TLR4 and an increase of functional CD14-TLR4 complexes (Suzuki et al., 2009). From this one might hypothesize that Tspan2 could comprise a similar mechanism for regulating the LPS response. Thus, in the absence of Tspan2, naive neutrophils might stay in a primed condition in which they can respond rapidly and effectively to bacterial infections, and even fungal pathogens, which, like *Candida albicans*, can be recognized via TLR4 (Netea et al., 2008, Figdor and van Spriel, 2010). To prevent an excessive or even chronic inflammation a balance might be established by the simultaneous upregulation of *Dusp1*, *Tnfaip3* and *Nfkbia*, which were found in the scRNA sequencing and are known to regulate and control inflammatory responses (Hammer et al., 2005, Lai et al., 2013, Rodrigues et al., 2008). This supports the idea that Tspan2-deficient BM neutrophils stay in a more active state, ready to react faster if needed but do not possess a strong dysfunctional phenotype.

6.4 Tspan2-deficient mice survive systemic *C. albicans* infection

Following the indication for an enhanced defense response against pathogens of bacterial and fungal origin, Tspan2-deficient and WT mice were challenged with high and low doses of i.v. administered *C. albicans*. Appropriate doses for this research question were chosen according to similarly performed experiments and time points of the onset of lethal symptoms were relatable (Taylor et al., 2007). Those receiving low doses (1 x 10^5 *C. albicans*) represented the control group of which all mice survived the infection. The second group received high doses (1 x 10^6 *C. albicans*) which were considered to be lethal leading to a mortality rate of 40-50 % in WT and Tspan2$^{-/-}$. Interestingly, only 10 % of females but 80 % of males died to the infection, suggesting that male mice are more susceptible to the infection independent of the genotype. This is an observation that has also been reported by others following i.v. administration of *C. albicans* (Arroyo-Mendoza et al., 2020). Although the exact mechanisms are still largely unknown, it is well documented that sex hormones, such as estrogens, progesterone and androgens, contribute decisively to the differences between the immune responses of the biological sexes. (Klein, 2000, Egger et al., 2022).

Additionally, Tspan2$^{-/-}$ mice showed a later onset of lethal symptoms compared to WT counterparts, indicating that the lack of Tspan2 might support their survival against systemic *C. albicans* infection by modulation of the immune response. Although not specifically on neutrophils, it has been shown that *Cd37*-deficient mice were better protected against *C. albicans* infection compared to WT counterparts (van Spriel et al., 2009). In contrast,

Cd82-deficient animals showed better survival of *C. albicans*, as the anti-fungal immune response of macrophages was significantly reduced (Tam et al., 2019).

Following both observations, the greater susceptibility of males and the later onset of lethal symptoms in Tspan2$^{-/-}$ mice, a larger group of males were challenged with an intermediate dose (5 x 10^5 *C. albicans*). While all Tspan2$^{-/-}$ mice survived the systemic infection, 20 % of WT developed lethal symptoms, supporting the previous hypothesis that the absence of Tspan2 has a positive impact on the arising immune response to *C. albicans* although it did not appear to be significant. This leads to the idea that perhaps Tspan2 and other Tspans expressed on neutrophils have redundant interaction partners and consequently redundant modulated functions. Thus, the loss of Tspan2 would affect certain functionalities, but not exclusively.

6.5 Neutrophil capacity to eliminate bacteria is influenced by Tspan2

Considering the recent findings that Tspan2-deficiency in neutrophils alters their expression profile with regard to pathogen recognition and functional response as well as the tendency towards a better survival against systemic *C. albicans* infection, functional capacities of Tspan2-deficient neutrophils were further investigated *in vitro*. Challenging them with the gram-negative bacteria *E. coli* resulted in a stronger kill capacity which supports the previously mentioned idea that the lack of Tspan2 is enhancing the immune response and in turn might increase the survival of the host to fungal and bacterial infection. This observation could be additionally explained by the scRNA sequencing findings that Tspan2-deficient neutrophils are potentially in a more active state and show, among other proinflammatory genes, higher expression of *Tlr4*. Furthermore, many other components need to contribute to this observation which cannot be fully explained to this time.

Although the overall advantage of Tspan2-deficiency in a direct bacterial encounter was demonstrated, individual key mechanisms such as phagocytosis, NET formation and ROS production remained surprisingly unchanged under the conditions tested. Within the scRNA sequencing part many genes were differentially expressed which associated with one or more functions analyzed here in vitro. However, a clear pattern, such as the upregulation of all genes related to phagocytosis, was not visible. Tspans are known to bind other membrane proteins and organize them into clusters which are called Tspan-enriched microdomains. With this unique feature they bring components of one signaling network, such as receptors and their modulators, in close proximity enabling a rapid extracellular to intracellular signal transduction (Kummer et al., 2020). While several interaction partners of Tspans could be classified into major groups, such as integrins, ICAMs, VCAMs, other Tspans and many more, one has to consider that every cell type at a given developmental stage has its own unique proteome making the Tspan-enriched microdomains a complex jigsaw puzzle (van Deventer et al., 2017,

Charrin et al., 2009). Furthermore, these microdomains typically consist of multiple Tspans indicating that the lack of one, here Tspan2, reduces the stability and structure of the microdomains potentially leading to reduced function of some interaction partners. Considering this, Tspan2 might not actively modulate one of these functions in neutrophils, raising the question why its loss increases the ability of neutrophils to eliminate *E. coli* bacteria more efficiently. Therefore, one might consider that the direct exposition to the pathogen makes the differences. However, there is no evidence to date that Tspans can interact directly with bacterial surface components, so it is more likely that direct Tspan interaction partners fulfil this role as it is described for multiple integrins in the context of viral infections (Storm et al., 2017, Rajan et al., 2018, Karam et al., 2020).

In Tspan2-deficient neutrophils, expression of *Tlr7* and *Ifitm* genes were significantly reduced which are directly related with the response to viruses. So far, only the interaction of CD82 (also known as Tspan27) with TLR7 was described, but without function, additionally considering that *Tlr7* expression was much lower in neutrophils compared to *Tlr4* (Khan et al., 2019). However, significantly decreased levels of genes involved in anti-viral responses might indicate a weaker initial response compared to the potentially beneficial priming of naive neutrophils to bacterial and fungal infections.

6.6 Tspan2 partially affects neutrophil recruitment and motility

Interestingly, although Tspan2-deficient neutrophils did not display altered intracellular ROS generation, for Tspan2 in human lung adenocarcinomas it was shown that Tspan2 scavenged intracellular ROS via CD44 and increased cell motility (Otsubo et al., 2014). CD44 was found to be strongly upregulated in the scRNA sequencing analysis, but unique to the M1_NTs subset, which accounted for about 40 % of the total population of neutrophils in the BM. Among the multiple DEGs and gene ontologies discussed in the scRNA sequencing section above, most of them were related to either cell motility, recruitment, migration or adhesion.

To investigate whether Tspan2 contributes to the recruitment machinery *in vivo*, *C. albicans* were administered i.p. into Tspan2-deficient and WT mice in order to establish a peritoneal inflammation over 4 hours. Among the immune cell that were recruited into the peritoneal cavity were only very few numbers of cDCs, followed by higher numbers of monocyte and macrophages. Neutrophils represented the immune cell population that were found most abundant in the peritoneal lavage fluid and in approximately 3-times higher numbers than monocyte and macrophages. However, there was no significant difference between the total amounts of neutrophils that were recruited in Tspan2-deficiency compared to WT. Interestingly, a similar study was performed featuring the Tspan CD37 and β_2 integrin-dependent adhesions on neutrophils. Surprisingly, *Cd37*-deficiency impaired neutrophil recruitment but β_2 integrin clustering remained unaffected. It was shown that the

lack of CD37 negatively influenced actin polymerization while accelerating β_2 integrin internalization and affecting further downstream processes (Wee et al., 2015).

Although in subsequent in vitro studies different mechanisms were featured, including the sensing of and reaction to attractions as well as the ability to efficiently remodel their cytoskeleton no significant impairments could be determined. In addition, when investigating neutrophil transmigration behavior, Tspan2-deficiency did not change the amount of cells that transmigrated in response to an attractant compared to WT counterparts. Interestingly, when conducting the same experiment with neutrophils from Tspan2 reporter mice, frequencies of Tspan2/EGFP-positive neutrophils were significantly increased among transmigrated cells. This would indicate that Tspan2 supports neutrophil transmigration behavior which is contradictory to the previously performed *in vivo* and *in vitro* studies. Following this observation, two possibilities are considered for explanation. The first and most likely explanation would be that the lack of Tspan2 on neutrophils might increase their adhesion capacity which was also indicated by the scRNA sequencing data. Stronger adhesion to the transwell membrane would result in lower amounts of neutrophils that transmigrate and finally detach which were counted as transmigrated cells. The second but less likely explanation could be that the transmigration process leads to an upregulation of Tspan2 resulting in increased frequencies of Tspan2/EGFP-positive neutrophils. However, the KO system is considered to be most reliable in questions of functionality.

6.7 Conclusion

This doctoral thesis shows for the first time that Tspan2 is expressed by several immune cells, including neutrophils which express Tspan2 at exclusively high levels.

Considering all aspects of the scRNA sequencing, Tspan2 potentially possesses a variety of influences on neutrophils. Tspan2-deficient neutrophils might be kept in a more active state enabling a quick release from the BM and following recruitment to sites of inflammation where they exert strong anti-microbial functions. However, important aspects of the recruitment machinery, such as the transmigration from the blood stream into the respective tissue might be negatively affected, slowing down the rapidly recruited neutrophils. Additionally, it has to be mentioned that on the one hand the functional situation is complex due to the huge amount of highly relevant differentially expressed genes. On the other hand, one has to take into consideration the heterogeneity in the degree of maturation of BM neutrophils, thus, mature neutrophil subsets showed higher amounts of unique genes differentially regulated in the absence of Tspan2.

From further studies one could conclude that Tspan2 negatively associates with the elimination of certain bacteria by neutrophils. However, despite several indications of Tspan2 influencing neutrophil motility, there were no significant changes found regarding their recruitment, migration and chemotaxis.

One has to take into account that Tspan2 is, as Tspans in general, a scaffolding protein that creates contacts with their partner proteins and mediates cluster formation. Therefore, many proteins within this cluster which rely primarily on Tspan2 might be abundant but lack effective functionality due to accelerated internalization, influences on actin polymerization or additional downstream processes. Furthermore, neutrophils express multiple Tspans from which one might consider the possibility of redundancy among their interaction partners.

6.8 Outlook

In order to continue building on the knowledge gained, a number of fundamental questions need to be answered through further studies. These include the conduction of *in vivo* studies in which Tspan2-deficient animals are challenged with bacterial pathogens such as gram-negative *Shigella* or gram-positive *Listeria* species, and eventually even with viruses. Especially with regard to bacterial infections, this doctoral thesis provides sufficient evidence that Tspan2-deficiency contributes to a greater protection of the host compared to WT.

Moreover, redundancy with regard to interaction partners and their related functions potentially occurs among the Tspan family. Therefore, first of all, Tspans that are expressed on neutrophils need to be identified together with their partner proteins shedding light into the complex network of Tspan-enriched microdomains on this specific cell type. Furthermore, it might be useful to focus on groups of fully matured neutrophils from the BM and the blood to evaluate differences in their interactome and anti-microbial functionalities during infection. Awareness of unique of redundant binding partners of Tspans may allow targeting of multiple Tspans in order to modulate a specific set of functions leading to rapid clearance of invading pathogens and increasing host survival.

7 Appendix

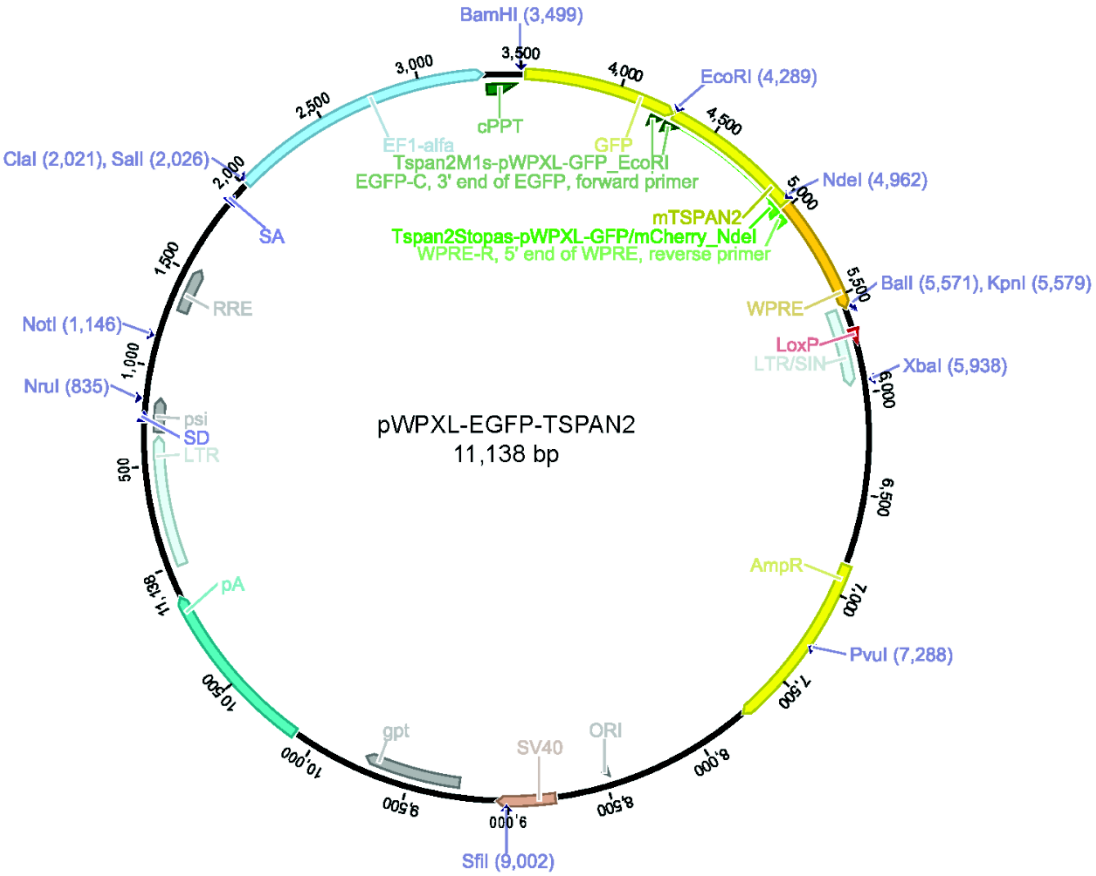

Supplementary Figure 1: Plasmid map of pWPXL-EGFP-TSPAN2. The Tspan2-encoding sequence was cloned to the C-terminus of the EGFP-encoding sequences including a 32-base pair (bp) spacer sequence between *Egfp* and Tspan2 gene sequences. Cells transfected with this plasmid results in expression of an EGFP-Tspan2 fusion protein.

List of figures

List of tables

List of supplementary figures

List of abbreviations

Abbreviation	Explanation
Acod1	Aconitate decarboxylase 1
Arhgap18	Rho GTPase activating protein 18
BAC	Bacterial artificial chromosome
BM	Bone marrow
BPI	Bactericidal permeability-increasing protein
C. albicans	Candida albicans
Camp	Antimicrobial cathelicidin peptide
Ccl6	C-C motif chemokine ligand 6
Ccr2	C-C motif chemokine receptor 2
cDCs	Conventional dendritic cells
CFU	Colony forming unit
CLR	C-type lectin receptor
Csf3r	Colony-stimulating factor 3 receptor
Cxcl2	C-X-C motif chemokine ligand 2
Cxcr4	C-X-C motif chemokine receptor 4
DAMP	Damage-associated molecular pattern
Data-dependent acquisition	DDA
DC	Dendritic cell
DEG	Differentially expressed genes
DHR-123	Dihydrorhodamine 123
Dusp1	Dual specificity phosphatase 1
E_NTs	Early stage neutrophils
ECM	Extracellular matrix
EGFP	Enhanced green fluorescent protein
Electron spray ionization	ESI
Elmo1	Engulfment and cell motility 1
EM_NTs	Early to mature stage neutrophils
Erdr1	Erythroid differentiation regulator 1

FC	Fold change
FDR	False discovery rate
Field asymmetric ion mobility spectrometry	FAIMS
fMLP	N-Formylmethionyl-leucyl-phenylalanine
Fpr2	Formyl peptide receptor 2
G-CSF	Granulocyte colony-stimulating factor
GO	Gene ontology
GPCR	G-protein coupled receptor
GSEA	Gene set enrichment analysis
HCMV	Human cytomegalovirus
HEK	Human embryonic kidney
HIV-1	Human immunodeficiency virus 1
HPV	Human papillomavirus
HTO	Hash tag oligos
I.p.	Intraperitoneally
I.v.	Intravenously
ICAM1	Intercellular adhesion molecule 1
Ifitm	Interferon-induced transmembrane
IFN	Type I interferon
IKK	IκB kinase
Il1b	Interleukin-1β
Itgb2	Integrin subunit beta 2
KEGG	Kyoto encyclopedia of genes and genomes
KO	Knockout
LB	Luria-Bertani
LFA1	Lymphocyte function-associated antigen 1
LTF	Lactoferrin
Ltf	Lactotransferrin
M1_NTs	Mature neutrophils 1

M2_NTs	Mature neutrophils 2
MACS	Magnetic activated cell sorting
MAPK	Mitogen-activated protein kinase
Mass spectrometry	MS
MEF	Mouse embryonic fibroblast
MFI	Mean fluorescence intensity
Mo/Ma	Monocytes/macrophages
MOI	Moiety of infection
MPO	Myeloperoxidase
Nanoscale liquid chromatography coupled to tandem mass spectrometry	NanoLC-MSMS
NE	Neutrophil elastase
NES	Normalized enrichment score
NET	Neutrophil extracellular trap
Nfkbia	Nuclear factor kappa-B inhibitor alpha
Ngp	Neutrophil granule protein
NK	Natural killer
NOD	Nucleotide-binding oligomerisation domain
NOX	NADPH oxidase
OD	Optical density
P_NTs	Proliferating neutrophils
PAMP	Pathogen-associated molecular pattern
PBS	Phosphate buffered saline
PCA	Principal component analysis
pDCs	Plasmacytoid dendritic cells
Plin2	Perilipin 2
PMA	Phorbol 12-myristate 13-acetate
Prdx5	Peroxiredoxin 5
PRR	Pattern recognition receptor

PSGL-1	P-selectin glycoprotein ligand-1
RIG	Retinoic acid-inducible gene
ROS	Reactive oxygen species
Rpl12	Ribosomal protein L12
scRNA	Single cell RNA
SDF-1	Stromal-derived factor-1
Selenok	Selenoprotein K
Significance analysis of microarrays	SAM
Single-pot, solid-phase-enhanced sample preparation	SP3
Slc7a11	Solute carrier family 7 member 11
SP	Spleen
SPF	Specific pathogen free
Standard deviation	S.d.
STRING	Search tool for recurring instances of neighboring genes
TLR	Toll-like receptor
Tmsb10	Thymosin beta-10
Tnfaip3	Tumour necrosis factor-alpha-induced protein 3
TNF-α	Tumor necrosis factor alpha
TRIF	TIR domain-containing adaptor inducing interferon-β
Tspan	Tetraspanin
Tuba1b	Tubulin alpha 1b
UAA	Under-agarose assay
UMAP	Uniform manifold approximation and projection
VCAM	Vascular cell adhesion molecule
WT	Wild type

8 References

ÁGUILA, S., DE LOS REYES-GARCÍA, A. M., FERNÁNDEZ-PÉREZ, M. P., REGUILÓN-GALLEGO, L., ZAPATA-MARTÍNEZ, L., RUIZ-LORENTE, I., VICENTE, V., GONZÁLEZ-CONEJERO, R. & MARTÍNEZ, C. 2021. MicroRNAs as New Regulators of Neutrophil Extracellular Trap Formation. *Int J Mol Sci,* 22.

ARAN, D., LOONEY, A. P., LIU, L., WU, E., FONG, V., HSU, A., CHAK, S., NAIKAWADI, R. P., WOLTERS, P. J., ABATE, A. R., BUTTE, A. J. & BHATTACHARYA, M. 2019. Reference-based analysis of lung single-cell sequencing reveals a transitional profibrotic macrophage. *Nature Immunology,* 20**,** 163-172.

ARROYO-MENDOZA, M., PERAZA, K., OLSON, J., ADLER-MOORE, J. P. & BUCKLEY, N. E. 2020. Effect of testosterone and estrogen supplementation on the resistance to systemic Candida albicans infection in mice. *Heliyon,* 6**,** e04437.

BAEUERLE, P. A. & BALTIMORE, D. 1988. IκB: a Specific Inhibitor of the NF-κB Transcription Factor. *Science,* 242**,** 540-546.

BARREIRO, O., YÁÑEZ-MÓ, M., SALA-VALDÉS, M., GUTIÉRREZ-LÓPEZ, M. D., OVALLE, S., HIGGINBOTTOM, A., MONK, P. N., CABAÑAS, C. & SÁNCHEZ-MADRID, F. 2005. Endothelial tetraspanin microdomains regulate leukocyte firm adhesion during extravasation. *Blood,* 105**,** 2852-2861.

BARTNECK, M. & WANG, J. 2019. Therapeutic Targeting of Neutrophil Granulocytes in Inflammatory Liver Disease. *Frontiers in Immunology,* 10.

BASSANI, S. & CINGOLANI, L. A. 2012. Tetraspanins: Interactions and interplay with integrins. *The International Journal of Biochemistry & Cell Biology,* 44**,** 703-708.

BEATTY, W. L. 2006. Trafficking from CD63-positive late endocytic multivesicular bodies is essential for intracellular development of Chlamydia trachomatis. *Journal of Cell Science,* 119**,** 350-359.

BEINERT, T., MÜNZING, S., POSSINGER, K. & KROMBACH, F. 2000. Increased expression of the tetraspanins CD53 and CD63 on apoptotic human neutrophils. *Journal of Leukocyte Biology,* 67**,** 369-373.

BENAYOUN, B. A., POLLINA, E. A., SINGH, P. P., MAHMOUDI, S., HAREL, I., CASEY, K. M., DULKEN, B. W., KUNDAJE, A. & BRUNET, A. 2019. Remodeling of epigenome and transcriptome landscapes with aging in mice reveals widespread induction of inflammatory responses. *Genome Research,* 29**,** 697-709.

BERDITCHEVSKI, F. 2001. Complexes of tetraspanins with integrins: more than meets the eye. *Journal of Cell Science,* 114**,** 4143-4151.

BIRLING, M.-C., TAIT, S., HARDY, R. J. & BROPHY, P. J. 1999. A Novel Rat Tetraspan Protein in Cells of the Oligodendrocyte Lineage. *Journal of Neurochemistry,* 73**,** 2600-2608.

BISSON-BOUTELLIEZ, C., MILLER, N., DEMARCH, D. & BENE, M. C. 2001. CD9 and HLA-DR expression by crevicular epithelial cells and polymorphonuclear neutrophils in periodontal disease. *Journal of Clinical Periodontology,* 28**,** 650-656.

BOND, D. R., KAHL, R., BRZOZOWSKI, J. S., JANKOWSKI, H., NAUDIN, C., PARIYAR, M., AVERY-KIEJDA, K. A., SCARLETT, C. J., BOUCHEIX, C., MULLER, W. J., ASHMAN, L. K., CAIRNS, M. J., ROSELLI, S. & WEIDENHOFER, J. 2020. Tetraspanin CD9 is Regulated by miR-518f-5p and Functions in Breast Cell Migration and In Vivo Tumor Growth. *Cancers,* 12**,** 795.

BORREGAARD, N. & COWLAND, J. B. 1997. Granules of the Human Neutrophilic Polymorphonuclear Leukocyte. *Blood,* 89**,** 3503-3521.

BORREGAARD, N., SØRENSEN, O. E. & THEILGAARD-MÖNCH, K. 2007. Neutrophil granules: a library of innate immunity proteins. *Trends in Immunology,* 28**,** 340-345.

BOUCHEIX, C. & RUBINSTEIN, E. 2001. Tetraspanins. *Cellular and Molecular Life Sciences CMLS,* 58**,** 1189-1205.

BRIMACOMBE, C. L., WILSON, G. K., HÜBSCHER, S. G., MCKEATING, J. A. & FARQUHAR, M. J. 2014. A Role for CD81 and Hepatitis C Virus in Hepatoma Mobility. *Viruses,* 6**,** 1454-1472.

BRINKMANN, V. & ZYCHLINSKY, A. 2007. Beneficial suicide: why neutrophils die to make NETs. *Nature Reviews Microbiology,* 5**,** 577-582.

BURN, G. L., FOTI, A., MARSMAN, G., PATEL, D. F. & ZYCHLINSKY, A. 2021. The Neutrophil. *Immunity,* 54**,** 1377-1391.

CASTRO-SANCHEZ, L., SOTO-GUZMAN, A., NAVARRO-TITO, N., MARTINEZ-OROZCO, R. & SALAZAR, E. P. 2010. Native type IV collagen induces cell migration through a CD9 and DDR1-dependent pathway in MDA-MB-231 breast cancer cells. *European Journal of Cell Biology,* 89**,** 843-852.

CHARRIN, S., LE NAOUR, F., SILVIE, O., MILHIET, P.-E., BOUCHEIX, C. & RUBINSTEIN, E. 2009. Lateral organization of membrane proteins: tetraspanins spin their web. *Biochemical Journal,* 420**,** 133-154.

CHEONG, C. M., CHOW, A. W. S., FITTER, S., HEWETT, D. R., MARTIN, S. K., WILLIAMS, S. A., TO, L. B., ZANNETTINO, A. C. W. & VANDYKE, K. 2015. Tetraspanin 7 (TSPAN7) expression is upregulated in multiple myeloma patients and inhibits myeloma tumour development in vivo. *Experimental Cell Research,* 332**,** 24-38.

CHERUKURI, A., SHOHAM, T., SOHN, H. W., LEVY, S., BROOKS, S., CARTER, R. & PIERCE, S. K. 2004. The Tetraspanin CD81 Is Necessary for Partitioning of Coligated CD19/CD21-B Cell Antigen Receptor Complexes into Signaling-Active Lipid Rafts 1. *The Journal of Immunology,* 172**,** 370-380.

CHOW, J. C., YOUNG, D. W., GOLENBOCK, D. T., CHRIST, W. J. & GUSOVSKY, F. 1999. Toll-like Receptor-4 Mediates Lipopolysaccharide-induced Signal Transduction*. *Journal of Biological Chemistry,* 274**,** 10689-10692.

CHRISTOPHER, M. J. & LINK, D. C. 2007. Regulation of neutrophil homeostasis. *Curr Opin Hematol,* 14**,** 3-8.

CLARKE, G., GOLDBERG, A. F. X., VIDGEN, D., COLLINS, L., PLODER, L., SCHWARZ, L., MOLDAY, L. L., ROSSANT, J., SZÉL, Á., MOLDAY, R. S., BIRCH, D. G. & MCINNES, R. R. 2000. Rom-1 is required for rod photoreceptor viability and the regulation of disk morphogenesis. *Nature Genetics,* 25**,** 67-73.

D'ORAZI, G. 2023. p53 Function and Dysfunction in Human Health and Diseases. *Biomolecules,* 13.

DANG, E. V., LEI, S., RADKOV, A., VOLK, R. F., ZARO, B. W. & MADHANI, H. D. 2022. Secreted fungal virulence effector triggers allergic inflammation via TLR4. *Nature,* 608**,** 161-167.

DE FILIPPO, K. & RANKIN, S. M. 2018. CXCR4, the master regulator of neutrophil trafficking in homeostasis and disease. *European Journal of Clinical Investigation,* 48**,** e12949.

DE MONASTERIO-SCHRADER, P., PATZIG, J., MÖBIUS, W., BARRETTE, B., WAGNER, T. L., KUSCH, K., EDGAR, J. M., BROPHY, P. J. & WERNER, H. B. 2013. Uncoupling of neuroinflammation from axonal degeneration in mice lacking the myelin protein tetraspanin-2. *Glia,* 61**,** 1832-1847.

DEHLER, C. E., BOUDINOT, P., COLLET, B. & MARTIN, S. M. 2023. Phylogeny and expression of tetraspanin CD9 paralogues in rainbow trout (Oncorhynchus mykiss). *Developmental & Comparative Immunology,* 146**,** 104735.

DELEO, F. R. & ALLEN, L. H. 2020. Phagocytosis and neutrophil extracellular traps. *Fac Rev,* 9**,** 25.

DELL'ANGELICA, E. C., MULLINS, C., CAPLAN, S. & BONIFACINO, J. S. 2000. Lysosome-related organelles. *The FASEB Journal,* 14**,** 1265-1278.

DEMARIA, M. C., YEUNG, L., PEETERS, R., WEE, J. L., MIHALJCIC, M., JONES, E. L., NASA, Z., ALDERUCCIO, F., HALL, P., SMITH, B. C., BINGER, K. J., HAMMERLING, G., KWOK, H. F., NEWMAN, A., AGER, A., VAN SPRIEL, A., HICKEY, M. J. & WRIGHT, M. D. 2020. Tetraspanin CD53 Promotes Lymphocyte Recirculation by Stabilizing L-Selectin Surface Expression. *iScience,* 23**,** 101104.

DONG, Y., TANG, X., ZHAO, W., LIU, P., YU, W., REN, J., CHEN, Y., CUI, Y., CHEN, J. & LIU, Y. 2024. TSPAN4 influences glioblastoma progression through regulating EGFR stability. *iScience,* 27.

EASH, K. J., GREENBAUM, A. M., GOPALAN, P. K. & LINK, D. C. 2010. CXCR2 and CXCR4 antagonistically regulate neutrophil trafficking from murine bone marrow. *The Journal of Clinical Investigation,* 120**,** 2423-2431.

EGGER, M., HOENIGL, M., THOMPSON III, G. R., CARVALHO, A. & JENKS, J. D. 2022. Let's talk about sex characteristics—As a risk factor for invasive fungal diseases. *Mycoses,* 65**,** 599-612.

EL-BENNA, J., HURTADO-NEDELEC, M., MARZAIOLI, V., MARIE, J. C., GOUGEROT-POCIDALO, M. A. & DANG, P. M. 2016. Priming of the neutrophil respiratory burst: role in host defense and inflammation. *Immunol Rev,* 273**,** 180-93.

ELLERMAN, D. A., HA, C., PRIMAKOFF, P., MYLES, D. G. & DVEKSLER, G. S. 2003. Direct Binding of the Ligand PSG17 to CD9 Requires a CD9 Site Essential for Sperm-Egg Fusion. *Molecular Biology of the Cell,* 14**,** 5098-5103.

EVRARD, M., KWOK, I. W. H., CHONG, S. Z., TENG, K. W. W., BECHT, E., CHEN, J., SIEOW, J. L., PENNY, H. L., CHING, G. C., DEVI, S., ADROVER, J. M., LI, J. L. Y., LIONG, K. H., TAN, L., POON, Z., FOO, S., CHUA, J. W., SU, I. H., BALABANIAN, K., BACHELERIE, F., BISWAS, S. K., LARBI, A., HWANG, W. Y. K., MADAN, V., KOEFFLER, H. P., WONG, S. C., NEWELL, E. W., HIDALGO, A., GINHOUX, F. & NG, L. G. 2018. Developmental Analysis of Bone Marrow Neutrophils Reveals Populations Specialized in Expansion, Trafficking, and Effector Functions. *Immunity,* 48**,** 364-379.e8.

FAST, L. A., LIEBER, D., LANG, T. & FLORIN, L. 2017. Tetraspanins in infections by human cytomegalo- and papillomaviruses. *Biochemical Society Transactions,* 45**,** 489-497.

FAURSCHOU, M. & BORREGAARD, N. 2003. Neutrophil granules and secretory vesicles in inflammation. *Microbes and Infection,* 5**,** 1317-1327.

FEIGELSON, S. W., GRABOVSKY, V., SHAMRI, R., LEVY, S. & ALON, R. 2003. The CD81 Tetraspanin Facilitates Instantaneous Leukocyte VLA-4 Adhesion Strengthening to Vascular Cell Adhesion Molecule 1 (VCAM-1) under Shear Flow*. *Journal of Biological Chemistry,* 278**,** 51203-51212.

FERWERDA, B., FERWERDA, G., PLANTINGA, T. S., WILLMENT, J. A., SPRIEL, A. B. V., VENSELAAR, H., ELBERS, C. C., JOHNSON, M. D., CAMBI, A., HUYSAMEN, C., JACOBS, L., JANSEN, T., VERHEIJEN, K., MASTHOFF, L., MORRÉ, S. A., VRIEND, G., WILLIAMS, D. L., PERFECT, J. R., JOOSTEN, L. A. B., WIJMENGA, C., MEER, J. W. M. V. D., ADEMA, G. J., KULLBERG, B. J., BROWN, G. D. & NETEA, M. G. 2009. Human Dectin-1 Deficiency and Mucocutaneous Fungal Infections. *New England Journal of Medicine,* 361**,** 1760-1767.

FIGDOR, C. G. & VAN SPRIEL, A. B. 2010. Fungal pattern-recognition receptors and tetraspanins: partners on antigen-presenting cells. *Trends in Immunology,* 31**,** 91-96.

FILIPPI, M.-D. 2016. Chapter Two - Mechanism of Diapedesis: Importance of the Transcellular Route. *In:* ALT, F. W. (ed.) *Advances in Immunology.* Academic Press.

FRANCO, M., MURATORI, C., CORSO, S., TENAGLIA, E., BERTOTTI, A., CAPPARUCCIA, L., TRUSOLINO, L., COMOGLIO, P. M. & TAMAGNONE, L. 2010. The Tetraspanin CD151 Is Required for Met-dependent Signaling and Tumor Cell Growth*. *Journal of Biological Chemistry,* 285**,** 38756-38764.

FRIEDL, P. & WOLF, K. 2009. Plasticity of cell migration: a multiscale tuning model. *Journal of Cell Biology,* 188**,** 11-19.

FURUYA, M., KATO, H., NISHIMURA, N., ISHIWATA, I., IKEDA, H., ITO, R., YOSHIKI, T. & ISHIKURA, H. 2005. Down-regulation of CD9 in Human Ovarian Carcinoma Cell Might Contribute to Peritoneal Dissemination: Morphologic Alteration and Reduced Expression of β1 Integrin Subsets. *Cancer Research,* 65**,** 2617-2625.

FURZE, R. C. & RANKIN, S. M. 2008. The role of the bone marrow in neutrophil clearance under homeostatic conditions in the mouse. *The FASEB Journal,* 22**,** 3111-3119.

GARCIA-ESPAÑA, A., CHUNG, P.-J., SARKAR, I. N., STINER, E., SUN, T.-T. & DESALLE, R. 2008. Appearance of new tetraspanin genes during vertebrate evolution. *Genomics,* 91**,** 326-334.

GEIGER, B. & YAMADA, K. M. 2011. Molecular Architecture and Function of Matrix Adhesions. *Cold Spring Harbor Perspectives in Biology,* 3.

GIRBL, T., LENN, T., PEREZ, L., ROLAS, L., BARKAWAY, A., THIRIOT, A., DEL FRESNO, C., LYNAM, E., HUB, E., THELEN, M., GRAHAM, G., ALON, R., SANCHO, D., VON ANDRIAN, U. H., VOISIN, M.-B., ROT, A. & NOURSHARGH, S. 2018. Distinct Compartmentalization of the Chemokines CXCL1 and CXCL2 and the Atypical

Receptor ACKR1 Determine Discrete Stages of Neutrophil Diapedesis. *Immunity,* 49**,** 1062-1076.e6.

GRÄßEL, L., FAST, L. A., SCHEFFER, K. D., BOUKHALLOUK, F., SPODEN, G. A., TENZER, S., BOLLER, K., BAGO, R., RAJESH, S., OVERDUIN, M., BERDITCHEVSKI, F. & FLORIN, L. 2016. The CD63-Syntenin-1 Complex Controls Post-Endocytic Trafficking of Oncogenic Human Papillomaviruses. *Scientific Reports,* 6**,** 32337.

GREENBERG, Z. J., MONLISH, D. A., BARTNETT, R. L., YANG, Y., SHEN, G., LI, W., BEDNARSKI, J. J. & SCHUETTPELZ, L. G. 2020. The Tetraspanin CD53 Regulates Early B Cell Development by Promoting IL-7R Signaling. *The Journal of Immunology,* 204**,** 58-67.

GRIESHABER-BOUYER, R., RADTKE, F. A., CUNIN, P., STIFANO, G., LEVESCOT, A., VIJAYKUMAR, B., NELSON-MANEY, N., BLAUSTEIN, R. B., MONACH, P. A. & NIGROVIC, P. A. 2021. The neutrotime transcriptional signature defines a single continuum of neutrophils across biological compartments. *Nat Commun,* 12**,** 2856.

GRIFFIN , F. M., JR, GRIFFIN , J. A., LEIDER , J. E. & SILVERSTEIN , S. C. 1975. Studies on the mechanism of phagocytosis. I. Requirements for circumferential attachment of particle-bound ligands to specific receptors on the macrophage plasma membrane. *Journal of Experimental Medicine,* 142**,** 1263-1282.

GUYON, A. 2014. CXCL12 chemokine and its receptors as major players in the interactions between immune and nervous systems. *Front Cell Neurosci,* 8**,** 65.

HAMMER , M., MAGES , J. R., DIETRICH , H., SERVATIUS , A., HOWELLS , N., CATO , A. C. B. & LANG , R. 2005. Dual specificity phosphatase 1 (DUSP1) regulates a subset of LPS-induced genes and protects mice from lethal endotoxin shock. *Journal of Experimental Medicine,* 203**,** 15-20.

HAO, Y., STUART, T., KOWALSKI, M. H., CHOUDHARY, S., HOFFMAN, P., HARTMAN, A., SRIVASTAVA, A., MOLLA, G., MADAD, S., FERNANDEZ-GRANDA, C. & SATIJA, R. 2023. Dictionary learning for integrative, multimodal and scalable single-cell analysis. *Nat Biotechnol*.

HASSUNA, N. A., MONK, P. N., ALI, F., READ, R. C. & PARTRIDGE, L. J. 2017. A role for the tetraspanin proteins in Salmonella infection of human macrophages. *Journal of Infection,* 75**,** 115-124.

HEIT, B. & KUBES, P. 2003. Measuring Chemotaxis and Chemokinesis: The Under-Agarose Cell Migration Assay. *Science's STKE,* 2003**,** pl5-pl5.

HEMLER, M. E. 2003. Tetraspanin Proteins Mediate Cellular Penetration, Invasion, and Fusion Events and Define a Novel Type of Membrane Microdomain. *Annual Review of Cell and Developmental Biology,* 19**,** 397-422.

HEMLER, M. E. 2005. Tetraspanin functions and associated microdomains. *Nature Reviews Molecular Cell Biology,* 6**,** 801-811.

HONG, I.-K., BYUN, H.-J., LEE, J., JIN, Y.-J., WANG, S.-J., JEOUNG, D.-I., KIM, Y.-M. & LEE, H. 2014. The Tetraspanin CD81 Protein Increases Melanoma Cell Motility by Up-regulating Metalloproteinase MT1-MMP Expression through the Pro-oncogenic Akt-dependent Sp1 Activation Signaling Pathways*. *Journal of Biological Chemistry,* 289**,** 15691-15704.

HOPKE, A., LIN, T., SCHERER, A. K., SHAY, A. E., TIMMER, K. D., WILSON-MIFSUD, B., MANSOUR, M. K., SERHAN, C. N., IRIMIA, D. & HURLEY, B. P. 2022. Transcellular biosynthesis of leukotriene B(4) orchestrates neutrophil swarming to fungi. *iScience,* 25**,** 105226.

HUGHES, C. S., MOGGRIDGE, S., MÜLLER, T., SORENSEN, P. H., MORIN, G. B. & KRIJGSVELD, J. 2019. Single-pot, solid-phase-enhanced sample preparation for proteomics experiments. *Nature Protocols,* 14**,** 68-85.

HUTTLIN, E. L., BRUCKNER, R. J., PAULO, J. A., CANNON, J. R., TING, L., BALTIER, K., COLBY, G., GEBREAB, F., GYGI, M. P., PARZEN, H., SZPYT, J., TAM, S., ZARRAGA, G., PONTANO-VAITES, L., SWARUP, S., WHITE, A. E., SCHWEPPE, D. K., RAD, R., ERICKSON, B. K., OBAR, R. A., GURUHARSHA, K. G., LI, K., ARTAVANIS-TSAKONAS, S., GYGI, S. P. & HARPER, J. W. 2017. Architecture of

the human interactome defines protein communities and disease networks. *Nature,* 545**,** 505-509.
HWANG, I. H., PARK, J., KIM, J. M., KIM, S. I., CHOI, J. S., LEE, K. B., YUN, S. H., LEE, M. G., PARK, S. J. & JANG, I. S. 2016. Tetraspanin-2 promotes glucotoxic apoptosis by regulating the JNK/β-catenin signaling pathway in human pancreatic β cells. *Faseb j,* 30**,** 3107-16.
HYNES, R. O. 2002. Integrins: Bidirectional, Allosteric Signaling Machines. *Cell,* 110**,** 673-687.
IDZERDA, R. L., CARTER, W. G., NOTTENBURG, C., WAYNER, E. A., GALLATIN, W. M. & ST JOHN, T. 1989. Isolation and DNA sequence of a cDNA clone encoding a lymphocyte adhesion receptor for high endothelium. *Proceedings of the National Academy of Sciences,* 86**,** 4659-4663.
INOUE, M. & SHINOHARA, M. L. 2014. Clustering of Pattern Recognition Receptors for Fungal Detection. *PLOS Pathogens,* 10**,** e1003873.
ISHIBASHI, T., DING, L., IKENAKA, K., INOUE, Y., MIYADO, K., MEKADA, E. & BABA, H. 2004. Tetraspanin Protein CD9 Is a Novel Paranodal Component Regulating Paranodal Junctional Formation. *The Journal of Neuroscience,* 24**,** 96-102.
IVASKA, J. 2012. Unanchoring integrins in focal adhesions. *Nature Cell Biology,* 14**,** 981-983.
JANEWAY, C. A., JR. & MEDZHITOV, R. 2002. Innate immune recognition. *Annu Rev Immunol,* 20**,** 197-216.
JANKOVIČOVÁ, J., NEUEROVÁ, Z., SEČOVÁ, P., BARTÓKOVÁ, M., BUBENÍČKOVÁ, F., KOMRSKOVÁ, K., POSTLEROVÁ, P. & ANTALÍKOVÁ, J. 2020. Tetraspanins in mammalian reproduction: spermatozoa, oocytes and embryos. *Medical Microbiology and Immunology,* 209**,** 407-425.
JIANG, X.-P., ZHANG, D.-X., TENG, M., ZHANG, Q., ZHANG, J.-P. & HUANG, Y.-S. 2013. Downregulation of CD9 in Keratinocyte Contributes to Cell Migration via Upregulation of Matrix Metalloproteinase-9. *PLOS ONE,* 8**,** e77806.
JIANG, X., ZHANG, J. & HUANG, Y. 2015. Tetraspanins in Cell Migration. *Cell Adhesion & Migration,* 9**,** 406-415.
JOVANOVIĆ, M., STANKOVIĆ, T., STOJKOVIĆ BURIĆ, S., BANKOVIĆ, J., DINIĆ, J., LJUJIĆ, M., PEŠIĆ, M. & DRAGOJ, M. 2022. Decreased TSPAN14 Expression Contributes to NSCLC Progression. *Life,* 12**,** 1291.
JUNG, K. K., LIU, X. W., CHIRCO, R., FRIDMAN, R. & KIM, H. R. C. 2006. Identification of CD63 as a tissue inhibitor of metalloproteinase‐1 interacting cell surface protein. *The EMBO Journal,* 25**,** 3934-3942.
JUNGE, H. J., YANG, S., BURTON, J. B., PAES, K., SHU, X., FRENCH, D. M., COSTA, M., RICE, D. S. & YE, W. 2009. TSPAN12 Regulates Retinal Vascular Development by Promoting Norrin- but Not Wnt-Induced FZD4/β-Catenin Signaling. *Cell,* 139**,** 299-311.
KAJI, K., ODA, S., SHIKANO, T., OHNUKI, T., UEMATSU, Y., SAKAGAMI, J., TADA, N., MIYAZAKI, S. & KUDO, A. 2000. The gamete fusion process is defective in eggs of Cd9-deficient mice. *Nature Genetics,* 24**,** 279-282.
KÄLLQUIST, L., HANSSON, M., PERSSON, A.-M., JANSSEN, H., CALAFAT, J., TAPPER, H. & OLSSON, I. 2008. The tetraspanin CD63 is involved in granule targeting of neutrophil elastase. *Blood,* 112**,** 3444-3454.
KARAM, J., MÉRESSE, S., KREMER, L. & DAHER, W. 2020. The roles of tetraspanins in bacterial infections. *Cellular Microbiology,* 22**,** e13260.
KARAMATIC CREW, V., BURTON, N., KAGAN, A., GREEN, C. A., LEVENE, C., FLINTER, F., BRADY, R. L., DANIELS, G. & ANSTEE, D. J. 2004. CD151, the first member of the tetraspanin (TM4) superfamily detected on erythrocytes, is essential for the correct assembly of human basement membranes in kidney and skin. *Blood,* 104**,** 2217-2223.
KAWAI, T. & AKIRA, S. 2006. TLR signaling. *Cell Death & Differentiation,* 13**,** 816-825.
KAWASAKI, T. & KAWAI, T. 2014. Toll-Like Receptor Signaling Pathways. *Frontiers in Immunology,* 5.

KHAN, N. S., LUKASON, D. P., FELIU, M., WARD, R. A., LORD, A. K., REEDY, J. L., RAMIREZ-ORTIZ, Z. G., TAM, J. M., KASPERKOVITZ, P. V., NEGORO, P. E., VYAS, T. D., XU, S., BRINKMANN, M. M., ACHARAYA, M., ARTAVANIS-TSAKONAS, K., FRICKEL, E. M., BECKER, C. E., DAGHER, Z., KIM, Y. M., LATZ, E., PLOEGH, H. L., MANSOUR, M. K., MIRANTI, C. K., LEVITZ, S. M. & VYAS, J. M. 2019. CD82 controls CpG-dependent TLR9 signaling. *Faseb j,* 33**,** 12500-12514.

KIENLE, K., GLASER, K. M., EICKHOFF, S., MIHLAN, M., KNÖPPER, K., REÁTEGUI, E., EPPLE, M. W., GUNZER, M., BAUMEISTER, R., TARRANT, T. K., GERMAIN, R. N., IRIMIA, D., KASTENMÜLLER, W. & LÄMMERMANN, T. 2021. Neutrophils self-limit swarming to contain bacterial growth in vivo. *Science,* 372.

KIM, M., LU, R. J. & BENAYOUN, B. A. 2022. Single-cell RNA-seq of primary bone marrow neutrophils from female and male adult mice. *Scientific Data,* 9**,** 442.

KIMBRELL, D. A. & BEUTLER, B. 2001. The evolution and genetics of innate immunity. *Nature Reviews Genetics,* 2**,** 256-267.

KLEIDONAS, D., KIRSCH, M., ANDRIEUX, G., PFEIFER, D., BOERRIES, M. & VLACHOS, A. 2023. Microglia modulate TNFα-mediated synaptic plasticity. *Glia,* 71**,** 2117-2136.

KLEIN, S. L. 2000. The effects of hormones on sex differences in infection: from genes to behavior. *Neuroscience & Biobehavioral Reviews,* 24**,** 627-638.

KNOBELOCH, K. P., WRIGHT, M. D., OCHSENBEIN, A. F., LIESENFELD, O., LÖHLER, J., ZINKERNAGEL, R. M., HORAK, I. & ORINSKA, Z. 2000. Targeted inactivation of the tetraspanin CD37 impairs T-cell-dependent B-cell response under suboptimal costimulatory conditions. *Mol Cell Biol,* 20**,** 5363-9.

KOLOSOWSKA, N., KEUTERS, M. H., WOJCIECHOWSKI, S., KEKSA-GOLDSTEINE, V., LAINE, M., MALM, T., GOLDSTEINS, G., KOISTINAHO, J. & DHUNGANA, H. 2019. Peripheral Administration of IL-13 Induces Anti-inflammatory Microglial/Macrophage Responses and Provides Neuroprotection in Ischemic Stroke. *Neurotherapeutics,* 16**,** 1304-1319.

KRAVETS, E., DEGRANDI, D., WEIDTKAMP-PETERS, S., RIES, B., KONERMANN, C., FELEKYAN, S., DARGAZANLI, J. M., PRAEFCKE, G. J. K., SEIDEL, C. A. M., SCHMITT, L., SMITS, S. H. J. & PFEFFER, K. 2012. The GTPase activity of murine guanylate-binding protein 2 (mGBP2) controls the intracellular localization and recruitment to the parasitophorous vacuole of Toxoplasma gondii. *The Journal of biological chemistry,* 287**,** 27452-27466.

KUMAGAI, Y. & AKIRA, S. 2010. Identification and functions of pattern-recognition receptors. *Journal of Allergy and Clinical Immunology,* 125**,** 985-992.

KUMAR, H., KAWAI, T. & AKIRA, S. 2011. Pathogen recognition by the innate immune system. *Int Rev Immunol,* 30**,** 16-34.

KUMMER, D., STEINBACHER, T., SCHWIETZER, M. F., THÖLMANN, S. & EBNET, K. 2020. Tetraspanins: integrating cell surface receptors to functional microdomains in homeostasis and disease. *Med Microbiol Immunol,* 209**,** 397-405.

KURT-JONES, E. A., POPOVA, L., KWINN, L., HAYNES, L. M., JONES, L. P., TRIPP, R. A., WALSH, E. E., FREEMAN, M. W., GOLENBOCK, D. T., ANDERSON, L. J. & FINBERG, R. W. 2000. Pattern recognition receptors TLR4 and CD14 mediate response to respiratory syncytial virus. *Nature Immunology,* 1**,** 398-401.

LAFLEUR, A. M., LUKACS, N. W., KUNKEL, S. L. & MATSUKAWA, A. 2004. Role of CC chemokine CCL6/C10 as a monocyte chemoattractant in a murine acute peritonitis. *Mediators of Inflammation,* 13**,** 601360.

LAI, T.-Y., WU, S.-D., TSAI, M.-H., CHUANG, E. Y., CHUANG, L.-L., HSU, L.-C. & LAI, L.-C. 2013. Transcription of Tnfaip3 Is Regulated by NF-κB and p38 via C/EBPβ in Activated Macrophages. *PLOS ONE,* 8**,** e73153.

LAMMERDING, J., KAZAROV, A. R., HUANG, H., LEE, R. T. & HEMLER, M. E. 2003. Tetraspanin CD151 regulates α6β1 integrin adhesion strengthening. *Proceedings of the National Academy of Sciences,* 100**,** 7616-7621.

LE NAOUR, F., RUBINSTEIN, E., JASMIN, C., PRENANT, M. & BOUCHEIX, C. 2000. Severely Reduced Female Fertility in CD9-Deficient Mice. *Science,* 287**,** 319-321.

LENTINI, G., FAMÀ, A., BIONDO, C., MOHAMMADI, N., GALBO, R., MANCUSO, G., IANNELLO, D., ZUMMO, S., GIARDINA, M., DE GAETANO, G. V., TETI, G.,

BENINATI, C. & MIDIRI, A. 2020. Neutrophils Enhance Their Own Influx to Sites of Bacterial Infection via Endosomal TLR-Dependent Cxcl2 Production. *The Journal of Immunology,* 204**,** 660-670.

LENZ, T. & STÜHLER, K. 2022. Small Molecule Arranged Thermal Proximity Coaggregation (smarTPCA)-A Novel Approach to Characterize Protein-Protein Interactions in Living Cells by Similar Isothermal Dose-Responses. *Int J Mol Sci,* 23.

LEVY, S. & SHOHAM, T. 2005a. Protein-Protein Interactions in the Tetraspanin Web. *Physiology,* 20**,** 218-224.

LEVY, S. & SHOHAM, T. 2005b. The tetraspanin web modulates immune-signalling complexes. *Nature Reviews Immunology,* 5**,** 136-148.

LEVY, S., TODD, S. C. & MAECKER, H. T. 1998. CD81 (TAPA-1): A MOLECULE INVOLVED IN SIGNAL TRANSDUCTION AND CELL ADHESION IN THE IMMUNE SYSTEM. *Annual Review of Immunology,* 16**,** 89-109.

LI, J., LIM, C. H., TAY, F., GOH, C. C., DEVI, S., MALLERET, B., LEE, B., BAKOCEVIC, N., CHONG, S. Z., EVRARD, M., TANIZAKI, H., YING, L., RUSSELL, B., RENIA, L., ZOLEZZI, F., POIDINGER, M., ANGELI, V., ST. JOHN, A., HARRIS, J. & NG, L. G. 2015. Neutrophils Self-Regulate Immune Complex-Mediated Cutaneous Inflammation Through CXCL2. *The Journal of investigative dermatology,* 136.

LI, J. L., LIM, C. H., TAY, F. W., GOH, C. C., DEVI, S., MALLERET, B., LEE, B., BAKOCEVIC, N., CHONG, S. Z., EVRARD, M., TANIZAKI, H., LIM, H. Y., RUSSELL, B., RENIA, L., ZOLEZZI, F., POIDINGER, M., ANGELI, V., ST. JOHN, A. L., HARRIS, J. E., TEY, H. L., TAN, S. M., KABASHIMA, K., WENINGER, W., LARBI, A. & NG, L. G. 2016a. Neutrophils Self-Regulate Immune Complex-Mediated Cutaneous Inflammation through CXCL2. *Journal of Investigative Dermatology,* 136**,** 416-424.

LI, P.-Y., LV, J., QI, W.-W., ZHAO, S.-F., SUN, L.-B., LIU, N., SHENG, J. & QIU, W.-S. 2016b. Tspan9 inhibits the proliferation, migration and invasion of human gastric cancer SGC7901 cells via the ERK1/2 pathway. *Oncol Rep,* 36**,** 448-454.

LI, P., DONG, M. & WANG, Z. 2019. Downregulation of TSPAN13 by miR-369-3p inhibits cell proliferation in papillary thyroid cancer (PTC). *Bosn J Basic Med Sci,* 19**,** 146-154.

LIU, L., HE, B., LIU, W. M., ZHOU, D., COX, J. V. & ZHANG, X. A. 2007. Tetraspanin CD151 Promotes Cell Migration by Regulating Integrin Trafficking*. *Journal of Biological Chemistry,* 282**,** 31631-31642.

LOMBARDO, S. D., MAZZON, E., BASILE, M. S., CAMPO, G., CORSICO, F., PRESTI, M., BRAMANTI, P., MANGANO, K., PETRALIA, M. C., NICOLETTI, F. & FAGONE, P. 2019. Modulation of Tetraspanin 32 (TSPAN32) Expression in T Cell-Mediated Immune Responses and in Multiple Sclerosis. *International Journal of Molecular Sciences,* 20**,** 4323.

LU, Y.-C., YEH, W.-C. & OHASHI, P. S. 2008. LPS/TLR4 signal transduction pathway. *Cytokine,* 42**,** 145-151.

MA, X., QIU, S., TANG, X., SONG, Q., WANG, P., WANG, J., XIA, Q., WANG, Z., ZHAO, Q. & LU, M. 2022. TSPAN31 regulates the proliferation, migration, and apoptosis of gastric cancer cells through the METTL1/CCT2 pathway. *Translational Oncology,* 20**,** 101423.

MACCALLUM, D. M. & ODDS, F. C. 2005. Temporal events in the intravenous challenge model for experimental Candida albicans infections in female mice. *Mycoses,* 48**,** 151-161.

MAECKER, H. T., TODD, S. C. & LEVY, S. 1997. The tetraspanin superfamily: molecular facilitators. *The FASEB Journal,* 11**,** 428-442.

MANTEGAZZA, A. R., BARRIO, M. M., MOUTEL, S., BOVER, L., WECK, M., BROSSART, P., TEILLAUD, J.-L. & MORDOH, J. 2004. CD63 tetraspanin slows down cell migration and translocates to the endosomal-lysosomal-MIICs route after extracellular stimuli in human immature dendritic cells. *Blood,* 104**,** 1183-1190.

MAZZOCCA, A., LIOTTA, F. & CARLONI, V. 2008. Tetraspanin CD81-Regulated Cell Motility Plays a Critical Role in Intrahepatic Metastasis of Hepatocellular Carcinoma. *Gastroenterology,* 135**,** 244-256.e1.

MCGOWAN, E. N. S., WONG, O., JONES, E., NGUYEN, J., WEE, J., DEMARIA, M. C., DELIYANTI, D., JOHNSON, C. J., HICKEY, M. J., MCCONVILLE, M. J.,

WILKINSON-BERKA, J. L., WRIGHT, M. D. & BINGER, K. J. 2022a. Tetraspanin CD82 restrains phagocyte migration but supports macrophage activation. *iScience,* 25**,** 104520.

MCGOWAN, E. N. S., WONG, O., JONES, E., NGUYEN, J., WEE, J., DEMARIA, M. C., DELIYANTI, D., JOHNSON, C. J., HICKEY, M. J., MCCONVILLE, M. J., WILKINSON-BERKA, J. L., WRIGHT, M. D. & BINGER, K. J. 2022b. Tetraspanin CD82 restrains phagocyte migration but supports macrophage activation. *iScience,* 25.

MEDZHITOV, R. 2008. Origin and physiological roles of inflammation. *Nature,* 454**,** 428-435.

MEDZHITOV, R. & JANEWAY, C. 2000. Innate Immunity. *New England Journal of Medicine,* 343**,** 338-344.

MEYER-WENTRUP, F., FIGDOR, C. G., ANSEMS, M., BROSSART, P., WRIGHT, M. D., ADEMA, G. J. & VAN SPRIEL, A. B. 2007. Dectin-1 Interaction with Tetraspanin CD37 Inhibits IL-6 Production1. *The Journal of Immunology,* 178**,** 154-162.

MEZU-NDUBUISI, O. J. & MAHESHWARI, A. 2021. The role of integrins in inflammation and angiogenesis. *Pediatric Research,* 89**,** 1619-1626.

MIHLAN, M., GLASER, K. M., EPPLE, M. W. & LÄMMERMANN, T. 2022. Neutrophils: Amoeboid Migration and Swarming Dynamics in Tissues. *Front Cell Dev Biol,* 10**,** 871789.

MISHRA, Y. G. & MANAVATHI, B. 2021. Focal adhesion dynamics in cellular function and disease. *Cellular Signalling,* 85**,** 110046.

MIYAZAKI, T., MÜLLER, U. & CAMPBELL, K. S. 1997. Normal development but differentially altered proliferative responses of lymphocytes in mice lacking CD81. *The EMBO Journal,* 16**,** 4217-4225-4225.

MOLLINEDO, F. 2019. Neutrophil Degranulation, Plasticity, and Cancer Metastasis. *Trends in Immunology,* 40**,** 228-242.

MOLOSTVOV, G., GACHECHILADZE, M., SHAABAN, A. M., HAYWARD, S., DEAN, I., DIAS, I. H. K., BADR, N., DANIAL, I., MOHAMMED, F., NOVITSKAYA, V., PANIUSHKINA, L., SPEIRS, V., HANBY, A., NAZARENKO, I., WITHERS, D. R., VAN LAERE, S., LONG, H. M. & BERDITCHEVSKI, F. 2023. Tspan6 stimulates the chemoattractive potential of breast cancer cells for B cells in an EV- and LXR-dependent manner. *Cell Reports,* 42.

MURAYAMA, Y., SHINOMURA, Y., ORITANI, K., MIYAGAWA, J.-I., YOSHIDA, H., NISHIDA, M., KATSUBE, F., SHIRAGA, M., MIYAZAKI, T., NAKAMOTO, T., TSUTSUI, S., TAMURA, S., HIGASHIYAMA, S., SHIMOMURA, I. & HAYASHI, N. 2008. The tetraspanin CD9 modulates epidermal growth factor receptor signaling in cancer cells. *Journal of Cellular Physiology,* 216**,** 135-143.

NAKAMURA, Y., IWAMOTO, R. & MEKADA, E. 1996. Expression and distribution of CD9 in myelin of the central and peripheral nervous systems. *Am J Pathol,* 149**,** 575-83.

NAKANISHI, Y., MATSUGAKI, A., KAWAHARA, K., NINOMIYA, T., SAWADA, H. & NAKANO, T. 2019. Unique arrangement of bone matrix orthogonal to osteoblast alignment controlled by Tspan11-mediated focal adhesion assembly. *Biomaterials,* 209**,** 103-110.

NAVARRO-HERNANDEZ, I. C., LÓPEZ-ORTEGA, O., ACEVEDO-OCHOA, E., CERVANTES-DÍAZ, R., ROMERO-RAMÍREZ, S., SOSA-HERNÁNDEZ, V. A., MEZA-SÁNCHEZ, D. E., JUÁREZ-VEGA, G., PÉREZ-MARTÍNEZ, C. A., CHÁVEZ-MUNGUÍA, B., GALVÁN-HERNÁNDEZ, A., ANTILLÓN, A., ORTEGA-BLAKE, I., SANTOS-ARGUMEDO, L., HERNÁNDEZ-HERNÁNDEZ, J. M. & MARAVILLAS-MONTERO, J. L. 2020. Tetraspanin 33 (TSPAN33) regulates endocytosis and migration of human B lymphocytes by affecting the tension of the plasma membrane. *The FEBS Journal,* 287**,** 3449-3471.

NETEA, M. G., BROWN, G. D., KULLBERG, B. J. & GOW, N. A. R. 2008. An integrated model of the recognition of Candida albicans by the innate immune system. *Nature Reviews Microbiology,* 6**,** 67-78.

NETEA, M. G., GOW, N. A. R., MUNRO, C. A., BATES, S., COLLINS, C., FERWERDA, G., HOBSON, R. P., BERTRAM, G., HUGHES, H. B., JANSEN, T., JACOBS, L., BUURMAN, E. T., GIJZEN, K., WILLIAMS, D. L., TORENSMA, R., MCKINNON, A.,

MACCALLUM, D. M., ODDS, F. C., VAN DER MEER, J. W. M., BROWN, A. J. P. & KULLBERG, B. J. 2006. Immune sensing of Candida albicans requires cooperative recognition of mannans and glucans by lectin and Toll-like receptors. *The Journal of Clinical Investigation,* 116**,** 1642-1650.

NG, L. G., OSTUNI, R. & HIDALGO, A. 2019. Heterogeneity of neutrophils. *Nature Reviews Immunology,* 19**,** 255-265.

NISHIUCHI, R., SANZEN, N., NADA, S., SUMIDA, Y., WADA, Y., OKADA, M., TAKAGI, J., HASEGAWA, H. & SEKIGUCHI, K. 2005. Potentiation of the ligand-binding activity of integrin α3β1 via association with tetraspanin CD151. *Proceedings of the National Academy of Sciences,* 102**,** 1939-1944.

NOURSHARGH, S. & ALON, R. 2014. Leukocyte Migration into Inflamed Tissues. *Immunity,* 41**,** 694-707.

O′ MEARA, R. W., MICHALSKI, J.-P. & KOTHARY, R. 2011. Integrin Signaling in Oligodendrocytes and Its Importance in CNS Myelination. *Journal of Signal Transduction,* 2011**,** 354091.

ONO, M., HANDA, K., WITHERS, D. A. & HAKOMORI, S. 1999. Motility inhibition and apoptosis are induced by metastasis-suppressing gene product CD82 and its analogue CD9, with concurrent glycosylation. *Cancer Res,* 59**,** 2335-9.

OREN, R., TAKAHASHI, S., DOSS, C., LEVY, R. & LEVY, S. 1990a. TAPA-1, the target of an antiproliferative antibody, defines a new family of transmembrane proteins. *Molecular and Cellular Biology,* 10**,** 4007-4015.

OREN, R., TAKAHASHI, S., DOSS, C., LEVY, R. & LEVY, S. 1990b. TAPA-1, the target of an antiproliferative antibody, defines a new family of transmembrane proteins. *Mol Cell Biol,* 10**,** 4007-15.

OSORIO, D. & CAI, J. J. 2020. Systematic determination of the mitochondrial proportion in human and mice tissues for single-cell RNA-sequencing data quality control. *Bioinformatics,* 37**,** 963-967.

OTSUBO, C., OTOMO, R., MIYAZAKI, M., MATSUSHIMA-HIBIYA, Y., KOHNO, T., IWAKAWA, R., TAKESHITA, F., OKAYAMA, H., ICHIKAWA, H., SAYA, H., KIYONO, T., OCHIYA, T., TASHIRO, F., NAKAGAMA, H., YOKOTA, J. & ENARI, M. 2014. TSPAN2 Is Involved in Cell Invasion and Motility during Lung Cancer Progression. *Cell Reports,* 7**,** 527-538.

PAPAYANNOPOULOS, V. 2018. Neutrophil extracellular traps in immunity and disease. *Nature Reviews Immunology,* 18**,** 134-147.

PAPAYANNOPOULOS, V., METZLER, K. D., HAKKIM, A. & ZYCHLINSKY, A. 2010. Neutrophil elastase and myeloperoxidase regulate the formation of neutrophil extracellular traps. *Journal of Cell Biology,* 191**,** 677-691.

PATIN, E. C., THOMPSON, A. & ORR, S. J. 2019. Pattern recognition receptors in fungal immunity. *Seminars in Cell & Developmental Biology,* 89**,** 24-33.

PEROT, B. P., GARCÍA-PAREDES, V., LUKA, M. & MÉNAGER, M. M. 2020. Dendritic Cell Maturation Regulates TSPAN7 Function in HIV-1 Transfer to CD4+ T Lymphocytes. *Frontiers in Cellular and Infection Microbiology,* 10.

PILERI, P., UEMATSU, Y., CAMPAGNOLI, S., GALLI, G., FALUGI, F., PETRACCA, R., WEINER, A. J., HOUGHTON, M., ROSA, D., GRANDI, G. & ABRIGNANI, S. 1998. Binding of Hepatitis C Virus to CD81. *Science,* 282**,** 938-941.

PILLAY, J., DEN BRABER, I., VRISEKOOP, N., KWAST, L. M., DE BOER, R. J., BORGHANS, J. A. M., TESSELAAR, K. & KOENDERMAN, L. 2010. In vivo labeling with 2H2O reveals a human neutrophil lifespan of 5.4 days. *Blood,* 116**,** 625-627.

POWNER, D., KOPP, PETRA M., MONKLEY, SUSAN J., CRITCHLEY, DAVID R. & BERDITCHEVSKI, F. 2011. Tetraspanin CD9 in cell migration. *Biochemical Society Transactions,* 39**,** 563-567.

PRADEU, T., THOMMA, B. P. H. J., GIRARDIN, S. E. & LEMAITRE, B. 2024. The conceptual foundations of innate immunity: Taking stock 30 years later. *Immunity,* 57**,** 613-631.

QU, J., JIN, J., ZHANG, M. & NG, L. G. 2023. Neutrophil diversity and plasticity: Implications for organ transplantation. *Cellular & Molecular Immunology,* 20**,** 993-1001.

QUAST, T., EPPLER, F., SEMMLING, V., SCHILD, C., HOMSI, Y., LEVY, S., LANG, T., KURTS, C. & KOLANUS, W. 2011. CD81 is essential for the formation of membrane protrusions and regulates Rac1-activation in adhesion-dependent immune cell migration. *Blood,* 118**,** 1818-1827.

R CORE TEAM 2021. R: A Language and Environment for Statistical Computing. Vienna, Austria: R Foundation for Statistical Computing.

RADFORD, K. J., THORNE, R. F. & HERSEY, P. 1996. CD63 Associates with Transmembrane 4 Superfamily Members, CD9 and CD81, and with β1 Integrins in Human Melanoma. *Biochemical and Biophysical Research Communications,* 222**,** 13-18.

RAJAN, A., PERSSON, B. D., FRÄNGSMYR, L., OLOFSSON, A., SANDBLAD, L., HEINO, J., TAKADA, Y., MOULD, A. P., SCHNAPP, L. M., GALL, J. & ARNBERG, N. 2018. Enteric Species F Human Adenoviruses use Laminin-Binding Integrins as Co-Receptors for Infection of Ht-29 Cells. *Scientific Reports,* 8**,** 10019.

RANKIN, S. M. 2010. The bone marrow: a site of neutrophil clearance. *J Leukoc Biol,* 88**,** 241-51.

REÁTEGUI, E., JALALI, F., KHANKHEL, A. H., WONG, E., CHO, H., LEE, J., SERHAN, C. N., DALLI, J., ELLIOTT, H. & IRIMIA, D. 2017. Microscale arrays for the profiling of start and stop signals coordinating human-neutrophil swarming. *Nature Biomedical Engineering,* 1**,** 0094.

REICHEL, C. A., KHANDOGA, A., ANDERS, H.-J., SCHLÖNDORFF, D., LUCKOW, B. & KROMBACH, F. 2005. Chemokine receptors Ccr1, Ccr2, and Ccr5 mediate neutrophil migration to postischemic tissue. *Journal of Leukocyte Biology,* 79**,** 114-122.

REYAT, J. S., CHIMEN, M., NOY, P. J., SZYROKA, J., RAINGER, G. E. & TOMLINSON, M. G. 2017. ADAM10-Interacting Tetraspanins Tspan5 and Tspan17 Regulate VE-Cadherin Expression and Promote T Lymphocyte Transmigration. *The Journal of Immunology,* 199**,** 666-676.

REYES, R., CARDEÑES, B., MACHADO-PINEDA, Y. & CABAÑAS, C. 2018. Tetraspanin CD9: A Key Regulator of Cell Adhesion in the Immune System. *Frontiers in Immunology,* 9.

REYNOLDS, J. L. & MAHAJAN, S. D. 2020. Transmigration of Tetraspanin 2 (Tspan2) siRNA Via Microglia Derived Exosomes across the Blood Brain Barrier Modifies the Production of Immune Mediators by Microglia Cells. *Journal of Neuroimmune Pharmacology,* 15**,** 554-563.

ROCHELEAU, A. D., WANG, W. & KING, M. R. 2016. Effect of Pseudopod Extensions on Neutrophil Hemodynamic Transport Near a Wall. *Cell Mol Bioeng,* 9**,** 85-95.

RODRIGUES, A., QUEIRÓZ, D. B. C., HONDA, L., SILVA, E. J. R., HALL, S. H. & AVELLAR, M. C. W. 2008. Activation of Toll-Like Receptor 4 (TLR4) by In Vivo and In Vitro Exposure of Rat Epididymis to Lipopolysaccharide from Escherichia Coli1. *Biology of Reproduction,* 79**,** 1135-1147.

RSTUDIO TEAM 2019. RStudio: Integrated Development for R. Boston, MA: RStudio, Inc.

RUBINSTEIN, E., LE NAOUR, F., LAGAUDRIÈRE-GESBERT, C., BILLARD, M., CONJEAUD, H. & BOUCHEIX, C. 1996. CD9, CD63, CD81, and CD82 are components of a surface tetraspan network connected to HLA-DR and VLA integrins. *European Journal of Immunology,* 26**,** 2657-2665.

SCAPINI, P., MARINI, O., TECCHIO, C. & CASSATELLA, M. A. 2016. Human neutrophils in the saga of cellular heterogeneity: insights and open questions. *Immunological Reviews,* 273**,** 48-60.

SERRU, V., DESSEN, P., BOUCHEIX, C. & RUBINSTEIN, E. 2000. Sequence and expression of seven new tetraspans. *Biochimica et Biophysica Acta (BBA) - Protein Structure and Molecular Enzymology,* 1478**,** 159-163.

SERRU, V., LE NAOUR, F., BILLARD, M., AZORSA, D. O., LANZA, F., BOUCHEIX, C. & RUBINSTEIN, E. 1999. Selective tetraspan-integrin complexes (CD81/alpha4beta1, CD151/alpha3beta1, CD151/alpha6beta1) under conditions disrupting tetraspan interactions. *Biochem J,* 340 (Pt 1)**,** 103-11.

SETO, S., MATSUMOTO, S., TSUJIMURA, K. & KOIDE, Y. 2010. Differential recruitment of CD63 and Rab7-interacting-lysosomal-protein to phagosomes containing Mycobacterium tuberculosis in macrophages. *Microbiology and Immunology,* 54**,** 170-174.

SHEMER, A., SCHEYLTJENS, I., FRUMER, G. R., KIM, J.-S., GROZOVSKI, J., AYANAW, S., DASSA, B., VAN HOVE, H., CHAPPELL-MAOR, L., BOURA-HALFON, S., LESHKOWITZ, D., MUELLER, W., MAGGIO, N., MOVAHEDI, K. & JUNG, S. 2020. Interleukin-10 Prevents Pathological Microglia Hyperactivation following Peripheral Endotoxin Challenge. *Immunity,* 53**,** 1033-1049.e7.

SILVESTRE-ROIG, C., HIDALGO, A. & SOEHNLEIN, O. 2016. Neutrophil heterogeneity: implications for homeostasis and pathogenesis. *Blood,* 127**,** 2173-2181.

SINATRA, L., YANG, J., SCHLIEHE-DIECKS, J., DIENSTBIER, N., VOGT, M., GEBING, P., BACHMANN, L. M., SÖNNICHSEN, M., LENZ, T., STÜHLER, K., SCHÖLER, A., BORKHARDT, A., BHATIA, S. & HANSEN, F. K. 2022. Solid-Phase Synthesis of Cereblon-Recruiting Selective Histone Deacetylase 6 Degraders (HDAC6 PROTACs) with Antileukemic Activity. *Journal of Medicinal Chemistry,* 65**,** 16860-16878.

SPELLBERG, B., IBRAHIM, A. S., EDWARDS, J. E., JR. & FILLER, S. G. 2005. Mice with Disseminated Candidiasis Die of Progressive Sepsis. *The Journal of Infectious Diseases,* 192**,** 336-343.

SPODEN, G., FREITAG, K., HUSMANN, M., BOLLER, K., SAPP, M., LAMBERT, C. & FLORIN, L. 2008. Clathrin- and Caveolin-Independent Entry of Human Papillomavirus Type 16—Involvement of Tetraspanin-Enriched Microdomains (TEMs). *PLOS ONE,* 3**,** e3313.

STADELMANN, C., TIMMLER, S., BARRANTES-FREER, A. & SIMONS, M. 2019. Myelin in the Central Nervous System: Structure, Function, and Pathology. *Physiological Reviews,* 99**,** 1381-1431.

STADTMANN, A., GERMENA, G., BLOCK, H., BORAS, M., ROSSAINT, J., SUNDD, P., LEFORT, C., FISHER, C. I., BUSCHER, K., GELSCHEFARTH, B., URZAINQUI, A., GERKE, V., LEY, K. & ZARBOCK, A. 2013. The PSGL-1–L-selectin signaling complex regulates neutrophil adhesion under flow. *Journal of Experimental Medicine,* 210**,** 2171-2180.

STIPP, C. S., KOLESNIKOVA, T. V. & HEMLER, M. E. 2003. Functional domains in tetraspanin proteins. *Trends in Biochemical Sciences,* 28**,** 106-112.

STORM, R. J., PERSSON, B. D., SKALMAN, L. N., FRÄNGSMYR, L., LINDSTRÖM, M., RANKIN, G., LUNDMARK, R., DOMELLÖF, F. P. & ARNBERG, N. 2017. Human Adenovirus Type 37 Uses α(V)β(1) and α(3)β(1) Integrins for Infection of Human Corneal Cells. *J Virol,* 91.

SUÁREZ, H., ROCHA-PERUGINI, V., ÁLVAREZ, S. & YÁÑEZ-MÓ, M. 2018. Tetraspanins, Another Piece in the HIV-1 Replication Puzzle. *Frontiers in Immunology,* 9.

SUMMERS, C., RANKIN, S. M., CONDLIFFE, A. M., SINGH, N., PETERS, A. M. & CHILVERS, E. R. 2010. Neutrophil kinetics in health and disease. *Trends in Immunology,* 31**,** 318-324.

SUZUKI, M., TACHIBANA, I., TAKEDA, Y., HE, P., MINAMI, S., IWASAKI, T., KIDA, H., GOYA, S., KIJIMA, T., YOSHIDA, M., KUMAGAI, T., OSAKI, T. & KAWASE, I. 2009. Tetraspanin CD9 Negatively Regulates Lipopolysaccharide-Induced Macrophage Activation and Lung Inflammation1. *The Journal of Immunology,* 182**,** 6485-6493.

SZKLARCZYK, D., KIRSCH, R., KOUTROULI, M., NASTOU, K., MEHRYARY, F., HACHILIF, R., GABLE, A. L., FANG, T., DONCHEVA, NADEZHDA T., PYYSALO, S., BORK, P., JENSEN, LARS J. & VON MERING, C. 2022. The STRING database in 2023: protein–protein association networks and functional enrichment analyses for any sequenced genome of interest. *Nucleic Acids Research,* 51**,** D638-D646.

TADA, H., NEMOTO, E., SHIMAUCHI, H., WATANABE, T., MIKAMI, T., MATSUMOTO, T., OHNO, N., TAMURA, H., SHIBATA, K., AKASHI, S., MIYAKE, K., SUGAWARA, S. & TAKADA, H. 2002. Saccharomyces cerevisiae- and Candida albicans-derived mannan induced production of tumor necrosis factor alpha by human monocytes in a CD14- and Toll-like receptor 4-dependent manner. *Microbiol Immunol,* 46**,** 503-12.

TAKAHASHI, M., SUGIURA, T., ABE, M., ISHII, K. & SHIRASUNA, K. 2007. Regulation of c-Met signaling by the tetraspanin KAI-1/CD82 affects cancer cell migration. *International Journal of Cancer,* 121**,** 1919-1929.

TAKEUCHI, O. & AKIRA, S. 2010. Pattern Recognition Receptors and Inflammation. *Cell,* 140**,** 805-820.

TAM, J. M., REEDY, J. L., LUKASON, D. P., KUNA, S. G., ACHARYA, M., KHAN, N. S., NEGORO, P. E., XU, S., WARD, R. A., FELDMAN, M. B., DUTKO, R. A., JEFFERY, J. B., SOKOLOVSKA, A., WIVAGG, C. N., LASSEN, K. G., LE NAOUR, F., MATZARAKI, V., GARNER, E. C., XAVIER, R. J., KUMAR, V., VAN DE VEERDONK, F. L., NETEA, M. G., MIRANTI, C. K., MANSOUR, M. K. & VYAS, J. M. 2019. Tetraspanin CD82 Organizes Dectin-1 into Signaling Domains to Mediate Cellular Responses to Candida albicans. *J Immunol,* 202**,** 3256-3266.

TARRANT, J. M., ROBB, L., VAN SPRIEL, A. B. & WRIGHT, M. D. 2003. Tetraspanins: molecular organisers of the leukocyte surface. *Trends in Immunology,* 24**,** 610-617.

TAYLOR, P. R., TSONI, S. V., WILLMENT, J. A., DENNEHY, K. M., ROSAS, M., FINDON, H., HAYNES, K., STEELE, C., BOTTO, M., GORDON, S. & BROWN, G. D. 2007. Dectin-1 is required for β-glucan recognition and control of fungal infection. *Nature Immunology,* 8**,** 31-38.

TEBBE, L., KAKAKHEL, M., MAKIA, M. S., AL-UBAIDI, M. R. & NAASH, M. I. 2020. The Interplay between Peripherin 2 Complex Formation and Degenerative Retinal Diseases. *Cells,* 9**,** 784.

TEJERA, E., ROCHA-PERUGINI, V., LÓPEZ-MARTÍN, S., PÉREZ-HERNÁNDEZ, D., BACHIR, A. I., HORWITZ, A. R., VÁZQUEZ, J., SÁNCHEZ-MADRID, F. & YÁÑEZ-MO, M. 2013. CD81 regulates cell migration through its association with Rac GTPase. *Molecular Biology of the Cell,* 24**,** 261-273.

TERADA, N., BARACSKAY, K., KINTER, M., MELROSE, S., BROPHY, P. J., BOUCHEIX, C., BJARTMAR, C., KIDD, G. & TRAPP, B. D. 2002. The tetraspanin protein, CD9, is expressed by progenitor cells committed to oligodendrogenesis and is linked to β1 integrin, CD81, and Tspan-2. *Glia,* 40**,** 350-359.

TERMINI, C. M., COTTER, M. L., MARJON, K. D., BURANDA, T., LIDKE, K. A. & GILLETTE, J. M. 2014. The membrane scaffold CD82 regulates cell adhesion by altering α4 integrin stability and molecular density. *Molecular Biology of the Cell,* 25**,** 1560-1573.

THAM, T. N., GOUIN, E., RUBINSTEIN, E., BOUCHEIX, C., COSSART, P. & PIZARRO-CERDA, J. 2010. Tetraspanin CD81 is required for Listeria monocytogenes invasion. *Infect Immun,* 78**,** 204-9.

TIPPETT, E., CAMERON, P. U., MARSH, M. & CROWE, S. M. 2013. Characterization of tetraspanins CD9, CD53, CD63, and CD81 in monocytes and macrophages in HIV-1 infection. *Journal of Leukocyte Biology,* 93**,** 913-920.

TIWARI-WOODRUFF, S. K., KAPLAN, R., KORNBLUM, H. I. & BRONSTEIN, J. M. 2004. Developmental expression of OAP-1/Tspan-3, a member of the tetraspanin superfamily. *Journal of Neuroscience Research,* 77**,** 166-173.

TODD, S. C., DOCTOR, V. S. & LEVY, S. 1998. Sequences and expression of six new members of the tetraspanin/TM4SF family. *Biochimica et Biophysica Acta (BBA) - Gene Structure and Expression,* 1399**,** 101-104.

TUGUES, S., HONJO, S., KÖNIG, C., PADHAN, N., KROON, J., GUALANDI, L., LI, X., BARKEFORS, I., THIJSSEN, V. L., GRIFFIOEN, A. W. & CLAESSON-WELSH, L. 2013. Tetraspanin CD63 Promotes Vascular Endothelial Growth Factor Receptor 2-β1 Integrin Complex Formation, Thereby Regulating Activation and Downstream Signaling in Endothelial Cells in Vitro and in Vivo*. *Journal of Biological Chemistry,* 288**,** 19060-19071.

TUSHER, V. G., TIBSHIRANI, R. & CHU, G. 2001. Significance analysis of microarrays applied to the ionizing radiation response. *Proceedings of the National Academy of Sciences,* 98**,** 5116-5121.

ULLAH, M., AKBAR, A., NG, N. N., CONCEPCION, W. & THAKOR, A. S. 2019. Mesenchymal stem cells confer chemoresistance in breast cancer via a CD9 dependent mechanism. *Oncotarget,* 10.

URBAN, C. F., ERMERT, D., SCHMID, M., ABU-ABED, U., GOOSMANN, C., NACKEN, W., BRINKMANN, V., JUNGBLUT, P. R. & ZYCHLINSKY, A. 2009. Neutrophil Extracellular Traps Contain Calprotectin, a Cytosolic Protein Complex Involved in Host Defense against Candida albicans. *PLOS Pathogens,* 5**,** e1000639.

URBAN, C. F., REICHARD, U., BRINKMANN, V. & ZYCHLINSKY, A. 2006. Neutrophil extracellular traps capture and kill Candida albicans yeast and hyphal forms. *Cellular Microbiology,* 8**,** 668-676.

VAN DEVENTER, S. J., DUNLOCK, V.-M. E. & VAN SPRIEL, A. B. 2017. Molecular interactions shaping the tetraspanin web. *Biochemical Society Transactions,* 45**,** 741-750.

VAN SPRIEL, A. B., SOFI, M., GARTLAN, K. H., VAN DER SCHAAF, A., VERSCHUEREN, I., TORENSMA, R., RAYMAKERS, R. A., LOVELAND, B. E., NETEA, M. G., ADEMA, G. J., WRIGHT, M. D. & FIGDOR, C. G. 2009. The tetraspanin protein CD37 regulates IgA responses and anti-fungal immunity. *PLoS Pathog,* 5**,** e1000338.

VENCES-CATALÁN, F., RAJAPAKSA, R., SRIVASTAVA, M. K., MARABELLE, A., KUO, C.-C., LEVY, R. & LEVY, S. 2015. Tetraspanin CD81 Promotes Tumor Growth and Metastasis by Modulating the Functions of T Regulatory and Myeloid-Derived Suppressor Cells. *Cancer Research,* 75**,** 4517-4526.

WACK, A., SOLDAINI, E., TSENG, C.-T. K., NUTI, S., KLIMPEL, G. R. & ABRIGNANI, S. 2001. Binding of the hepatitis C virus envelope protein E2 to CD81 provides a co-stimulatory signal for human T cells. *European Journal of Immunology,* 31**,** 166-175.

WANG, J., ZHOU, Y., LI, D., SUN, X., DENG, Y. & ZHAO, Q. 2017. TSPAN31 is a critical regulator on transduction of survival and apoptotic signals in hepatocellular carcinoma cells. *FEBS Letters,* 591**,** 2905-2918.

WANG, Q. & DOERSCHUK, C. M. 2002. The Signaling Pathways Induced by Neutrophil-Endothelial Cell Adhesion. *Antioxidants & Redox Signaling,* 4**,** 39-47.

WEE, J. L., SCHULZE, K. E., JONES, E. L., YEUNG, L., CHENG, Q., PEREIRA, C. F., COSTIN, A., RAMM, G., VAN SPRIEL, A. B., HICKEY, M. J. & WRIGHT, M. D. 2015. Tetraspanin CD37 Regulates β2 Integrin–Mediated Adhesion and Migration in Neutrophils. *The Journal of Immunology,* 195**,** 5770-5779.

WITKO-SARSAT, V., RIEU, P., DESCAMPS-LATSCHA, B., LESAVRE, P. & HALBWACHS-MECARELLI, L. 2000. Neutrophils: Molecules, Functions and Pathophysiological Aspects. *Laboratory Investigation,* 80**,** 617-653.

WRIGHT, M. D., GEARY, S. M., FITTER, S., MOSELEY, G. W., LAU, L.-M., SHENG, K.-C., APOSTOLOPOULOS, V., STANLEY, E. G., JACKSON, D. E. & ASHMAN, L. K. 2004a. Characterization of Mice Lacking the Tetraspanin Superfamily Member CD151. *Molecular and Cellular Biology,* 24**,** 5978-5988.

WRIGHT, M. D., MOSELEY, G. W. & VAN SPRIEL, A. B. 2004b. Tetraspanin microdomains in immune cell signalling and malignant disease. *Tissue Antigens,* 64**,** 533-542.

WU, L., YANG, S., LI, H., ZHANG, Y., FENG, L., ZHANG, C., WEI, J., GU, X., XU, G., WANG, Z. & WANG, F. 2022. TSPAN4-positive migrasome derived from retinal pigmented epithelium cells contributes to the development of proliferative vitreoretinopathy. *Journal of Nanobiotechnology,* 20**,** 519.

WU, X. R., SUN, T. T. & MEDINA, J. J. 1996. In vitro binding of type 1-fimbriated Escherichia coli to uroplakins Ia and Ib: relation to urinary tract infections. *Proceedings of the National Academy of Sciences,* 93**,** 9630-9635.

WU, Y., CHEN, W., GONG, Y., LIU, H. & ZHANG, B. 2021. Tetraspanin 1 (TSPAN1) promotes growth and transferation of breast cancer cells via mediating PI3K/Akt pathway. *Bioengineered,* 12**,** 10761-10770.

XIE, Q., GUO, H., HE, P., DENG, H., GAO, Y., DONG, N., NIU, W., LIU, T., LI, M., WANG, S., WU, Y. & LI, J.-L. 2021. Tspan5 promotes epithelial–mesenchymal transition and tumour metastasis of hepatocellular carcinoma by activating Notch signalling. *Molecular Oncology,* 15**,** 3184-3202.

XIE, X., SHI, Q., WU, P., ZHANG, X., KAMBARA, H., SU, J., YU, H., PARK, S.-Y., GUO, R., REN, Q., ZHANG, S., XU, Y., SILBERSTEIN, L. E., CHENG, T., MA, F., LI, C. & LUO, H. R. 2020. Single-cell transcriptome profiling reveals neutrophil heterogeneity in homeostasis and infection. *Nature Immunology,* 21**,** 1119-1133.

YASEEN, I. H., MONK, P. N. & PARTRIDGE, L. J. 2017. Tspan2: a tetraspanin protein involved in oligodendrogenesis and cancer metastasis. *Biochem Soc Trans,* 45**,** 465-475.

YAUCH, R. L., BERDITCHEVSKI, F., HARLER, M. B., REICHNER, J. & HEMLER, M. E. 1998. Highly Stoichiometric, Stable, and Specific Association of Integrin α3β1 with CD151 Provides a Major Link to Phosphatidylinositol 4-Kinase, and May Regulate Cell Migration. *Molecular Biology of the Cell,* 9**,** 2751-2765.

YEUNG, L., HICKEY, M. J. & WRIGHT, M. D. 2018. The Many and Varied Roles of Tetraspanins in Immune Cell Recruitment and Migration. *Frontiers in Immunology,* 9.

YIPP, B. G., PETRI, B., SALINA, D., JENNE, C. N., SCOTT, B. N. V., ZBYTNUIK, L. D., PITTMAN, K., ASADUZZAMAN, M., WU, K., MEIJNDERT, H. C., MALAWISTA, S. E., DE BOISFLEURY CHEVANCE, A., ZHANG, K., CONLY, J. & KUBES, P. 2012. Infection-induced NETosis is a dynamic process involving neutrophil multitasking in vivo. *Nature Medicine,* 18**,** 1386-1393.

YONEYAMA, H., MATSUNO, K. & MATSUSHIMA, K. 2005. Migration of Dendritic Cells. *International Journal of Hematology,* 81**,** 204-207.

YU, G., WANG, L. G., HAN, Y. & HE, Q. Y. 2012. clusterProfiler: an R package for comparing biological themes among gene clusters. *Omics,* 16**,** 284-7.

YU, H., LIN, L., ZHANG, Z., ZHANG, H. & HU, H. 2020. Targeting NF-κB pathway for the therapy of diseases: mechanism and clinical study. *Signal Transduction and Targeted Therapy,* 5**,** 209.

ZARBOCK, A., LEY, K., MCEVER, R. P. & HIDALGO, A. 2011. Leukocyte ligands for endothelial selectins: specialized glycoconjugates that mediate rolling and signaling under flow. *Blood,* 118**,** 6743-6751.

ZHANG, B., ZHANG, Z., LI, L., QIN, Y.-R., LIU, H., JIANG, C., ZENG, T.-T., LI, M.-Q., XIE, D., LI, Y., GUAN, X.-Y. & ZHU, Y.-H. 2018. TSPAN15 interacts with BTRC to promote oesophageal squamous cell carcinoma metastasis via activating NF-κB signaling. *Nature Communications,* 9**,** 1423.

ZHANG, C., DU, F. H., WANG, R. X., HAN, W. B., LV, X., ZENG, L. H. & CHEN, G. Q. 2024. TSPAN6 reinforces the malignant progression of glioblastoma via interacting with CDK5RAP3 and regulating STAT3 signaling pathway. *Int J Biol Sci,* 20**,** 2440-2453.

ZHANG, H.-S., LIU, H.-Y., ZHOU, Z., SUN, H.-L. & LIU, M.-Y. 2020. TSPAN8 promotes colorectal cancer cell growth and migration in LSD1-dependent manner. *Life Sciences,* 241**,** 117114.

ZHOU, C., LIANG, Y., ZHOU, L., YAN, Y., LIU, N., ZHANG, R., HUANG, Y., WANG, M., TANG, Y., ALI, D. W., WANG, Y., MICHALAK, M., CHEN, X.-Z. & TANG, J. 2021. TSPAN1 promotes autophagy flux and mediates cooperation between WNT-CTNNB1 signaling and autophagy via the MIR454-FAM83A-TSPAN1 axis in pancreatic cancer. *Autophagy,* 17**,** 3175-3195.

ZHOU, J., FUJIWARA, T., YE, S., LI, X. & ZHAO, H. 2014. Downregulation of Notch Modulators, Tetraspanin 5 and 10, Inhibits Osteoclastogenesis in Vitro. *Calcified Tissue International,* 95**,** 209-217.

ZHOU, Q., CHEN, X., YAO, K., ZHANG, Y., HE, H., HUANG, H., CHEN, H., PENG, S., HUANG, M., CHENG, L., ZHANG, Q., XIE, R., LI, K., LIN, T. & HUANG, H. 2023. TSPAN18 facilitates bone metastasis of prostate cancer by protecting STIM1 from TRIM32-mediated ubiquitination. *Journal of Experimental & Clinical Cancer Research,* 42**,** 195.

ZIMMERMAN, B., KELLY, B., MCMILLAN, B. J., SEEGAR, T. C. M., DROR, R. O., KRUSE, A. C. & BLACKLOW, S. C. 2016. Crystal Structure of a Full-Length Human Tetraspanin Reveals a Cholesterol-Binding Pocket. *Cell,* 167**,** 1041-1051.e11.

ZUIDSCHERWOUDE, M., WORAH, K., VAN DER SCHAAF, A., BUSCHOW, S. I. & VAN SPRIEL, A. B. 2017. Differential expression of tetraspanin superfamily members in dendritic cell subsets. *PLOS ONE,* 12**,** e0184317.

9 Danksagung

Eine Doktorarbeit ist vieles, ein großes Projekt, ein Meilenstein und nahezu unmöglich im Alleingang zu bewältigen. Daher möchte ich hier meinen besonderen Dank an all jene richten, die mich auf diesem Weg unterstützt haben.

An erster Stelle gilt mein Dank meiner Erstbetreuerin Stefanie Scheu. Du hast mich vom ersten Moment an unermüdlich unterstützt und hast trotz vollem Kalender immer noch einen freien Termin gefunden. Nicht zuletzt gaben mir dein konstruktives Lob und Kritik immer ein positives Gefühl und reichlich Motivation. Das weiß ich sehr zu schätzen!

Gleichermaßen möchte ich Lutz Schmitt danken, der sich bereit erklärte, als Zweitbetreuer meiner Arbeit zu fungieren und stets Fragen parat hatte, die das Projekt voranbrachten und zum Weiterdenken anregten.

Ich danke der Jürgen Manchot Stiftung für die Finanzierung meines Projekts und meinem Kollegium innerhalb der MOI Graduiertenschule. Ein besonderer Dank geht an die AGs Pfeffer und Fleig, die durch den kontinuierlichen Austausch von Daten, Wissen und Material den Fortschritt meines Projekts mit unterstützt haben.

Des Weiteren möchte ich Rafael Leite-Dantas und Judith Alferink für den wissenschaftlichen Austausch und die Bereitstellung von Probenmaterial danken. Danke Rafael, ohne dich wäre so vieles kaum machbar gewesen!

Vielen Dank an die ganze AG Scheu und allen weiteren Kollegen:innen des Instituts. Neben dem wissenschaftlichen Austausch, waren auch private Gespräche an der Tagesordnung und haben eine ganz wunderbare Atmosphäre geschaffen (viele Grüße an den coolsten Schreibraum 4ever).

Danke Sonja, ohne dich wären so viele Experimente einfach nicht möglich gewesen, mein Nervenkostüm punktiert und der Alltag schlichter, öder und ohne Kekse.

Liebe Sofie, du warst immer bedingungslos für mich da und hast mich aus jeder Tiefe wieder zurück ans Licht geholt. Du bist mein Feuerherz, das mir Mut und Kraft schenkt. Danke!

Mein Dank gilt zudem meinen Eltern und meiner Schwester, die vom Studium bis zur Promotion jederzeit mit Stolz hinter mir standen. Ihr habt mich in jeder Situation unterstützt und standet mir mit Rat und Tat zur Seite. Danke!

Zuletzt noch einen großen Dank an die Korrekturleser:innen. Ihr habt mir viele neue und fortführende Ideen gegeben, mit denen ich diese Arbeit zu meiner Zufriedenheit gestalten konnte.